VOL. 14 NO. 2 JUNE 1967
PUBLISHED MONTHLY

JOURNAL OF

ELECTROANALYTICAL CHEMISTRY

AND INTERFACIAL ELECTROCHEMISTRY

International Journal devoted to all Aspects of Electroanalytical Chemistry, Double Layer Studies, Electrokinetics, Colloid Stability, and Electrode Kinetics.

ELSEVIER

GENERAL INFORMATION

See also Suggestions and Instructions to Authors which will be sent free, on request to the Publishers.

Types of contributions

(a) Original research work not previously published in other periodicals.
(b) Reviews on recent developments in various fields.
(c) Short communications.
(d) Bibliographical notes and book reviews.

Languages

Papers will be published in English, French or German.

Submission of papers

Papers should be sent to one of the following Editors:
Professor J. O'M. Bockris, John Harrison Laboratory of Chemistry, University of Pennsylvania, Philadelphia 4, Pa. 19104, U.S.A.
Dr. R. H. Ottewill, Department of Chemistry, The University, Bristol 8, England.
Dr. R. Parsons, Department of Chemistry, The University, Bristol 8, England. Until June 1967: Gates and Crellin Laboratories of Chemistry, California Institute of Technology, Pasadena, Calif. 91109, U.S.A.
Professor C. N. Reilley, Department of Chemistry, University of North Carolina, Chapel Hill, N.C. 27515, U.S.A.

Authors should preferably submit two copies in double-spaced typing on pages of uniform size. Legends for figures should be typed on a separate page. The figures should be in a form suitable for reproduction, drawn in Indian ink on drawing paper or tracing paper, with lettering etc. in thin pencil. The sheets of drawing or tracing paper should preferably be of the same dimensions as those on which the article is typed. Photographs should be submitted as clear black and white prints on glossy paper. Standard symbols should be used in line drawings, the following are available to the printers:

All references should be given at the end of the paper. They should be numbered and the numbers should appear in the text at the appropriate places.
A summary of 50 to 200 words should be included.

Reprints

Fifty reprints will be supplied free of charge. Additional reprints can be ordered at quoted prices. They must be ordered on order forms which are sent together with the proofs.

Publication

The *Journal of Electroanalytical Chemistry and Interfacial Electrochemistry* appears monthly and has four issues per volume and three volumes per year.

Subscription price: £ 18.18.0 or $ 52.50 or Dfl. 189.00 per year; £ 6.6.0 or $ 17.50 or Dfl. 63.00 per volume; plus postage. Additional cost for copies by air mail available on request. For advertising rates apply to the publishers.

ubscriptions

Subscriptions should be sent to:

ELSEVIER PUBLISHING COMPANY, P.O. Box 211, Amsterdam, The Netherlands.

ELECTROANALYTICAL CHEMISTRY AND INTERFACIAL ELECTROCHEMISTRY
Elsevier Publishing Company, Amsterdam – Printed in The Netherlands

THEORETICAL EVALUATION OF EFFECTS OF ELECTRODE SPHERICITY ON STATIONARY ELECTRODE POLAROGRAPHY

CASE OF A CHEMICAL REACTION FOLLOWING REVERSIBLE ELECTRON TRANSFER

MICHAEL L. OLMSTEAD AND RICHARD S. NICHOLSON*
Chemistry Department, Michigan State University, East Lansing, Michigan (U.S.A.)
(Received July 6th, 1966)

INTRODUCTION

Stationary electrode polarography (cyclic voltammetry) is finding wide application in the investigation of electrolysis mechanisms, and in particular in detection of the presence of coupled chemical reactions. The detection of coupled reactions is especially facilitated by application of diagnostic criteria developed on the basis of recent theoretical calculations for stationary electrode polarography[1]. In addition to providing diagnostic information, in some cases these criteria permit quantitative evaluation of the rates of coupled reactions[2]. Essentially all of these theoretical calculations, however, have been based on equations for linear diffusion. From an experimental point of view, applications of stationary electrode polarography frequently involve use of a hanging mercury drop electrode, or slowly dropping D.M.E., and in these cases differences between theory and experiment may be expected. Therefore, it appeared important to examine the theory of stationary electrode polarography for the case of a coupled chemical reaction and a model based on spherical diffusion, to determine quantitatively the effects of electrode geometry.

The mechanism chosen for investigation was the case in which a chemical reaction deactivates the initially-formed product of the electron transfer. This mechanism is of general interest and, moreover, is readily amenable to study with stationary electrode polarography[3]. Thus, in addition to diagnostic criteria, an extremely convenient method has been presented for determining the rate constant of the succeeding reaction simply by measuring the ratio of anodic to cathodic peak currents[1,4].

Attempts to evaluate the effects of electrode geometry on stationary electrode polarography were directed along two lines: the determination of the influence of sphericity on diagnostic criteria and on the correlation between the ratio of anodic to cathodic peak currents used to measure rate constants. The latter point seemed particularly important because of the usefulness of the method and recent experiments which indicated the importance of sphericity, especially in measuring anodic peak currents[5].

* To whom correspondence should be addressed.

THEORY

We assume the following mechanism

$$O + ne \rightleftarrows R \qquad \text{I}$$

$$R \xrightarrow{k_f} Z \qquad \text{II}$$

System I is reversible (Nernstian) and species O, R, and Z are soluble in the solution phase. The homogeneous chemical reaction (System II) having rate constant, k_f, is assumed to be first-order (or pseudo-first-order) and irreversible.

Boundary value problem

Diffusion to a spherical electrode is assumed to be the only means of mass transport, and thus Fick second-law equations for a stationary sphere may be applied to substances O and R. It is convenient to write these differential equations in the following dimensionless form

$$\frac{\partial U(z,y)}{\partial y} = \phi^2 \frac{\partial^2 U(z,y)}{\partial z^2} \qquad (1)$$

$$\frac{\partial V(z,y)}{\partial y} = \phi^2 \frac{\partial^2 V(z,y)}{\partial z^2} - \psi V(z,y) \qquad (2)$$

Terms in eqns. (1) and (2) have the following definitions

$$y = at \qquad (3)$$

$$z = r/r_0 \qquad (4)$$

$$\psi = k_f/a \qquad (5)$$

$$\phi = \sqrt{D}/r_0\sqrt{a} \qquad (6)$$

$$U = z(C_O/C_O^* - 1) \qquad (7)$$

$$V = -z(C_R/C_O^*) \qquad (8)$$

There, C represents concentration as a function of radial distance, r, from the center of a sphere of radius, r_0, and time, t. C_O^* is the initial concentration of O and the parameter a is defined as

$$a = nFv/RT \qquad (9)$$

where v is the scan rate, dE/dt, and other terms have their usual significance[1].

Usual initial and boundary conditions are assumed to hold

$$y = 0,\ z \geq 1 \qquad U = 0; \quad V = 0 \qquad (10)$$

$$y \geq 0,\ z \to \infty \qquad U \to 0; \quad V \to 0 \qquad (11)$$

$$y \geq 0,\ z = 1 \qquad \frac{\partial U}{\partial z} - U = \frac{\partial V}{\partial z} - V \qquad (12)$$

$$\frac{U+1}{-V} = \begin{cases} \theta \exp(-y) & y \leq a\lambda \\ \theta \exp(y-2a\lambda) & y > a\lambda \end{cases} \tag{13}$$

$$= \theta S_{a\lambda}(y) \tag{14}$$

Equation (14) represents the Nernst equation with the triangular-wave potential variation characteristic of stationary electrode polarography included. Thus, λ is the time at which the direction of potential variation is reversed, and θ is $\exp[(nF/RT)-(E_i-E^0)]$, where E_i is the initial potential of the triangular wave. A detailed derivation of boundary condition (14) has been given previously[1].

It is apparent from the formulation of the preceding boundary value problem that current–potential curves will depend on the two variables, ψ and ϕ, defined by eqns. (5) and (6). ψ is a kinetic parameter involving the rate constant, k_t, and scan rate, v; ϕ is a spherical parameter involving the radius, r_0, and scan rate.

Whereas ψ may assume any finite value, the parameter, ϕ, seldom exceeds 0.1 for reasonable experimental conditions[1]. Thus, discussions that follow are restricted to values of ϕ in the range $0 < \phi < 0.1$.

Conversion of boundary value problem to integral equations

With the aid of Laplace transforms and the convolution theorem[6] the boundary value problem may be solved for the surface values of U and V in terms of the surface fluxes of U and V. Equations (12) and (13) are used to eliminate the surface values of U and V, which results in the following linear integral equations

$$1 - \int_0^y \frac{\omega(x)\mathrm{d}x}{\sqrt{y-x}} = \theta S_{a\lambda}(y) \int_0^y \frac{\zeta(x) \exp\{-\psi(y-x)\}\,\mathrm{d}x}{\sqrt{y-x}} \tag{15}$$

$$\omega(y) - \zeta(y) = \frac{\phi}{\sqrt{\pi}} \int_0^y \frac{[\zeta(x) \exp\{-\psi(y-x)\} - \omega(x)]\,\mathrm{d}x}{\sqrt{y-x}} \tag{16}$$

The following definitions apply to eqns. (15) and (16)

$$\omega(y) = \frac{\phi}{\sqrt{\pi}} \left(\frac{\partial U}{\partial z}\right)_{z=1} \tag{17}$$

$$\zeta(y) = \frac{\phi}{\sqrt{\pi}} \left(\frac{\partial V}{\partial z}\right)_{z=1} \tag{18}$$

Solution of eqns. (15) and (16) provides values of $\omega(y)$ and $\zeta(y)$. Equations (12), (14), (17), and (18) relate $\omega(y)$ and $\zeta(y)$ to the current function, $\chi(y)$

$$\chi(y) = \frac{\omega(y) + \theta S_{a\lambda}(y)\zeta(y) + (\phi/\sqrt{\pi})}{1 + \theta S_{a\lambda}(y)} \tag{19}$$

The current function, $\chi(y)$, is directly proportional to current

$$i = nFA\sqrt{aD}\, C_0^* \sqrt{\pi}\, \chi(y) \tag{20}$$

Alternatively, the boundary value problem may be solved directly for surface concentrations of O and R. The derivation is similar to that given elsewhere[7,8], and results in the following linear integral equation in the unknown function, $\chi(y)$

$$1 - \int_0^y \chi(x)K(y-x)\,dx = \theta S_{a\lambda}(y) \int_0^y \chi(x)K(y-x)\exp\{-\psi(y-x)\}dx \qquad (21)$$

The kernel of eqn. (21) is defined as

$$K(y-x) = 1/\sqrt{y-x} - \sqrt{\pi}\,\phi \exp\{\phi^2(y-x)\}\,\mathrm{erfc}(\phi\sqrt{y-x}) \qquad (22)$$

where erfc denotes the complement of the error function.

Solution of integral equations

It can readily be shown that the following is a solution of eqn. (21)

$$\sqrt{\pi}\,\chi(y) = \sum_{j=1}^{\infty} \frac{(-1)^{j+1}\prod_{i=1}^{j}(\phi+\sqrt{\psi+i})\exp[(-jnF/RT)(E-E^0)]}{\prod_{i=1}^{j-1}(\phi+\sqrt{i})} \qquad (23)$$

For $\phi = 0$, eqn. (23) is identical with the result obtained previously for the case of a succeeding reaction and linear diffusion[1].

Equation (23) can be used to evaluate $\sqrt{\pi}\,\chi(y)$ for potentials anodic of E^0. For potentials cathodic of E^0, the series diverges and may not be used. Therefore, to calculate complete current–potential curves, it is necessary to solve the integral equations derived above. Although these integral equations cannot be solved analytically, because they are dimensionless, they may be solved numerically without loss of generality. Because of the complex form of the kernel of eqn. (21), we chose to solve eqns. (15) and (16) simultaneously, and have used the numerical method of HUBER[9]. This method has been used previously by GOKHSHTEIN AND GOKHSHTEIN to solve simultaneous integral equations[10,11], and recently DE VRIES[12] has outlined the specific manner of application of HUBER's method. To solve eqns. (15) and (16), an integration increment of 0.2 was used and values of $\sqrt{\pi}\,\chi(y)$ are accurate to ± 0.002. All calculations were performed with the Michigan State University Control Data 3600 digital computer.

To present results of numerical calculations in a manner directly related to real systems, in some cases it was convenient to define a new variable directly related to experimentally measurable parameters. Thus, by elimination of a between the spherical and kinetic parameters, a new variable, ϱ, is obtained

$$\varrho = \phi^2/\psi = D/r_0^2 k_f \qquad (24)$$

In this way, calculations performed for various values of ϕ and ψ, with ϱ held constant, reflect the manner in which experimental observables such as peak potential and peak current vary with scan rate.

RESULTS OF CALCULATIONS

Single scan method

Spherical corrections. It would be especially convenient if existing theoretical data for linear diffusion could be corrected simply for effects of sphericity. In some cases this can be done readily. For example, for values of $\psi \leq 0.01$, eqn. (23) reduces to

the form given previously for reversible electron transfer at a spherical electrode[1]. Therefore, for this case the spherical correction term derived in closed form by REINMUTH[13] is directly applicable.

For large values of ψ (greater than *ca.* 10) eqn. (23) becomes

$$\sqrt{\pi}\,\chi(y) = \sum_{j=1}^{\infty} \frac{(-1)^{j+1}(\sqrt{\pi})^{j} \exp[(-jnF/RT)(E-E^{0}-(RT/nF)\ln\sqrt{\psi/\pi})]}{\prod_{i=1}^{j-1}[\phi+\sqrt{i}]} \qquad (25)$$

which is of the same form as that given by REINMUTH for the case of totally irreversible charge transfer at a spherical electrode[14]. Therefore, for this limiting case the empirical spherical correction previously tabulated is directly applicable (ref. 1, Table III).

It is interesting to note that for the conditions under which eqn. (25) is applicable, kinetic and spherical effects are separable. Thus, it can be seen from eqn. (25) that the only effect of the kinetic parameter, ψ, is to determine the position of the polarographic wave on the potential axis. However, the spherical parameter, ϕ, primarily affects the magnitude of the current, and causes only minor variations in the potential dependence of the wave.

Spherical correction data for values of ψ not included in the range discussed above — *i.e.*, $0.01 < \psi < 10$ — cannot be obtained from existing tabulations. However, within this range of ψ, values of the current function $\sqrt{\pi}\,\chi(y)$ for the case of linear diffusion have been given previously (ref. 1, Table X). Therefore, an attempt was made to develop accurate spherical corrections in the range $0.01 < \psi < 10$ which could be applied directly to the existing plane electrode data.

A number of theoretical curves were calculated for relevant values of ϕ and ψ, and it was found that the spherical correction (relative to a plane electrode) differed from REINMUTH's correction[13] by a function of potential which accurately could be expressed in the form

$$\frac{\alpha\phi+\beta}{\exp[\gamma(n(E-E^{0})+E_{s})^{2}]} \qquad (26)$$

There, α, β, γ and E_s are empirically-determined constants for given values of the kinetic parameter. The pre-exponential term containing α and β yields the maximum value of this correction.

With the aid of (26) the current function for a spherical electrode may be written

$$\sqrt{\pi}\,\chi(\text{sphere}) = \sqrt{\pi}\,\chi(\text{plane}) + \phi\left[\frac{1}{1+\exp[(nF/RT)(E-E^{0})]} + \frac{\alpha\phi+\beta}{\exp[\gamma(n(E-E^{0})+E_{s})^{2}]}\right] \qquad (27)$$

for $0.01 < \psi < 10$.

Table I gives the empirical constants for use with eqn. (27). Values of $\sqrt{\pi}\,\chi$(sphere) calculated from eqn. (27) and Table I are accurate to ± 0.002

Diagnostic criteria. An important application of stationary electrode polarography involves the use of diagnostic criteria. Because sphericity may effect quanti-

tative application of these criteria, it is important to evaluate effects of spherical geometry.

Three diagnostic criteria have been proposed previously[1] and all of these are based on variations with scan rate of the experimentally observable parameters, peak current, peak potential, and the ratio of anodic to cathodic peak currents. The first two of these criteria are discussed in this section, and a discussion of the third is implicit in the section on the cyclic method.

TABLE 1

EMPIRICAL CONSTANTS FOR SPHERICAL CORRECTION OF SINGLE SCAN DATA

ψ	α	β	$\gamma \cdot 10^4$	E_s (mV)
0.05	−0.0058	0.0057	2.989	51.9
0.20	−0.0218	0.0218	3.283	48.5
0.50	−0.0481	0.0504	3.912	40.5
1.00	−0.0797	0.0907	4.292	34.4
1.60	−0.1095	0.1267	4.743	28.0
4.00	−0.1480	0.2238	5.353	16.6
10.00	−0.2080	0.3403	4.808	5.5

Variation of $i_p/\sqrt{v}$ (or equivalently, current function $\sqrt{\pi}\,\chi(y)$) with scan rate has been described previously for linear diffusion[1]. There it was shown that $\sqrt{\pi}\,\chi(y)$ varies between the limit corresponding to uncomplicated reversible electron transfer at high scan rates (small ψ) and the limit corresponding to totally irreversible charge transfer at low scan rates (large ψ). For linear diffusion these limits are independent of scan rate. However, under the influence of spherical diffusion both limits are subject to increases at low scan rates. This behavior is illustrated in Fig. 1 where peak current

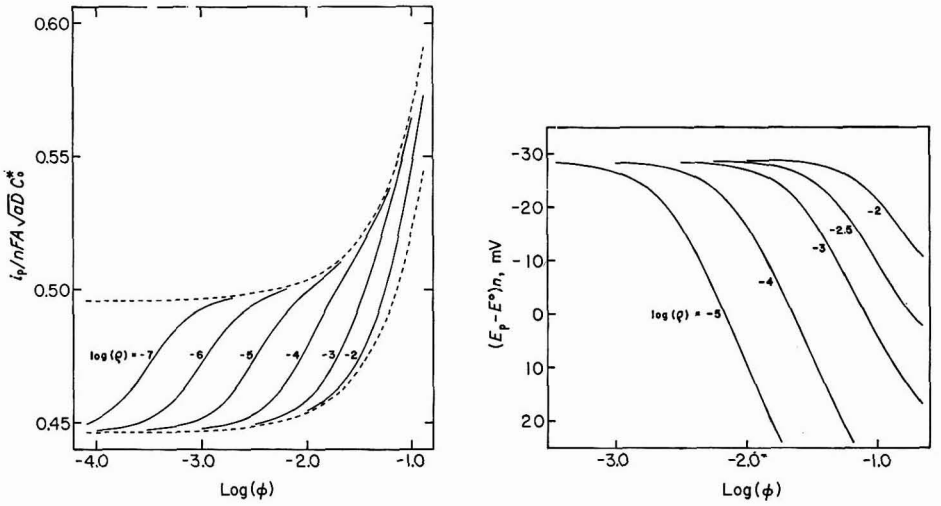

Fig. 1. Variation of peak current function with ϕ. Dashed curves are reversible and irreversible limits.

Fig. 2. Variation of peak potential with ϕ.

functions for constant values of ϱ are plotted *versus* the logarithm of ϕ*. The upper and lower dashed curves are the limiting values of the current function for a spherical electrode. The solid curves of Fig. 1 show the combined influence on peak current functions of sphericity and the kinetic process. Thus, for large values of ϕ and ϱ the curves rise more sharply from the reversible limit to the irreversible limit than for the case of linear diffusion. This effect becomes important to the correct interpretation of diagnostic criteria when ϱ is larger than about 10^{-4}, or for typical values of diffusion coefficient and electrode radius, a value of k_f smaller than about 20 sec^{-1}.

The trends exhibited in Fig. 1 are qualitatively similar to those of the catalytic case as scan rate is decreased (ref. 1, Fig. 17). Ambiguities between these two mechanisms, however, may be resolved by application of the other diagnostic criteria.

Sphericity also affects variations of peak potential with scan rate, but to a lesser extent, because effects of electrode geometry are manifested primarily as variations of current rather than position of the polarographic wave on the potential axis. This fact is illustrated in Fig. 2 where peak potential is plotted *versus* ϕ for typical values of ϱ. Thus, all the curves of Fig. 2 have essentially the same shape, and the magnitude of ϱ merely determines the scan rate at which deviations from the reversible limit become apparent. Nevertheless, some minor variations do result for sufficiently large values of ϱ, where the curves of Fig. 2 are no longer strictly linear. In addition, for large values of ϱ the slopes of the curves in the nearly linear portions are less than the $30/n$ mV expected for linear diffusion[1].

Because peak potential variations are relatively insensitive to electrode geometry, interpretation of diagnostic criteria based on peak potential variations may be made without regard to electrode geometry. It is expected that this result would be generally true for electrolysis mechanisms other than the one considered here.

Cyclic triangular wave method

Figure 3 illustrates the effect of electrode geometry on cyclic stationary electrode polarograms. The curves of Fig. 3 were calculated for a fixed value of the kinetic parameter ($\psi = 0.1$) and two values of the spherical parameter ($\phi = 0.0, 0.1$). It can be seen from Fig. 3 that sphericity causes a major effect on the cathodic portion of the curves in the manner already discussed. Effects of sphericity on the anodic curves are much less pronounced, because there the predominant factor is loss of R through kinetics rather than spherical diffusion. Thus, measurements involving a ratio of anodic to cathodic peaks will show significant differences between planar and spherical electrodes. This fact is especially important because the most convenient method of quantitatively measuring rate constants involves this ratio. Thus, it has been shown for linear diffusion that the ratio of anodic to cathodic peak currents, i_a/i_c, depends only on a single parameter, $k_f\tau$ (τ is the time from E^0 to the switching potential, E_λ), provided the anodic currents are measured to the extension of the cathodic curve[1]. Therefore, for linear diffusion, rate constants can be measured with the aid of a single working curve relating i_a/i_c to $k_f\tau$. A similar correlation would be expected for spherical electrodes, but in view of the preceding discussion of Fig. 3, a marked dependence of the working curve on sphericity would be expected. Moreover, because sphericity affects the baseline for measuring anodic peak current (dashed

* Because ϕ is proportional to scan rate, this is equivalent to a plot of $i_p/\sqrt{v}$ *vs.* v.

curves of Fig. 3) more than the anodic peak current, ratios of i_a/i_c at constant $k_f\tau$ should be larger for spherical electrodes than for planar electrodes.

To test these ideas, cyclic polarograms were calculated for various values of $k_f\tau$ with ϕ held constant. As expected, current ratios calculated in this manner were independent of switching potential provided E_λ was between 90 and 150 mV cathodic of E^0. Thus, the procedure described previously for plane electrodes[1] may be used for spherical electrodes provided a suitable family of working curves is employed. Accurate data for construction of these curves are presented in Table 2.

It should be pointed out that to use the data of Table 2, only reasonably accurate estimates of the spherical parameter are required. For example, if $k_f\tau$ is 1.0 and the spherical parameter is 0.1, an uncertainty of 20% in the spherical parameter

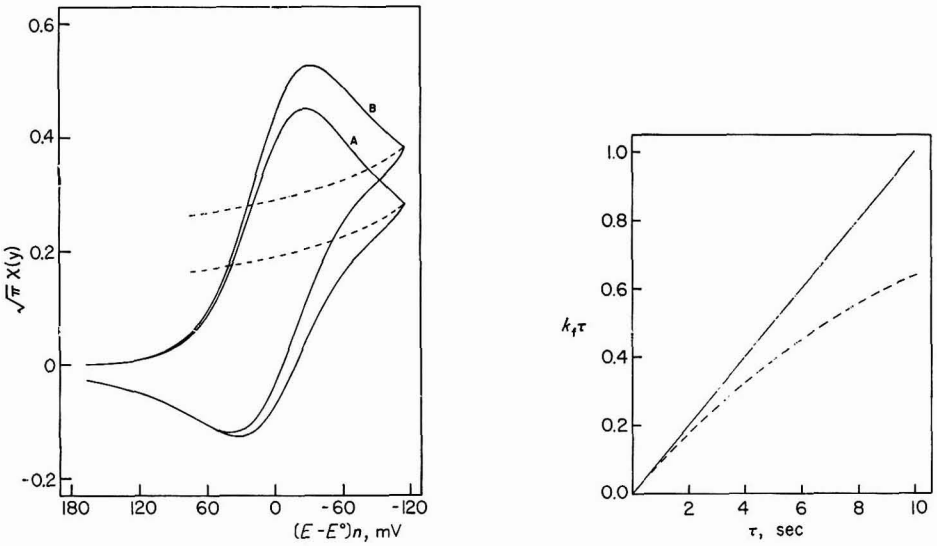

Fig. 3. Cyclic polarograms showing effect of sphericity. (A), $\psi=0.1$, $\phi=0.0$; (B), $\psi=0.1$, $\Phi=0.1$. Dashed curves are extensions of cathodic scans.

Fig. 4. Variation of $k_f\tau$ with τ for: $k_f = 0.1\ \text{sec}^{-1}$, $\varrho = 0.04$, $n(E_\lambda - E^0) = -115$ mV.

TABLE 2

RATIO OF ANODIC TO CATHODIC PEAK CURRENTS

	ϕ					
$k_f\tau$	*0.001*	*0.020*	*0.040*	*0.060*	*0.080*	*0.100*
0.01	0.989	0.990	0.990	0.991	0.991	0.992
0.10	0.904	0.909	0.914	0.918	0.922	0.926
0.20	0.824	0.833	0.842	0.850	0.857	0.864
0.35	0.727	0.740	0.753	0.765	0.777	0.787
0.50	0.651	0.668	0.684	0.699	0.713	0.726
0.65	0.591	0.610	0.629	0.647	0.663	0.678
0.85	0.529	0.551	0.572	0.592	0.611	0.628
1.05	0.483	0.507	0.530	0.552	0.572	0.591
1.25	0.448	0.473	0.498	0.521	0.542	0.562
1.50	0.416	0.442	0.468	0.492	0.514	0.535

will result in a 10% error in $k_f\tau$, and for $k_f\tau$ less than 1.0 the error always will be less than 10%. For values of the spherical parameter less than 0.1, the errors are correspondingly less.

It is interesting to note the direction and magnitude of errors that would occur if effects of sphericity were ignored in calculating rate constants. To evaluate these effects quantitatively, current ratios were calculated from the data of Table 2 for $k_f = 0.1$ sec^{-1} and typical values of other experimental parameters. These current ratios were then used to calculate the apparent values of $k_f\tau$ that would be measured if the working curve for a plane electrode were used. Figure 4 shows the results of these calculations. The solid line is the relationship obtained for a spherical electrode, and the slope is the true value of k_f. The dashed curve illustrates the behavior obtained if sphericity is neglected. Thus, apparent rate constants calculated from plane electrode theory will be smaller than the true rate constant, and plots similar to Fig. 4 will display curvature due to variations of the spherical parameter with scan rate.

ACKNOWLEDGEMENT

Support of this work by the National Science Foundation is gratefully acknowledged.

SUMMARY

Theory of stationary electrode polarography was developed for the case of spherical diffusion and a chemical reaction following reversible electron transfer. An empirical spherical correction based on these theoretical calculations and applicable to existing plane electrode data is presented. In addition, results of theoretical calculations indicate that interpretations of diagnostic criteria based on variations of peak current with scan rate must in general take account of effects of sphericity. However, criteria based on peak current ratios or peak potential variations with scan rate show negligible effects of sphericity, and therefore in many cases use of these latter diagnostic tests may be preferable. Finally, accurate data are presented which permit calculation of homogeneous rate constants from measurements with a spherical electrode of anodic to cathodic peak current ratios.

REFERENCES

1 R. S. NICHOLSON AND I. SHAIN, *Anal. Chem.*, 36 (1964) 706.
2 R. S. NICHOLSON AND I. SHAIN, *Anal. Chem.*, 37 (1965) 190.
3 D. G. DAVIS AND D. J. ORLERON, *Anal. Chem.*, 38 (1966) 179.
4 R. S. NICHOLSON, *Anal. Chem.*, 38 (1966) 1406.
5 M. L. OLMSTEAD AND R. S. NICHOLSON, *Anal. Chem.*, 38 (1966) 150.
6 W. H. REINMUTH, *Anal. Chem.*, 34 (1962) 1446.
7 P. DELAHAY AND G. MAMANTOV, *J. Am. Chem. Soc.*, 76 (1954) 5323.
8 H. D. HURWITZ, *J. Electroanal. Chem.*, 7 (1964) 368.
9 A. HUBER, *Monatsh. Mathematik und Physik*, 47 (1939) 240.
10 YA. P. GOKHSHTEIN AND A. YA. GOKHSHTEIN, *Dokl. Akad. Nauk SSSR*, 128 (1959) 985.
11 YA. P. GOKHSHTEIN AND A. YA. GOKHSHTEIN, *Advances in Polarography*, edited by I. S. LONGMUIR, Vol. II, Pergamon Press, New York, 1960, p. 465.
12 W. T. DE VRIES, *J. Electroanal. Chem.*, 9 (1965) 448.
13 W. H. REINMUTH, *J. Am. Chem. Soc.*, 79 (1957) 6358.
14 W. H. REINMUTH, *Anal. Chem.*, 33 (1961) 1793.

ELECTROANALYTICAL CHEMISTRY AND INTERFACIAL ELECTROCHEMISTRY
Elsevier Publishing Company, Amsterdam – Printed in The Netherlands

THE ANODIC RISE OF CAPACITY AT A MERCURY ELECTRODE IN FLUORIDE ION SOLUTIONS

R. D. ARMSTRONG, W. P. RACE AND H. R. THIRSK
Department of Physical Chemistry, University of Newcastle upon Tyne, Newcastle upon Tyne, 1 (England)
(Received July 22nd, 1966)

GRAHAME[1] first observed a steep rise in the capacity of a mercury electrode in sodium fluoride solutions at anodic potentials. FRUMKIN *et al.*[2], having prepared solutions in Teflon and platinum apparatus, suggested that this rise was due to the adsorption of silicofluoride ions derived from the attack of the glass vessels used by GRAHAME. Other possible explanations were subsequently considered by MOTT AND WATTS-TOBIN[3]. The most important of these attributed the effect to:

(a) mercurous adions;
(b) specific adsorption of hydroxyl ions;
(c) specific adsorption of fluoride ions;
(d) an electrochemical reaction.

The most recent work by PAYNE[4] showed that the potential at which the rise was observed was reversibly dependent on the pH, and he attributed this dependence to the adsorption of hydroxyl or carbonate ions.

Work carried out in these laboratories[5] has shown that on anodic polarisation of mercury in sodium hydroxide solution, $Hg(OH)_2$ is reversibly formed, giving rise to a faradaic pseudo-capacity. It seemed possible that a similar process occurred in fluoride ion solutions.

EXPERIMENTAL

Impedance measurements were made using a hanging mercury drop electrode and a smooth cylindrical platinum counter electrode. The size of the drop was controlled by a precision micro-syringe; a capillary of 0.15-mm bore diam. was used. The electrode was filled by suction, care being taken to exclude air from the capillary. The reproducibility of the drop area for a drop of $4 \cdot 10^{-2}$ cm^2 was within 1%.

Measurements were made at $25.5 \pm 0.2°$ in a Pyrex cell which incorporated a gas-lift device[6] to circulate the solution through purified charcoal. This purification was employed until no appreciable time-dependence of the measured impedance was observed.

All solutions were made up in triply-distilled water with AnalaR reagents. Mercury was purified by treatment with nitric acid, and distilled twice *in vacuo*.

The cell impedance was measured by an a.c. bridge, similar to that used by SLUYTERS[7], incorporating series resistance and capacitance decades in the measuring arm, resistive ratio arms, and a Wagner earthing system to eliminate the effect of

stray capacitance to earth. The accuracy of impedance measurement was better than 0.1% between 700 and 10000 c/sec; at lower frequencies the sensitivity was reduced, and at frequencies above 50 kc/sec, residual inductance in the components of the ratio and measuring arms became the predominant source of error. The polarising potential was applied across the bridge diagonal, the potential of the mercury drop being measured with respect to a saturated calomel electrode connected to the cell solution by means of a saturated ammonium nitrate salt bridge to minimise liquid junction potentials (except for the measurements with sodium hydroxide solutions when a mercury–mercuric oxide electrode in the same solution was employed).

RESULTS AND DISCUSSION

1 M NaOH solution

The electrode impedance was found to be purely capacitative between potentials corresponding to sodium deposition and that at which the faradaic impedance due to the dissolution of the mercury as $Hg(OH)_2$ became appreciable (about -100 mV with respect to Hg/HgO) as has been observed previously. In this anodic potential region, double-layer capacity (C_{dl}), and solution resistance (R_{so}) measurements were made at a frequency of 25 kc/sec, since (because the concentration of $Hg(OH)_2$ is less than $2 \cdot 10^{-4}$ M throughout) the current essentially bypasses the faradaic path at this frequency.

Cell impedance measurements were made at fixed potentials between -50 and -10 mV (on Hg/HgO) at a series of frequencies from 1000–200 c/sec. The measured resistance (R_s) and capacitance (C_s) values were then analysed after the method of RANDLES[8]. The electrode impedance was first found by subtracting R_{so}, and was expressed in terms of the equivalent parallel values of resistance (R_p) and capacitance (C_p), from which C_{dl} was subtracted. Finally the series values, R_{sf} and C_{sf}, due to the faradaic impedance alone, were calculated. These quantities should, ideally, obey the relationships[9]

$$R_{sf} = \sigma/\omega^{\frac{1}{2}} C_0 + R_{ct} \tag{1}$$

$$1/\omega C_{sf} = \sigma/\omega^{\frac{1}{2}} C_0 \tag{2}$$

Where $\sigma = (RT/n^2F^0)\ 1/2.303\sqrt{2}D^{\frac{1}{2}}$, D is the diffusion coefficient in $cm^2\ sec^{-1}$, ω the angular frequency in radians/sec, C_0 the concentration of the dissolving species in M and R_{ct} the charge-transfer resistance in $\Omega\ cm^2$.

Relationships (1) and (2) are tested in Fig. 1 which shows that they are obeyed within experimental error, and also that R_{ct} is small so that the exchange current, i_0, for the reaction is greater than 60 mA cm^2 at -30 mV (Hg/HgO). The slope of Fig. 1 yields the concentration of the dissolving species, and since this concentration shows a 30 mV/decade dependence on potential (Fig. 2), this is consistent with the view expressed earlier that the complex is $Hg(OH)_2$. The observed concentrations are also in good agreement with stability constant data[10].

The hydroxyl-ion concentration dependence of the complex has been treated earlier[5]. Finally, it is interesting to compare C_{dl} with C_s measured at 1000 c/sec (Fig. 3).

Thus it appears that part of the steep anodic rise in capacity observed at

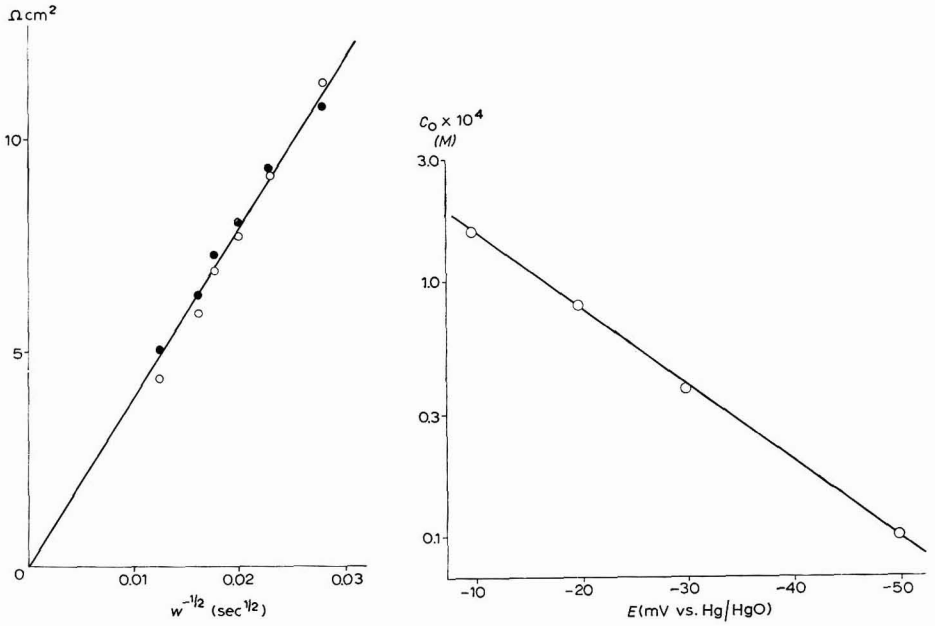

Fig. 1. 1 *M* NaOH. Variation of: (○), R_{sf}; (●), $(\omega C_{sf})^{-1}$ with $\omega^{-\frac{1}{2}}$ at 30 mV (Hg/HgO).

Fig. 2. Potential-dependence of $Hg(OH)_2$ concn. in 1 *M* NaOH.

1000 c/sec arises from the faradaic pseudo-capacity associated with the reversible dissolution of mercury as $Hg(OH)_2$.

0.9 M NaF solution

Small quantities of concentrated solution of hydrofluoric acid or sodium hydroxide were added to the neutral solution to give various measured pH-values at each of which C_{dl} was measured as before (Fig. 4).

The solution has appreciable buffer capacity only when the pH is near the pK of hydrofluoric acid, *viz.*, 3.17, so that at higher pH-values at anodic potentials, the formation of $Hg(OH)_2$ would produce local pH changes at the electrode, probably causing the insensitivity to pH of the anodic rise of C_s in solutions of pH 5–9. The formation of $Hg(OH)_2$ at anodic potentials was demonstrated by making faradaic impedance measurements as before in solutions of pH 5–7 (Fig. 5). Since the formation of OH^- ions from water is rapid, there is no restriction on the dissolution of mercury as $Hg(OH)_2$ even though the concentration of OH^- is low.

DE LEVIE[11] has shown that when R_{ct} is negligible, a graph of C_p against $(\omega R_p)^{-1}$ is linear with unit slope, with an intercept of C_{dl}. When such a test applied to our results gave a good straight line, values of the concentration of the complex were computed directly from the parallel circuit values after subtraction of C_{dl}.

The fact that the intercepts of such plots (Fig. 6) agree closely with the measured 25 kc/sec capacity confirms that, at this frequency, the observed capacity is essentially C_{dl}.

Measurements of faradaic impedance in sodium fluoride solutions were rather

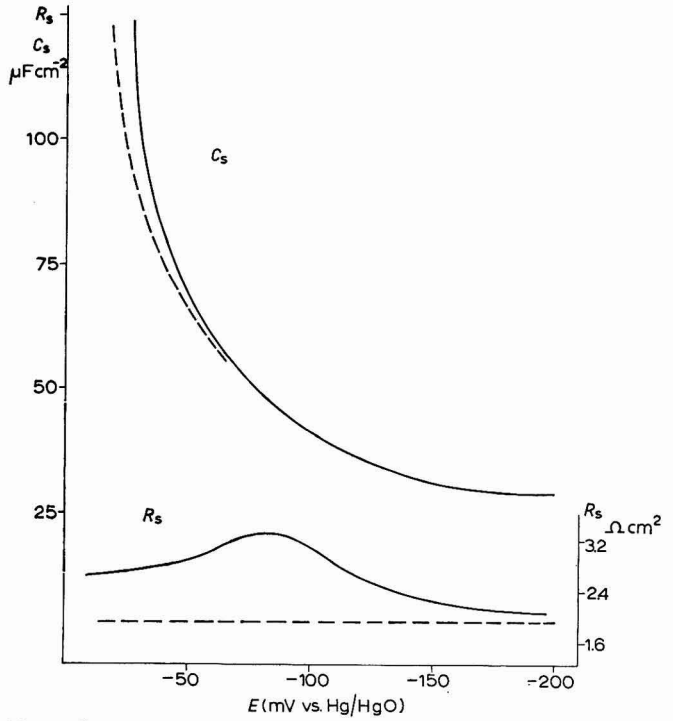

Fig. 3. Comparison of the potential-dependence of R_s and C_s in 1 M NaOH at: (—), 1; (– –), 25 kc/sec.

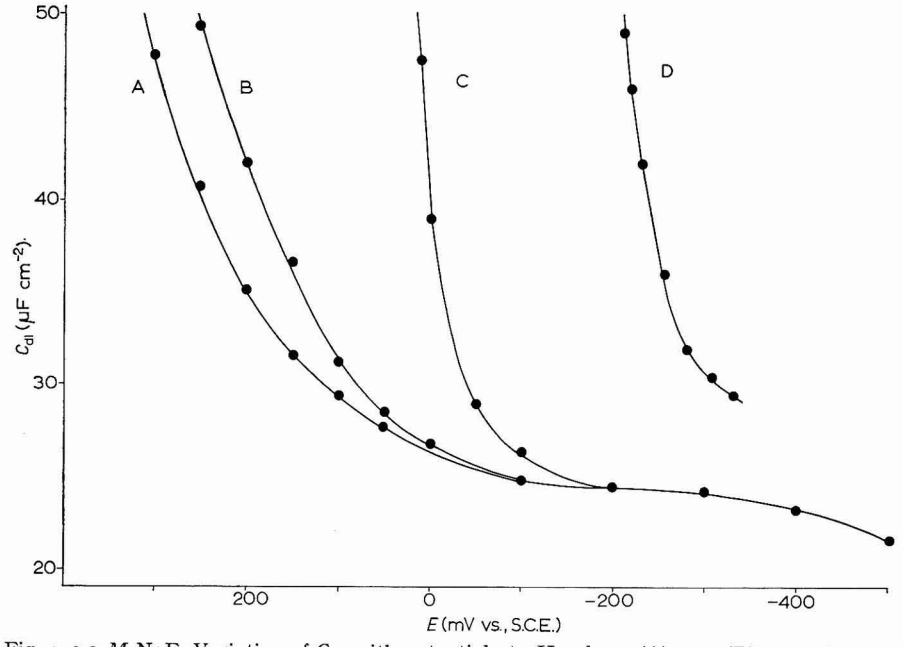

Fig. 4. 0.9 M NaF. Variation of C_{dl} with potential at pH-values: (A), 5.1; (B), 9.1; (C), 11. (D), corresponding curve for 1 M NaOH.

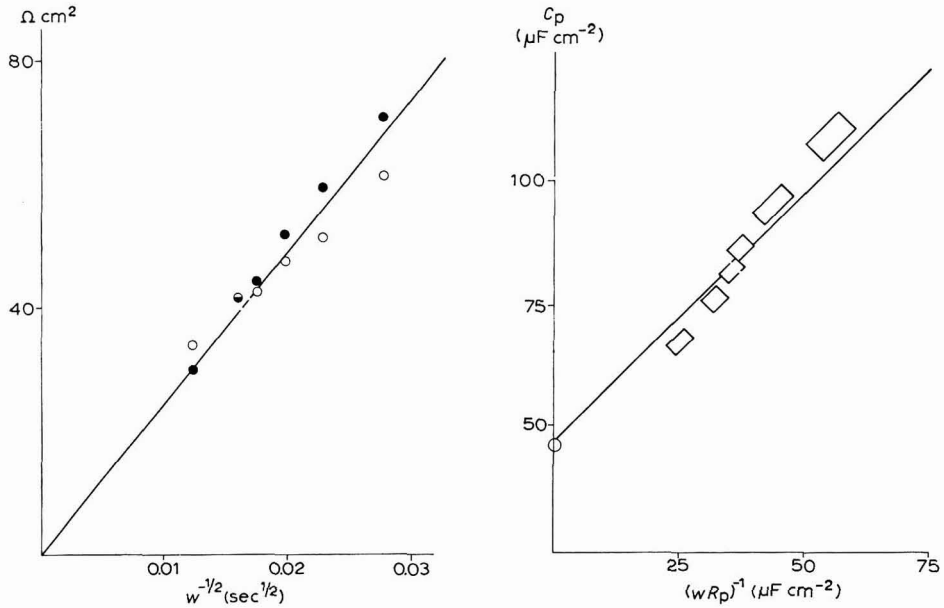

Fig. 5. 0.9 *M* NaF, pH 7.3. Variation of: (○), R_{sf}; (●), $(\omega C_{sf})^{-1}$ with $\omega^{-\frac{1}{2}}$ at 270 mV (S.C.E.).

Fig. 6. Variation of C_p with $(\omega R_p)^{-1}$ in 0.9 *M* NaF, pH 7.3 at 270 mV (S.C.E.). Error shown corresponds to $\pm 3\%$ in R_s and C_s.

TABLE 1

COMPARISON OF EXPERIMENTAL AND CALCULATED VALUES (FROM STABILITY CONSTANT DATA) OF $[Hg(OH)_2]$ IN NaF SOLUTIONS

pH	*Potential (mV, S.C.E.)*	*Observed concn.* $\cdot 10^5$ *(M)*	*Calcd. concn.* $\cdot 10^5$ *(M)*
7.3	230	3.2	3.0
5.95	320	2.8	1.7
5.2	350	2.5	1.1

less accurate than in *M* NaOH and NH_4F, because of the time-dependent adsorption of an unidentified impurity (suspected to be chloride ion) tending to give a rise of C_{dl} with time at anodic potentials. No improvement was noticed after exhaustive charcoal cleaning, or recrystallisation of sodium fluoride under a stream of nitrogen. There was also a pronounced tendency for the mercury thread to break in the more acidic solutions, necessitating the use of smaller drops.

There is still, however, a relationship of approximately 30 mV/decade of concentration of dissolving species at pH 5.2, and the actual values are in fair agreement with those predicted for $Hg(OH)_2$ (Table 1) in view of the difficulty in estimating the reversible potential arising from the local variations in pH occurring at the electrode.

At pH 7.3, the concentration of $Hg(OH)_2$ reaches a limiting value (Fig. 7) as

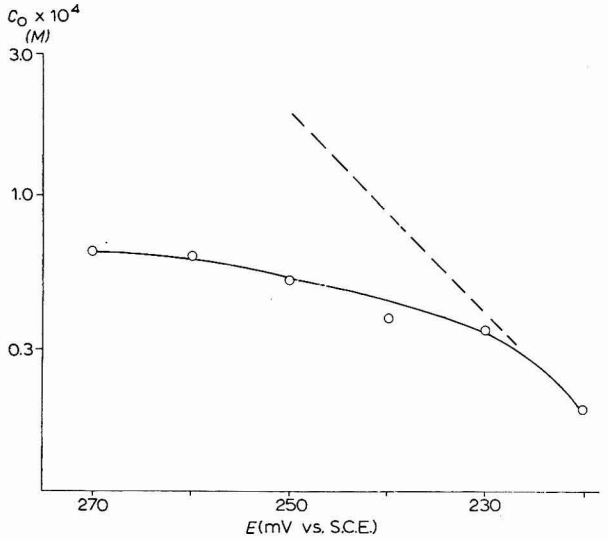

Fig. 7. 0.9 *M* NaF. Potential dependence of $Hg(OH)_2$ concn. at pH 7.3. (Broken line has slope 30 mV/decade.)

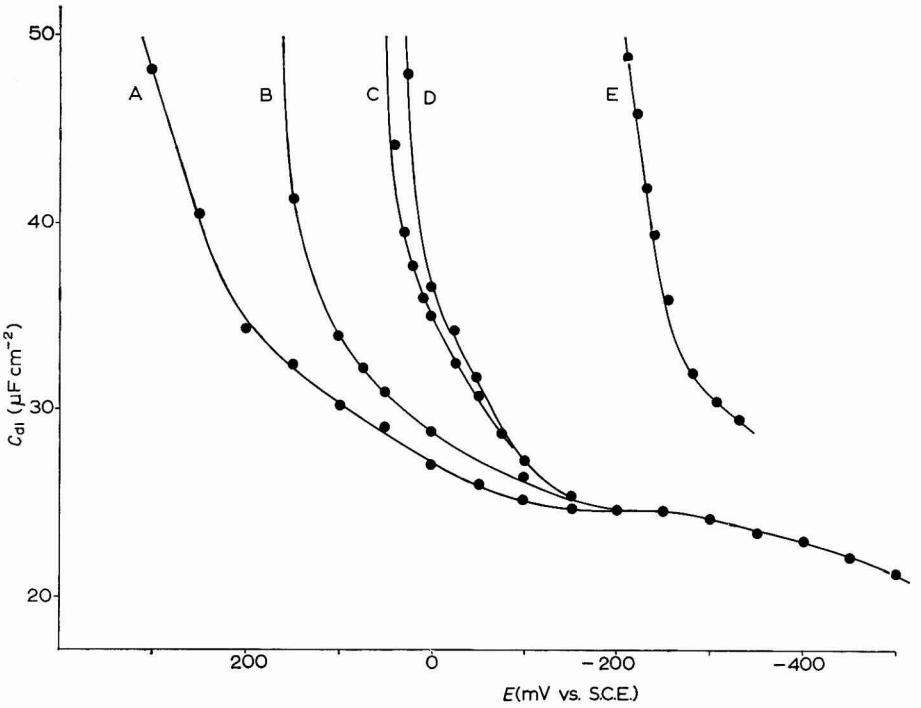

Fig. 8. 1 *M* NH_4F. pH and potential-dependence of C_{dl} at pH-values: (A), 5.1; (B), 6.75; (C), 8.35; (D), 8.75. (E), corresponding curve for 1 *M* NaOH.

the pH at the electrode decreases following further anodic polarisation, thus illustrating the ineffective buffering.

Thus, the nature of the pH-dependence of the anodic rise in capacity has been found to confirm PAYNE's results, the rise being due to a genuine increase in C_{dl}, together with a faradaic pseudo-capacity associated with the dissolution of mercury as $Hg(OH)_2$.

1 M ammonium fluoride solution

This solution has appreciable buffer capacity at the pK of ammonia, *i.e.* at pH 9.25 as well as at pH 3.17. C_{dl}, measured as before, is shown (in Fig. 8) for solutions of pH 5.1, 6.75, 8.35 and 8.75.

The potential at which the anodic rise in capacity becomes pronounced is moved about 60 mV more anodic for unit decrease of pH within the pH-range 5–9. This is also consistent with the pH-dependence of the anodic capacity rise in sodium hydroxide solutions.

Faradaic impedance measurements were made as before in all solutions at anodic polarisation, and the concentration of the dissolving species calculated directly from $C_p - C_{dl}$, and R_p as before (Fig. 9).

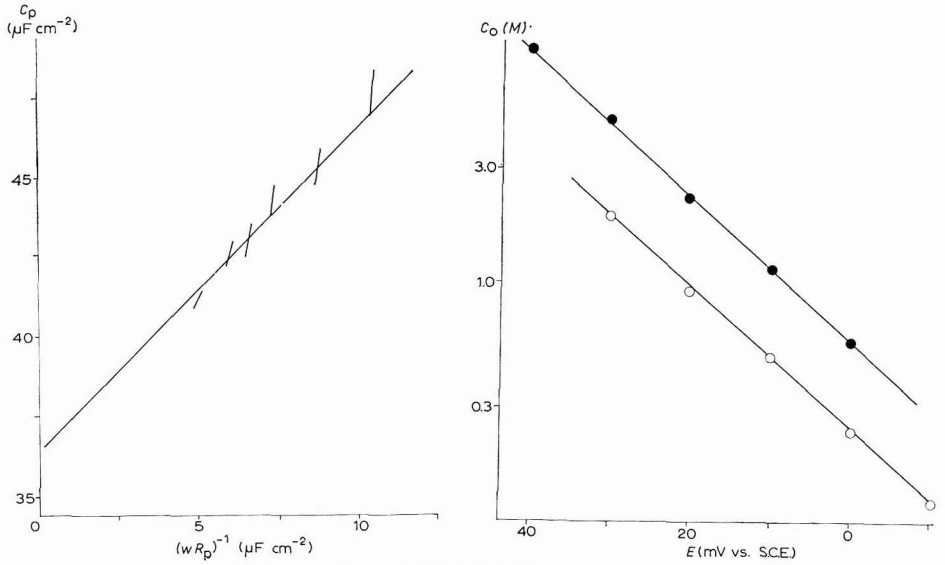

Fig. 9. 1 M NH_4F at pH 8.35 and 10 mV (S.C.E.). Variation of C_p with $(\omega R_p)^{-1}$. Error shown corresponds to $\pm 1\%$ in R_s and C_s.

Fig. 10. Potential-dependence of complex concn. in M NH_4F. (●), pH 8.35 ($C_0 \times 10^5$); (○), pH 8.75 ($C_0 \times 10^4$).

At pH 5.1, the concentration agrees with that predicted from stability constant data for $Hg(NH_3)_2^{2+}$ (Table 2). There was again a tendency for local pH-changes to take place at the electrode, and at some potentials a charge-transfer resistance was found, which necessitated the use of the full Randles procedure to estimate the concentration; this does show an approximate 30 mV/decade relationship with potential.

TABLE 2

COMPARISON OF EXPERIMENTAL, AND CALCULATED (FROM STABILITY CONSTANT DATA) VALUES OF COMPLEX CONCENTRATION IN NH_4F SOLUTIONS

pH	*Potential (mV, S.C.E.)*	*Calcd. complex concn. (M)*				*Total concn. (M)*	*Observed concn. (M)*
		$[Hg(NH_3)_2]^{2+}$	$[Hg(NH_3)_3]^{2+}$	$[Hg(NH_3)_4]^{2+}$	$Hg(OH)_2$		
5.5	170	$1.8 \cdot 10^{-5}$	$3 \cdot 10^{-8}$	negligible	$1.7 \cdot 10^{-11}$	$1.8 \cdot 10^{-5}$	$1.6 \cdot 10^{-5}$
6.75	140	$4.8 \cdot 10^{-4}$	$1.5 \cdot 10^{-5}$	$3 \cdot 10^{-7}$	$5.5 \cdot 10^{-11}$	$4.95 \cdot 10^{-4}$	$1.0 \cdot 10^{-4}$
8.35	30	$1.55 \cdot 10^{-4}$	$1.7 \cdot 10^{-4}$	$1.0 \cdot 10^{-4}$	$1.7 \cdot 10^{-10}$	$4.2 \cdot 10^{-4}$	$4.9 \cdot 10^{-5}$
8.75	30	$7.2 \cdot 10^{-4}$	$1.77 \cdot 10^{-3}$	$2.5 \cdot 10^{-3}$	negligible	$5.0 \cdot 10^{-3}$	$1.9 \cdot 10^{-4}$

At pH 6.75, there was no measurable charge-transfer resistance and concentrations were found which give a 34 mV/decade relationship with potential, probably reaching a limiting value as the pH changes in the ineffectively buffered solution.

Faradaic impedance measurements on solutions of pH 8.35 and 8.75 yielded concentrations showing a 33 mV/decade dependence (Fig. 10) on potential, being rather less than the total concentration predicted from stability constant data for the sum of the concentrations of $[Hg(NH_3)_2]^{2+} + [Hg(NH_3)_3]^{2+} + [Hg(NH_3)_4]^{2+}$ (Table 2). This discrepancy could be explained by the increasing sensitivity of the concentrations to small changes of free ammonia concentration, hence the pH.

Thus the anodic rise of capacity in ammonium fluoride solutions is partly due to a faradaic pseudo-capacity resulting from the dissolution of mercury as complexes, the nature of which depends on the pH of the solution at the electrode surface. There is also, however, a pH-dependent steep rise in C_{dl} in the solution, which, unlike sodium fluoride, has appreciable buffer capacity over a wide range of pH.

It was impracticable to use solutions at the ideally buffered pH 3.17, since attack of the cell and capillary by hydrofluoric acid would result in increasing pH with time, and possible silicofluoride adsorption.

CONCLUSIONS

The double-layer capacity curves for solutions of M NaOH, 0.9 M NaF, and M NH_4F have been determined. It has been shown that C_{dl} can be measured as C_s at 25 kc/sec in the presence of a dissolution reaction, when the concentration of the dissolving species is $\sim 10^{-4} M$.

The pH-dependence of the steep rise of C_{dl} with potential in ammonium fluoride solution demonstrates the adsorption of hydroxyl ion, whereas the slight pH-dependence in sodium fluoride solution can be attributed to the ineffective buffering of the solution at pH 5–9. It is improbable that any specific adsorption of carbonate ion or silicofluoride ion is responsible for the anodic rise of C_{dl}, since the adsorption of a small amount of an impurity at low concentration would lead to time-dependence of the electrode impedance.

At lower frequencies, the anodic rise in C_s is steepened by the pseudo-capacity associated with the reversible dissolution of mercury as $Hg(OH)_2$ in both sodium hydroxide and sodium fluoride, and as various ammonium complexes in ammonium

fluoride. It is possible to evaluate the concentration- and potential-dependence of these complexes by the faradaic impedance method.

APPENDIX I

THE DETECTION OF A REVERSIBLE ELECTROCHEMICAL REACTION FROM MEASUREMENTS OF R_s

It has been observed that when a reversible electrochemical reaction takes place at an electrode surface, there occurs (as well as an increase in C_s) an increase in R_s [4]. The latter effect cannot unambiguously be used to prove the presence of such a reaction since the detection of this change in R_s depends on the following factors:

(a) frequency: such a resistance increase may well become of the order of experimental error at frequencies above 10 kc/sec.

(b) rate of change of C_{dl} with potential;

(c) rate of change R_{ct} with potential.

The combination of the latter two effects often results in a maximum in the R_s–potential curve.

In the case of 1 M NaOH, as the potential is made progressively more anodic the rise in R_s is initially due to the dissolution reaction, but the subsequent fall is due mainly to the rapid increase in C_{dl}.

If in such a case C_{dl} were to increase more rapidly before the onset of dissolution, it is conceivable that the two effects could exactly cancel at a particular frequency, thus a dissolution reaction could take place without producing an increase in R_s. The only unambiguous way of observing an electrochemical reaction by impedance measurements is to analyse the frequency dispersion of R_s and C_s as outlined above.

APPENDIX II

REPRESENTATION OF EXPERIMENTAL ERROR IN DOUBLE-LAYER CAPACITY DETERMINATION AFTER THE METHOD OF DE LEVIE

In the analysis of faradaic impedance values DE LEVIE[11] has shown that when $R_{ct}=0$ a plot of C_p against $(\omega R_p)^{-1}$ is linear with unit slope and intercept, C_{dl}. SLUYTERS[12] has correctly pointed out that with a finite R_{ct} the line extrapolates below the true C_{dl}-value or takes the form of a curve exhibiting decreasing slope as $(\omega R_p)^{-1}$ tends to zero. This leads to an inherent systematic error in determining C_{dl} from this method when R_{ct} is significant.

There has also, however, been some uncertainty in the representation of actual experimental error of the measured values of R_s, C_s in the values of C_p and $(\omega R_p)^{-1}$ constituting the graph of unit slope.

DE LEVIE correctly represented the errors due to his uncertainty in R_p as segments of curves. We have computed the values of C_p and $(\omega R_p)^{-1}$ for a typical situation, taking $f=600$ c/sec, $R_s=100\ \Omega$ and $C_s=1.0\ \mu$F, considering errors of $\pm 5\%$ in the series values, assuming the frequency to be known exactly. The values where one of the components is $\pm 5\%$ in error, fall on the perimeter of an area (Fig. 11) bounded by four segments of curves (in this case almost linear) the corners representing values where both R_s and C_s are $\pm 5\%$ from the chosen values. All points corre-

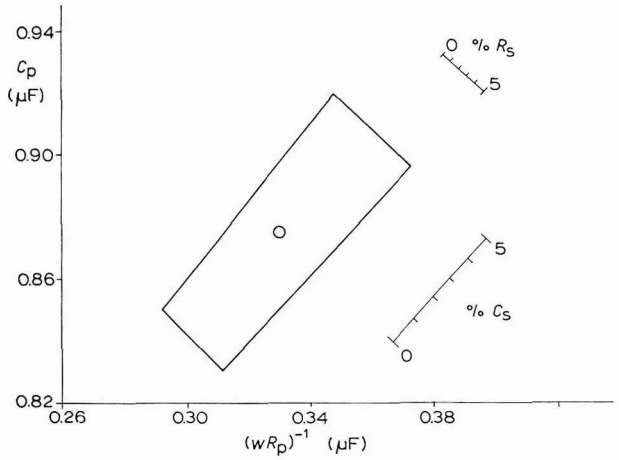

Fig. 11. Representation of $\pm 5\%$ error in R_s and C_s in parallel circuit values.

sponding to intermediate errors lie within the figure. It is seen that error in C_s does not necessarily affect the values of C_p more than those of R_p. In this case, 5% error in C_s has more effect on the values of $(\omega R_p)^{-1}$ than 5% error in R_s.

It is therefore preferable to represent such errors by an area, unless one series term is inherently much more erroneous than the other when representation by a curve is correct.

NOTATION

R_s = measured series resistance (Ω cm^2);
C_s = measured series capacity (μF cm^{-2})
C_{dl} = double-layer capacity (μF cm^{-2});
C_p = parallel interfacial capacity (μF cm^{-2});
C_{sf} = faradaic series capacity (μF cm^{-2});
R_p = parallel interfacial resistance (Ω cm^2);
R_{ct} = charge transfer resistance (Ω cm^2);
R_{so} = solution resistance (Ω);
R_{sf} = (faradaic series resistance) (Ω cm^2);
ω = angular frequency (radians sec^{-1});
n = charge of complex;
i_0 = exchange current (mA cm^2).

ACKNOWLEDGEMENT

One of us (W.P.R.) thanks the Science Research Council for the provision of a research studentship, during the tenure of which this work was carried out.

SUMMARY

The sudden rise in the capacity of a mercury electrode at anodic potentials in fluoride ion solutions has been shown to be due to:

(i) the presence of a faradaic pseudo-capacity associated with the dissolution of Hg as various complexes;

(ii) the specific adsorption of hydroxyl ions.

REFERENCES

1 D. C. GRAHAME, *J. Am. Chem. Soc.*, 76 (1954) 4819.
2 B. B. DAMASKIN, N. V. NIKOLAEVA-FEDOROVICH AND A. N. FRUMKIN, *Dokl. Akad. Nauk SSSR*, 121 (1958) 129.
3 N. F. MOTT AND R. J. WATTS-TOBIN, *Electrochim. Acta*, 4 (1961) 79.
4 R. PAYNE, *J. Electroanal. Chem.*, 7 (1964) 343–358.
5 R. D. ARMSTRONG, M. FLEISCHMANN AND H. R. THIRSK, *J. Electroanal. Chem.*, 11 (1966) 208.
6 D. C. CORNISH, S. N. DAS, D. J. G. IVES AND R. W. PITTMAN, *J. Chem. Soc.*, A (1966) 111.
7 M. SLUYTERS-REHBACH AND J. H. SLUYTERS, *Rec. Trav. Chim.*, 82 (1963) 535.
8 J. E. B. RANDLES, *Discussions Faraday Soc.*, 1 (1947) 11.
9 P. DELAHAY, *New Instrumental Methods in Electrochemistry*, Interscience, New York, 1954, p. 151.
10 *Stability Constants of Metal Ion Complexes*, Chem. Soc., London, *Spec. Publ. No. 17*, 1964.
11 R. DE LEVIE, *Electrochim. Acta*, 10 (1965) 395.
12 M. SLUYTERS-REHBACH AND J. H. SLUYTERS, *Electrochim. Acta*, 11 (1966) 73.

ELECTROANALYTICAL CHEMISTRY AND INTERFACIAL ELECTROCHEMISTRY
Elsevier Publishing Company, Amsterdam – Printed in The Netherlands

THE BOUNDARY CONDITION IN THE ELECTROSTATIC CHARGING OF MOVING FLUIDS

J. C. GIBBINGS AND R. W. VERYARD
Department of Mechanical Engineering, Fluid Mechanics Division, University of Liverpool (England)
(Received August 3rd, 1966)

1. INTRODUCTION

When a liquid, containing ions of opposite signs, is placed in contact with a solid surface, a separation of the charges takes place, so that an excess of the ions of one sign is left in the liquid. On the liquid being set in motion, the resulting charge is convected with the flow resulting in what has been called an electrostatic streaming current.

Attempts have been made to explain this phenomena by drawing an analogy with either heat or mass transfer.

In experiments to determine the streaming current for the flow through a pipe, care is usually taken to reproduce an analytical model in which the liquid enters the pipe in an electrically neutral state, having a voltage equal to that of the pipe wall[1–3].

With this inlet boundary condition, there is no potential difference between the bulk of the fluid and the wall to initiate charging, and so there is no analogy with the inlet temperature difference in the heating phenomena. This analogy cannot be used to explain the electrostatic charging in a fluid in the absence of an externally applied field.

2. MOBILITY BOUNDARY CONDITION

A boundary condition which provides an explanation for the initiation of charging has been proposed[4]. At the initial instant of contact, at a pipe inlet, between the liquid and the surface, and when the liquid is electrically neutral, a wall current density, j_w is given by

$$j_w \propto \Sigma C_i z_i k_i$$

In this equation, C is the ion concentration, z the ion valency and k the ion mobility. In a liquid with ions of two kinds of valency so that

$$z_+ = -z_-$$

this becomes

$$j_w \propto (C_+ k_+ - C_- k_-)$$

Thus, as the charge density, σ, is given by

$$\sigma = z_+ F (C_+ - C_-) ,$$

where F is the Faraday constant,
then initially, when $\sigma = 0$,

$$j_w \propto C_{\pm}(k_+ - k_-) \tag{1}$$

This boundary condition indicates a charging current that arises from a difference in the ionic mobilities.

3. CHARGING CURRENT MEASUREMENTS

To see if the charging current could be measured, experiments were performed with a conductivity cell containing kerosene.

The cell, illustrated in Fig. 1, consisted of a stainless-steel cylindrical beaker within which a stainless-steel sphere was suspended on a stainless-steel rod, and supported by P.T.F.E. bars.

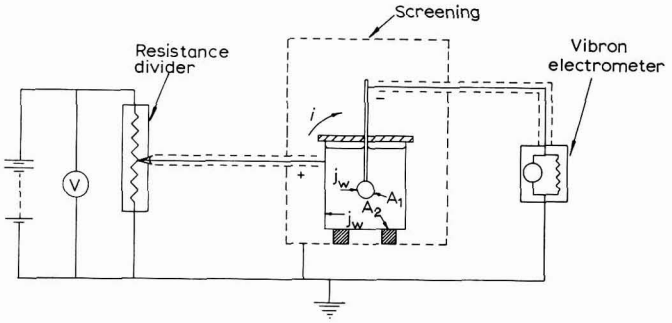

Fig. 1. Conductivity measuring apparatus.

The electrical circuit is also shown in this figure. The applied electrical potential was obtained from dry batteries, its value being controlled by a Muirhead voltage dividing resistance D-801-D, 10,000 Ω. The current passing through the cell being completely negligible compared with that passing through the dividing box, the output applied voltage could be calculated from the box ratio and the input voltage. The current passing through the cell was obtained by measuring the voltage drop, using an E.I.L. Vibron 33c electrometer, that occurred across a resistor in the E.I.L. Electrometer converter unit B33c-2.

The usual precautions, of providing earthed screening, were made as indicated in Fig. 1. The experiments were performed in a room that was supplied with filtered air and that was kept at constant temperature. Movement and draughts within the room were kept as small as possible and the screen box and conductivity cell were supported upon foam rubber.

As the current density, j_w, is a constant, the charging current, i_{w0}, flowing through the cell in the direction indicated in Fig. 1 is,

$$i_{w0} \propto j_w(A_1 - A_2) \tag{2}$$
$$= j_w \Delta A$$

where A_1 and A_2 are the surface areas of the electrodes.

A range of values of the area difference, ΔA, was obtained by varying the

height of the liquid in the beaker, a change always being made by syphoning off some liquid.

Results for three values of ΔA are plotted in Fig. 2. These results confirm that a charging current exists at zero potential.

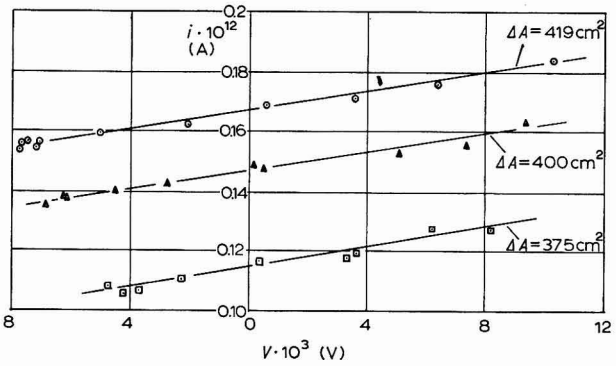

Fig. 2. Variation of cell current with applied voltage for a range of differences in area of the electrodes.

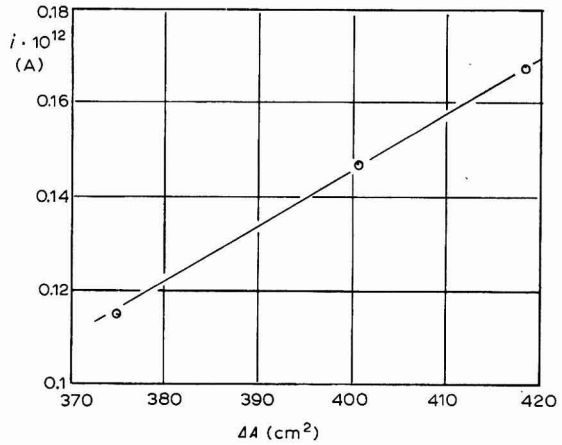

Fig. 3. Variation of cell current at zero potential difference across the electrodes as a function of the difference in area of the electrodes.

A cross-plot of the results at zero potential is shown in Fig. 3. This confirms the linear variation of i_{w0} with ΔA. However, the curve obtained does not go through the origin. The relation obtained is

$$10^{12} i_{w0} = 1.24 \cdot 10^{-3} \Delta A - 0.351$$

where ΔA is measured in cm^2.

There are several possible explanations for the occurrence of a current when ΔA is zero. First, although the potential difference across the cell is zero, it is not expected that the applied field would be the mirror image of that due to the charge distribution within the liquid and so it is not likely that the field at the electrode surfaces would be zero or even uniform over the surfaces. Secondly, the presence of a very small-scale roughness has been found to have a significant effect upon the

charging of a liquid flowing through a stainless-steel tube[5]. It seems unlikely that the surface of the two electrodes had sufficiently similar roughnesses, the sphere being machined and the beaker being drawn. Thirdly, it is possible that the stainless-steel alloy had a different composition in each electrode.

4. CONSISTENCY WITH CONDUCTIVITY MEASUREMENTS

From the arrangement sketched in Fig. 1,

$A_2 > A_1$

Also from the measurements

$i_{w0} > 0$

in the direction shown in this figure and thus from eqn. (2),

$j_w < 0$

Inspection of eqn. (1) then shows that for ions of only two types as specified,

$$k_- > k_+ \tag{3}$$

It has been shown[4] that the rate of change of conductivity, λ, with charge density, σ, is given by,

$$\frac{d\lambda}{d\sigma} = \tfrac{1}{2}(k_+ - k_-) \tag{4}$$

With a negative potential difference across the cell, the positive voltage on the smaller electrode will correspond to a negative charge in the region of the sphere that will be more than counterbalanced by the greater positive charge that is associated with the larger surface area of the other electrode. Thus, a positive total charge being associated with a negative voltage, $d\sigma/dV < 0$. This relation combined with eqn. (4) and substituted from eqn. (3) shows that $d\lambda/dV > 0$.

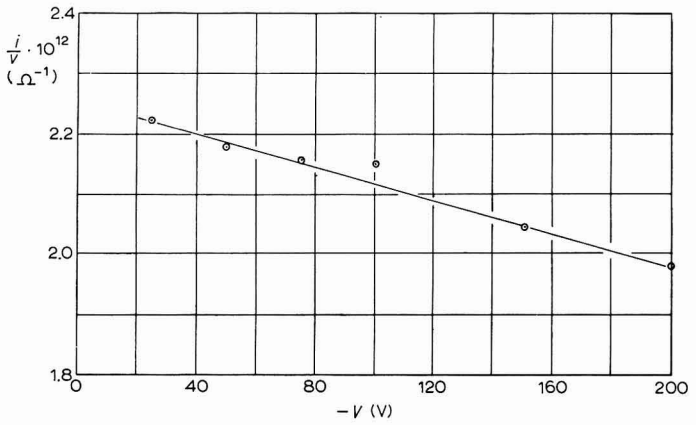

Fig. 4. Variation of current: voltage ratio as a function of applied voltage.

This is confirmed by the measurements, shown in Fig. 4 of i/V against negative voltage. Thus, there is a consistency of sign between the results of Figs. 2 and 4 if the relationship of eqn. (1) is valid.

5. FUTURE WORK

More detailed experiments to evaluate the effects of other surface materials, of other liquids and of varying surface roughness, and to investigate the presence of a charging current when $\Delta A = 0$, are in preparation.

SUMMARY

A boundary condition, proposed to explain electrostatic charging in moving fluids, has been given a preliminary experimental test. The presence of the suggested charging current has been measured for one liquid in one conductivity cell and has been shown to be consistent with the existence of a variation of conductivity with charge density.

NOTATION

A_1, A_2, surface areas of electrodes (cm^2);
ΔA, $\equiv A_1 - A_2$;
C, ion concentration;
F, Faraday number;
i_{w0}, zero-field wall charging current (A);
j_w, wall current density (A cm^{-2});
k, ion mobility;
V, voltage across cell;
z, ion valency;
λ, conductivity;
σ charge density.

REFERENCES

1 E. T. HIGNETT AND J. C. GIBBINGS, *J. Electroanal. Chem.*, 9 (1965) 260.
2 I. KOSZMAN AND J. GAVIS, *Chem. Eng. Sci.*, 17 (1962) 1023.
3 A. KLINKENBERG AND J. L. VAN DER MINNE, *Electrostatics in the Petroleum Industry*, Elsevier, London, 1958.
4 J. C. GIBBINGS AND E. T. HIGNETT, *Electrochim. Acta*, 11 (1966) 815.
5 E. T. HIGNETT AND J. C. GIBBINGS, in manuscript.

ELECTROANALYTICAL CHEMISTRY AND INTERFACIAL ELECTROCHEMISTRY
Elsevier Publishing Company, Amsterdam – Printed in The Netherlands

ZUR POLAROGRAPHIE DES TECHNETIUMS II. RADIOMETRISCHE BESTIMMUNG VON SELBSTDIFFUSIONSKOEFFIZIENTEN FÜR PERTECHNETAT-IONEN IN WÄSSERIGEN LÖSUNGEN*

L. ASTHEIMER, K. SCHWOCHAU UND W. HERR
Arbeitsgruppe "Institut für Radiochemie" der Kernforschungsanlage Jülich
*Institut für Kernchemie der Universität Köln***
(Eingegangen am 16. Juni 1966)

EINLEITUNG

In der Polarographie begnügt man sich zur Bestimmung von Elektronenübergängen nach der Ilkovič-Gleichung meistens mit Diffusionskoeffizienten, die nach der Nernstschen Beziehung $D^0 = R \cdot T \cdot l^0/|z| \cdot F^2$ aus der Äquivalent-Leitfähigkeit l^0 des betreffenden Ions bei unendlicher Verdünnung ermittelt werden. Die konduktometrische Methode[2] setzt die Abwesenheit von Fremdelektrolyt voraus, so dass der aus Leitfähigkeitsmessungen gewonnene Diffusionskoeffizient im allgemeinen nicht den polarographischen Gegebenheiten gerecht wird[3]. Allerdings geht in die Ilkovič-Gleichung nur der Wurzelwert des Diffusionskoeffizienten ein; der Unterschied zum tatsächlichen Diffusionskoeffizienten ist deshalb nicht immer von ausschlaggebender Bedeutung. Um den Einfluss der unter polarographischen Bedingungen ermittelten Diffusionskoeffizienten auf die für Pertechnetat-Ionen gefundenen Elektronenübergänge (n-Werte) festzustellen, bestimmten wir die Selbstdiffusionskoeffizienten von Pertechnetat-Ionen in Gegenwart und Abwesenheit von Grundelektrolyten. Zum Vergleich wurden auch die Selbstdiffusionskoeffizienten der in Struktur und Grösse sehr ähnlichen Perrhenat-Ionen[4] ermittelt.

Neuerdings wurde von BEARMAN[5] nachgewiesen, dass bei niedrigen Depolarisatorkonzentrationen nach

$$D_P = \frac{R \cdot T}{\sum_{\substack{\beta=1 \\ \neq A}}^{\varkappa} c_\beta \cdot \zeta_{A\beta} - \frac{\nu_R}{\nu_A} \cdot c_A \cdot \zeta_{RA}} \qquad (1)$$

und

$$D = \frac{R \cdot T}{\sum_{\beta=1}^{\varkappa} c_\beta \cdot \zeta_{A\beta}} \qquad (2)$$

* Für I. Mitteilung siehe Lit. (1).
** Die Untersuchungen wurden im Rahmen des Euratom-Forschungsvertrages 064-64 RISD durchgeführt.

der polarographische Diffusionskoeffizient D_P und der Selbstdiffusionskoeffizient D ineinander übergehen. A ist das Depolarisator-Ion, R (Index) sein Gegenion, c_β die Konzentration der Ionenart β, ζ ein konzentrationsabhängiger sog. Reibungskoeffizient (friction coefficient); ν_R, ν_A sind einfache positive ganze Zahlen der Eigenschaft, dass $\nu_R/\nu_A = -z_A/z_R$ ist, wobei z_A, z_R die Ladungszahlen der Ionenarten A und R bedeuten. Der bei gebräuchlichen polarographischen Konzentrationen von etwa 10^{-3} M bestimmte Selbstdiffusionskoeffizient darf danach in die Ilkovič-Gleichung eingesetzt werden.

EXPERIMENTELLES

Zur experimentellen Bestimmung des Selbstdiffusionskoeffizienten wurde die Kapillar-Methode[6] verwendet. Sie ist eine Absolut-Methode mit relativ einfacher Arbeitstechnik und einem vergleichsweise kleinen Adsorptionsfehler[7]. Der Diffusionsraum ist eine mit indizierter Lösung gefüllte, einseitig verschlossene Kapillare, die mit der Öffnung nach oben in eine nichtindizierte Lösung sonst gleicher Zusammensetzung taucht (Abb. 1).

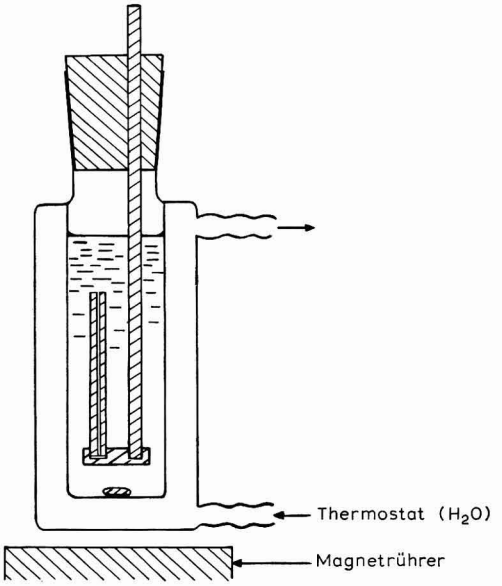

Abb. 1. Versuchsanordnung zur Bestimmung des Selbstdiffusionskoeffizienten nach der Kapillar-Methode. Das Volumen der thermostatisierten Badlösung beträgt 100 ml, die Kapillarenlänge ~ 5 cm, ihr Innendurchmesser ~ 0.05 cm[8].

Unter Verwendung einer 10 μl-Spritze kann die Kapillare mit der indizierten Lösung gefüllt werden, wobei sorgfältig auf Ausschluss von Luftbläschen zu achten ist. Durch Rühren mit einem Magnetrührer wird die Konzentration des Leitisotops an der Kapillarenöffnung nahezu gleich null gehalten. Nach Abbruch der Diffusion wird der Kapillareninhalt in ein Messschälchen zur Aktivitätsmessung überführt. Auf

einige Fehlermöglichkeiten soll hingewiesen werden. Beim Eintauchen der Kapillare in das Bad und beim Herausnehmen kann Lösung aus der Kapillare herausgewirbelt werden. Der Eintaucheffekt lässt sich weitgehend ausschalten, wenn man vorher auf die Kapillarenendfläche einen Tropfen der indizierten Lösung gibt. Weitere Fehler können durch Turbulenz bei zu starkem Rühren und durch Konvektion bei Temperaturunterschieden zwischen Kapillareninhalt und Badlösung zustande kommen. Weiter ist darauf zu achten, dass sich Vibrationen des Magnetrührers nicht auf das Badgefäss übertragen.

Auf die Diffusion des Leitisotops aus der Kapillare in die Badlösung wird das 2. Ficksche Gesetz angewendet. Für Grenzbedingungen, die durch die Versuchsanordnung gegeben sind, erhält man folgende Gleichung[9]:

$$\frac{\bar{c}}{c_0} = \sum_{n=0}^{n=\infty} \frac{8}{\pi^2(2n+1)^2} \exp\left[-\pi^2(2n+1)^2 \frac{Dt}{4l^2}\right] \tag{3}$$

mit

$\bar{c}$ = mittlere Konzentration des Leitisotops in der Kapillare bei Versuchsende,
c_0 = Konzentration des Leitisotops bei Versuchsbeginn,
n = 0, 1, 2, ...,
t = Diffusionsdauer (sec)
l = Kapillarenlänge (cm).

An Stelle des Konzentrationsverhältnisses $\bar{c}/c_0$ kann der Quotient der entsprechenden Aktivitätsraten A/A_0 eingesetzt werden. Sorgt man durch genügend lange Versuchsdauer dafür, dass $Dt/l^2 > 0.2$ wird, so muss nur das erste Glied der Reihe in Gl. (3) berücksichtigt werden, so dass sich

$$D = \frac{4l^2}{\pi^2 t} \ln \frac{8A_0}{\pi^2 A} \tag{4}$$

ergibt. Für die beschriebene Versuchsanordung ist zur Anwendung von Gl. (4) eine Mindestdiffusionsdauer von etwa vier Tagen erforderlich.

Zur Indizierung des langlebigen, β^--aktiven ^{99}Tc wurde ^{95m}Tc, ein β^+- und γ-Strahler mit einer Halbwertszeit von 60 Tagen, verwendet; es entsteht neben ^{97m}Tc und einigen anderen kurzlebigen Nukliden im Zyklotron durch Deuteronenbestrahlung von natürlichem Molybdän. Das mit 21 MeV-Deuteronen (Intensität 80 μA) eine Stunde lang bestrahlte Molybdänblech wurde zur Isolierung des Indikatornuklids in Salpetersäure gelöst, nach Zusatz von $K^{99}TcO_4$ als Träger die Salpetersäure weitgehend abdestilliert und die Lösung des Rückstandes in 2 M Natronlauge nach Harnstoffzusatz zwischen Platinelektroden bei 1.5 V elektrolysiert. 80 bis 90% des eingesetzten Technetiums konnten so abgeschieden werden. Zur Reinigung des Tc-Beschlages musste die Elektrolyse wiederholt werden. Durch Aufnahme des γ-Spektrums und Bestimmung der Halbwertszeit liess sich ^{95m}Tc nachweisen. Die Aktivität der Proben wurde mit einem Einkanal-Impulshöhenanalysator bei 0.20 MeV, der Energie des γ-Quants grösster Häufigkeit, gemessen. Die Indizierung der ReO_4^--Lösungen erfolgte mit den Radionukliden ^{186}Re ($T_{\frac{1}{2}} = 90h$) und ^{188}Re ($T_{\frac{1}{2}} = 17h$), die durch (n,γ)-Reaktionen aus natürlichem Rhenium entstehen.

ERGEBNISSE UND DISKUSSION

In Tab. 1 ist als Beispiel zur Bestimmung von Selbstdiffusionskoeffizienten nach der Kapillar-Methode eine Messreihe angeführt.

TABELLE 1

MESSREIHE ZUR BESTIMMUNG DES SELBSTDIFFUSIONSKOEFFIZIENTEN VON TcO_4^- IN ALKALISCHER LÖSUNG

10^{-3} *M* TcO_4^-, 1 *M* NaOH, 25°

Kapillar-länge l (cm)	*Diffusions-dauer t (Tage)*	*Aktivitätsraten (Imp./min)*		*Selbstdiffusions-koeffizient D nach Gl. (4)* $(10^{-5} \cdot cm^2\ sec^{-1})$
		A_0	A	
4.74	8.740	15443	4482	1.24
4.74	10.774	11335	2444	1.29
4.93	11.938	13114	2720	1.30
4.93	10.809	10931	2709	1.25
4.96	10.743	11937	2968	1.27

Nach einer Diffusionsdauer von 9 bis 12 Tagen betrug die Rate A der in der Kapillare verbliebenen Aktivität 20–30% der Ausgangsaktivitätsrate A_0. Der relative mittlere Fehler des Selbstdiffusionskoeffizienten entspricht dem in der Literatur für die Kapillar-Methode angegebenen[7].

Die Selbstdiffusionskoeffizienten von TcO_4^- und ReO_4^- wurden für 1 *M* Natronlauge und 1 *M* LiCl-Lösung bestimmt, da in diesen Grundelektrolyten sich gut ausgebildete polarographische Reduktionsstufen ergaben[1]. Um den Einfluss des Grundelektrolyten auf die Selbstdiffusion festzustellen, waren auch die Selbstdiffusionskoeffizienten in Abwesenheit von Grundelektrolyt zu ermitteln. In der Tab. 2 sind neben den nach der Kapillar-Methode radiometrisch bestimmten Selbstdiffusionskoeffizienten sowohl die nach NERNST konduktometrisch gefundenen Werte als auch die nach ONSAGER[10] sowie GOSTING UND HARNED[11] berechneten Selbstdiffusionskoeffizienten angeführt. Für die Messungen wurden $KTcO_4$- bzw. $KReO_4$-Lösungen verwendet.

Die in Tab. 2 zusammengestellten Selbstdiffusionskoeffizienten sind Mittelwerte aus jeweils 5 Einzelmessungen. Die mittleren Fehler der Mittelwerte von ~ 1% werden bei den Versuchen ohne Fremdelektrolyt-Zusatz merklich überschritten und betragen hier 3–4%; eine Erklärung für den grösseren Fehler mag die erhöhte Anfälligkeit der fremdelektrolytfreien Lösungen gegenüber Turbulenz sein.

In 1 *M* Natronlauge oder 1 *M* LiCl-Lösung sind nach Tab. 2 die Selbstdiffusionskoeffizienten des TcO_4^--Ions um ungefähr 15–17% kleiner als für die Lösungen ohne Elektrolyt-Zusatz. Der Einfluss des Grundelektrolyten auf den Selbstdiffusionskoeffizienten und somit auch auf den polarographischen Diffusionskoeffizienten ist danach recht erheblich. Da der Elektrolyt-Zusatz die Viskosität der Lösungen erhöht, ist nach STOKES–EINSTEIN[9] eine Abnahme des Selbstdiffusionskoeffizienten zu erwarten. Eine Theorie, die die quantitative Deutung der Ergebnisse gestattet, ist noch nicht bekannt.

Der nach der Kapillar-Methode erhaltene Selbstdiffusionskoeffizient des

TcO_4^- ohne Fremdelektrolyt-Einfluss steht mit dem nach der Onsagerschen Theorie berechneten Selbstdiffusionskoeffizienten in befriedigender Übereinstimmung; nahezu gleich ist auch der konduktometrisch für unendliche Verdünnung gefundene Wert.

Die für die analogen Perrhenat-Lösungen unter den gleichen Bedingungen ermittelten Koeffizienten unterscheiden sich von den für Pertechnetat gefundenen Werten nur geringfügig; die Abweichungen liegen innerhalb des Messfehlers.

TABELLE 2

SELBSTDIFFUSIONSKOEFFIZIENTEN VON PERTECHNETAT- UND PERRHENAT-IONEN BEI 25°

Substanzen	*Grundelektrolyt*	*Methode*	*Selbstdiffusionskoeffizient D* ($10^{-5} \cdot cm^2\ sec^{-1}$)
10^{-3} *M* TcO_4^- 10^{-3} *M* ReO_4^-	1 *M* NaOH	Kapillar-Methode	1.27 ± 0.01 1.27 ± 0.02
10^{-3} *M* TcO_4^- 10^{-3} *M* ReO_4^-	1 *M* LiCl	Kapillar-Methode	1.24 ± 0.01 1.27 ± 0.02
10^{-3} *M* TcO_4^- 10^{-3} *M* ReO_4^-		Kapillar-Methode	1.49 ± 0.06 1.54 ± 0.05
TcO_4^- in unendl. Verd. ReO_4^- in unendl. Verd.		Konduktometrie	1.48 ± 0.01 1.46[12,13]
10^{-3} *M* TcO_4^- 10^{-3} *M* ReO_4^-		Onsagersche Theorie	1.47 1.45

Bei der polarographischen Reduktion von Pertechnetat-Ionen werden in neutralen und alkalischen wässerigen Lösungen vier Stufen beobachtet, von denen nur die beiden ersten mit den Halbstufenpotentialen $\simeq -0.8$ V und $\simeq -1.1$ V konzentrationsproportional sind[1]. Über die diesen Stufen zu Grunde liegenden Elektronenübergänge findet man in der Literatur (vgl. ref. 1 und die dort zit. Lit.) unterschiedliche Angaben. Die erste Stufe wird der Reduktion des siebenwertigen Technetiums zum fünf- oder vierwertigen zugeschrieben, die folgende zweite Stufe dem Übergang zum vier- bzw. dreiwertigen Zustand. Die nach der Ilkovič-Gleichung berechneten n-Werte weichen in allen Fällen erheblich von der Ganzzahligkeit ab. Allerdings wurde bisher zur Ermittlung der Elektronenübergänge nur der konduktometrisch bestimmte Diffusionskoeffizient $D^0_{TcO_4^-}$ verwendet. In Tab. 3 sind die Mittelwerte $\bar{n}$ der Elektronenübergänge für die erste und zweite Reduktionsstufe in 1 *M* Grundelektrolyten angegeben, berechnet unter Anwendung der einfachen und der nach KOUTECKÝ[14] verbesserten Ilkovič-Gleichung* sowie des Diffusionskoeffizienten D^0 und des radiometrisch bestimmten, den polarographischen Bedingungen eher gerecht werdenden Selbstdiffusionskoeffizienten D.

* Da bei der von uns verwendeten Rapidpolarographie der Verarmungseffekt vernachlässigbar ist, wurde die von KOUTECKÝ abgeleitete Gleichung $i_d = 607 D^{1/2} m^{2/3} \tau^{1/6} n c (1 + 34\ D^{1/2} m^{-1/3} \tau^{1/6})$ benutzt.

Die zweite Reduktionsstufe setzt sich nur in alkalischer Grundlösung in einer auswertbaren Form von der ersten Stufe ab.

Der Vergleich der verschieden berechneten Elektronenübergänge $\bar{n}$ zeigt, dass auch nach Einsetzen des Selbstdiffusionskoeffizienten D in die nach KOUTECKÝ

TABELLE 3

ELEKTRONENÜBERGANGE $\bar{n}$ FÜR DIE 1. UND 2. POLAROGRAPHISCHE REDUKTIONSSTUFE DES TcO_4^-

Reduktionsstufe	*Grundelektrolyt*	*Elektronenübergänge $\bar{n}$*			
		einfache Ilkovič-Gl. mit D^0	*verbesserte Ilkovič-Gl. mit D^0*	*einfache Ilkovič-Gl. mit D*	*verbesserte Ilkovič-Gl. mit D*
1.	1 M NaOH	2.30	2.12	(2.48)	2.29
	1 M LiCl	1.95	1.80	(2.13)	1.96
2.	1 M NaOH	3.04	2.80	(3.28)	3.02

verbesserte Ilkovič-Gleichung die Elektronenübergänge für die erste Reduktionsstufe $\simeq 2$ und für die zweite Reduktionsstufe $\simeq 3$ bleiben. Die annähernde Übereinstimmung der nach der einfachen Ilkovič-Gleichung mit D^0 und nach der verbesserten Gleichung mit D errechneten $\bar{n}$-Werte beruht darauf, dass sich hier der grössere D^0-Wert in der einfachen Gleichung wie der Korrekturfaktor in der verbesserten Gleichung auswirkt. Es ist deshalb nicht sinnvoll, in die einfache Ilkovič-Gleichung den Selbstdiffusionskoeffizienten D einzusetzen. Bei der polarographischen Reduktion des Pertechnetat-Ions findet danach sowohl in neutraler als auch in alkalischer Grundlösung zunächst der Übergang Tc(VII) → Tc(V) statt, dem die Reduktion Tc(VII) → Tc(IV) folgt.

DANK

Der Europäischen Atomgemeinschaft danken wir für die im Rahmen eines Forschungsvertrages gewährte finanzielle Unterstützung.

ZUSAMMENFASSUNG

Selbstdiffusionskoeffizienten D des TcO_4^- wurden radiometrisch nach der Kapillar-Methode in Gegenwart von Grundelektrolyten bestimmt, um deren Einfluss auf die Diffusion und auf die bei der polarographischen Reduktion von TcO_4^- ermittelten Wertigkeitsänderungen festzustellen. Für 10^{-3} M TcO_4^- ergab sich in 1 M Natronlauge $D = 1.27 \cdot 10^{-5}$, in 1 M LiCl-Lösung $D = 1.24 \cdot 10^{-5}$ cm^2 sec^{-1}. Der in Abwesenheit von Grundelektrolyt gefundene Selbstdiffusionskoeffizient $D = 1.49 \cdot 10^{-5}$ cm^2 sec^{-1} stimmt mit dem nach der Onsagerschen Theorie berechneten Wert nahezu überein. Obgleich die Grundelektrolyte die Selbstdiffusion des TcO_4^- merklich beeinflussen, sind die hierdurch bedingten Änderungen der Elektronenübergänge vernachlässigbar. Sowohl in neutraler als auch in alkalischer Grundlösung findet zu-

nächst der Übergang Tc(VII) → Tc(V) statt, dem die Reduktion Tc(VII) → Tc(IV) folgt. Die unter den gleichen Bedingungen bestimmten Selbstdiffusionskoeffizienten des ReO_4^- unterscheiden sich innerhalb des Messfehlers nicht von den für TcO_4^- gefundenen Werten.

SUMMARY

The self-diffusion coefficients D for the TcO_4^- were determined by the capillary method in the presence of supporting electrolytes, in order to evaluate their influence on the diffusion and on the electron transfers established for the polarographic reduction of TcO_4^-. At 10^{-3} M TcO_4^- in 1 M NaOH soln., $D = 1.27 \cdot 10^{-5}$, in 1 M LiCl soln., $D = 1.24 \cdot 10^{-5}$ cm^2 sec^{-1} were obtained. The self-diffusion coefficient found in the absence of supporting electrolyte, $D = 1.49 \cdot 10^{-5}$ cm^2 sec^{-1}, is in agreement with the value calculated by the Onsager theory. Whereas the supporting electrolytes affect the self-diffusion of the TcO_4^-, the changes of the electron transfers hereby induced can be neglected. Both in neutral and in alkaline supporting electrolyte solutions first there is the reduction Tc(VII) → Tc(V), followed by Tc(VII) → Tc(IV). The self-diffusion coefficients of the ReO_4^- determined under the same conditions, do not differ from the values for TcO_4^- within the experimental error.

LITERATUR

1 L. ASTHEIMER UND K. SCHWOCHAU, Gleichstrom- und wechselstrompolarographische Untersuchungen an Pertechnetat-Lösungen, *J. Electroanal. Chem.*, 8 (1964) 382.
2 J. M. KOLTHOFF UND J. J. LINGANE, *Polarography*, Vol. 1, Interscience, New York–London, 2nd ed., 1952.
3 R. MILLS, *J. Electroanal. Chem.*, 9 (1965) 57.
4 K. SCHWOCHAU, *Angew. Chem.*, 76 (1964) 9.
5 R. J. BEARMAN, *J. Phys. Chem.*, 66 (1962) 2072.
6 J. S. ANDERSON UND K. SADDINGTON, *J. Chem. Soc.*, (1949) 381.
7 R. MILLS, *Rev. Pure Appl. Chem.*, 11 (1961) 78.
8 L. ASTHEIMER, *Dissertation*, Köln, 1965.
9 R. A. ROBINSON UND R. H. STOKES, *Electrolyte solutions*, Butterworths, London, 2nd ed., 1959.
10 L. ONSAGER, *Ann. N. Y. Acad. Sci.*, 46 (1945) 241.
11 L. GOSTING UND H. HARNED, *J. Am. Chem. Soc.*, 73 (1951) 159.
12 J. H. JONES, *J. Am. Chem. Soc.*, 68 (1946) 240.
13 K. SCHWOCHAU UND L. ASTHEIMER, *Z. Naturforschg.*, 17a (1962) 820.
14 J. KOUTECKÝ, *Czech. J. Phys.*, 2 (1953) 50.

ELECTROANALYTICAL CHEMISTRY AND INTERFACIAL ELECTROCHEMISTRY
Elsevier Publishing Company, Amsterdam – Printed in The Netherlands

ON THE IMPEDANCE OF GALVANIC CELLS

XVIII. THE POTENTIAL DEPENDENCE OF THE FARADAIC IMPEDANCE IN THE CASE OF AN IRREVERSIBLE ELECTRODE REACTION, AND ITS APPLICATION TO A.C. POLAROGRAPHY

B. TIMMER, M. SLUYTERS-REHBACH AND J. H. SLUYTERS
Laboratory of Analytical Chemistry, State University, Utrecht (The Netherlands)
(Received March 5th, 1966; in revised form May 27th, 1966)

INTRODUCTION

The study of the faradaic impedance has proved to be useful in fundamental investigations of electrode reactions, especially for the determination of the kinetic parameters of comparatively fast reactions *i.e.*, reactions, that are reversible with respect to d.c. current. Until now few practical applications are known of the analysis of irreversible reactions by means of the faradaic impedance, probably because the importance of such a study is not sufficiently recognized. In particular, cell impedance measurements as a function of potential may be useful, not only as a check of the d.c. analysis, but also for the evaluation of double-layer parameters and possibly for obtaining more information about the reaction mechanism itself. Examples of irreversible electrode reactions, that have been studied in this way, are the H^+/H_2 reaction[1] at a dropping mercury electrode (D.M.E.) and the $Zn^{2+}/Zn(Hg)$ reaction[2,3] at a streaming mercury electrode (S.M.E.). For the latter system, unexpectedly, two peaks in the impedance plot were observed; these were misinterpreted for lack of a good theory for the faradaic impedance, as will be shown.

It is worthwhile, therefore, to have theoretical expressions of the faradaic impedance as a function of potential in the case of an irreversible reaction, particularly if both the oxidized (O) and reduced (R) form of the reactant are present. Such expressions might be derived from the work of MATSUDA[4], who gives a rigorous theory of the faradaic alternating current as a function of potential, or from the less rigorous, but more accessible treatment of AYLWARD *et al.*[5] on the same subject. In both treatments, however, it is supposed that only O is present and that the D.M.E. is used. Moreover, little attention has been paid to general conclusions which can be drawn in relation to a.c. polarography. In this paper an analogous treatment will be given for the case in which both O and R of the reactant are present and for different kinds of electrodes (such as the S.M.E.). The relevant consequences of the resulting equations will be discussed as an introduction to experimental studies to be described in the near future.

THEORY

In order to obtain expressions for the faradaic impedance, it will be assumed that the mass transfer due to the a.c. current and due to the d.c. current do not in-

fluence each other and that it is permissible to treat these two processes separately, as is done by most authors[5-7,10]. The current–voltage relationship for an electrode reaction is

$$i = nFk_{sh}\left[C_R \exp\left\{\frac{\alpha nF}{RT}(E-E_0)\right\} - C_O \exp\left\{\frac{-\beta nF}{RT}(E-E_0)\right\}\right] \quad (1)$$

where C_O and C_R, the concentrations at the electrode surface, are functions of the potential, E, and the bulk concentrations, C_O^* and C_R^*; $\beta = 1-\alpha$, and the other symbols have their usual meaning. For impedance measurements a small alternating voltage, V_{ac}, is superposed on the d.c. voltage, E_{dc}, so that $E-E_0 = V_{ac}+E_{dc}-E_0$. The surface concentrations in that case are $C_O = \bar{C}_O + \Delta C_O(t)$ and $C_R = \bar{C}_R - \Delta C_R(t)$, in which $\bar{C}$ is the surface concentration due to the direct current, i_{dc}, and $\Delta C(t)$ is caused by the alternating current, $i_m \sin \omega t$. Equation (1) becomes

$$i_{dc}+i_m \sin\omega t = nFk_{sh}\left[(\bar{C}_R - \Delta C_R(t)) \exp\left\{\alpha\varphi + \frac{\alpha nF}{RT}V_{ac}\right\}\right.$$
$$\left. - (\bar{C}_O + \Delta C_O(t)) \exp\left\{-\left(\beta\varphi + \frac{\beta nF}{RT}V_{ac}\right)\right\}\right] \quad (2)$$

in which $\varphi = (nF/RT)(E-E_0)$. If the terms $\exp((\alpha nF/RT)V_{ac})$ and $\exp(-(\beta nF/RT)V_{ac})$ in eqn. (2) are expanded as a Fourier series and terms containing products of V_{ac} and ΔC or powers of V_{ac} higher than unity are neglected (because $V_{ac} \ll RT/nF$) eqn. (2) reduces to

$$i_{dc}+i_m \sin\omega t = nFk_{sh}\left[\left(1 + \frac{\alpha nF}{RT}V_{ac}\right)\bar{C}_R \exp(\alpha\varphi) - \left(1 - \frac{\beta nF}{RT}V_{ac}\right)\bar{C}_O \exp(-\beta\varphi)\right.$$
$$\left. - \Delta C_R(t) \exp(\alpha\varphi) - \Delta\bar{C}_O(t) \exp(-\beta\varphi)\right] \quad (3)$$

The direct current density is given by

$$i_{dc} = nFk_{sh}[\bar{C}_R \exp(\alpha\varphi) - \bar{C}_O \exp(-\beta\varphi)] \quad (4)$$

Subtraction of (4) from (3) yields

$$i_m \sin\omega t = nFk_{sh}\left[\frac{nF}{RT}V_{ac}\{\alpha\bar{C}_R \exp(\alpha\varphi) + \beta\bar{C}_O \exp(-\beta\varphi)\}\right.$$
$$\left. - \{\Delta C_R(t) \exp(\alpha\varphi) + \Delta C_O(t) \exp(-\beta\varphi)\}\right] \quad (5)$$

Equations for $\Delta C_O(t)$ and $\Delta C_R(t)$ have been given by WARBURG[8]

$$\Delta C(t) = \frac{i_m}{nF}\left(\frac{1}{2\omega D}\right)^{\frac{1}{2}}(\sin\omega t - \cos\omega t) \quad (6)$$

Substitution of (6) into (5) and rearrangement leads to

$$V_{ac} = \frac{RTi_m \sin\omega t}{n^2F^2k_{sh}\{\alpha\bar{C}_R \exp(\alpha\varphi) + \beta\bar{C}_O \exp(-\beta\varphi)\}} + \frac{RT}{n^2F^2\sqrt{2\omega}}$$
$$\cdot \frac{D_R^{-\frac{1}{2}} \exp(\alpha\varphi) + D_O^{-\frac{1}{2}} \exp(-\beta\varphi)}{\alpha\bar{C}_R \exp(\alpha\varphi) + \beta\bar{C}_O \exp(-\beta\varphi)} \cdot i_m(\sin\omega t - \cos\omega t) \quad (7)$$

Equation (7) can be presented in the form of the faradaic impedance, Z_f, with

$$Z_f = \theta + \sigma\omega^{-\frac{1}{2}}(1-j) \tag{8}$$

$$\theta = \frac{RT}{n^2F^2k_{sh}\{\alpha\bar{C}_R \exp(\alpha\varphi) + \beta\bar{C}_O \exp(-\beta\varphi)\}} \tag{9}$$

$$\sigma = \frac{RT}{n^2F^2\sqrt{2}} \cdot \frac{D_R^{-\frac{1}{2}} \exp(\alpha\varphi) + D_O^{-\frac{1}{2}} \exp(-\beta\varphi)}{\alpha\bar{C}_R \exp(\alpha\varphi) + \beta\bar{C}_O \exp(-\beta\varphi)} \tag{10}$$

In the reversible case, $\exp\varphi = \bar{C}_O/\bar{C}_R$ may be introduced, reducing (9) and (10) to the well-known expressions of RANDLES[11]. The same holds for the equilibrium potential, φ_{eq}.

The next step is to obtain expressions for $\bar{C}_O$ and $\bar{C}_R$ as a function of φ. These expressions may be derived from the theory of semi-infinite linear diffusion or from the steady-state theory[9,10]; in this paper the latter will be followed, since its mathematics are less involved. Moreover, the steady-state concept may be used as a model for different types of electrodes, as only a suitable estimation has to be made for the thickness of the diffusion layer, δ. According to the steady-state theory, the surface concentrations are[3,6]:

$$\bar{C}_O = \frac{C_O^*\left[a_O + \frac{a_O}{a_R}\exp(\alpha\varphi)\right] + C_R^* \exp(\alpha\varphi)}{a_O + \frac{a_O}{a_R}\exp(\alpha\varphi) + \exp(-\beta\varphi)} \tag{11a}$$

$$\bar{C}_R = \frac{C_O^* \exp(-\beta\varphi) + C_R^*\left[a_R + \frac{a_R}{a_O}\exp(-\beta\varphi)\right]}{a_R + \exp(\alpha\varphi) + \frac{a_R}{a_O}\exp(-\beta\varphi)} \tag{11b}$$

in which the terms $a_O = D_O/\delta_O k_{sh}$ and $a_R = D_R/\delta_R k_{sh}$ reflect the influence of the irreversibility of the electrode reaction. Substitution of (11) into (9) and (10) leads to the desired equations for θ and σ.

$$\theta = \frac{RT}{n^2F^2k_{sh}} \cdot \frac{a_O + \frac{a_O}{a_R}\exp(\alpha\varphi) + \exp(-\beta\varphi)}{a_O \exp(-\beta\varphi)\left[\beta + \frac{1}{a_R}\exp(\alpha\varphi)\right]C_O^* + \exp(\alpha\varphi)\left[\alpha a_O + \exp(-\beta\varphi)\right]C_R^*} \tag{12a}$$

$$\sigma = \frac{RT}{n^2F^2\sqrt{2}}\{D_R^{-\frac{1}{2}}\exp(\alpha\varphi) + D_O^{-\frac{1}{2}}\exp(-\beta\varphi)\} \times \frac{a_O + \frac{a_O}{a_R}\exp(\alpha\varphi) + \exp(-\beta\varphi)}{a_O \exp(-\beta\varphi)\left[\beta + \frac{1}{a_R}\exp(\alpha\varphi)\right]C_O^* + \exp(\alpha\varphi)\left[\alpha a_O + \exp(-\beta\varphi)\right]C_R^*} \tag{12b}$$

In the derivation of these equations no special assumptions have been made; they are valid for reversible as well as irreversible reactions.

In part III and VI of this series[6,7] also, expressions for Z_f were derived as a function of potential assuming, however, that the reaction behaves reversibly with

respect to d.c. current. The *reversible* equations for θ and σ are, in the present notation

$$\theta = \frac{RT}{n^2F^2k_{sh}} \cdot \frac{\exp(\beta\varphi) + \frac{a_R}{a_O}\exp(-\alpha\varphi)}{C_O^* + \frac{a_R}{a_O}C_R^*} \tag{13a}$$

$$\sigma = \frac{RT}{n^2F^2\sqrt{2D_R}} \cdot \frac{\left[\exp(\tfrac{1}{2}\varphi) + \frac{a_R}{a_O}\exp(-\tfrac{1}{2}\varphi)\right]^2}{C_O^* + \frac{a_R}{a_O}C_R^*} \tag{13b}$$

These equations will now be discussed.

ANALYSIS OF CELL IMPEDANCES IN THE CASE OF IRREVERSIBLE ELECTRODE REACTIONS

Measurements of the cell impedance at the equilibrium potential as a function of frequency are useful for the determination[11,12] of k_{sh} from the value of θ. For low k_{sh}-values, however, θ becomes large with respect to the double-layer impedance; consequently the ohmic resistance, R_Ω, and the double-layer capacitance, C_d, dominate the cell impedance which for this reason contains little information about the electrode reaction. In part VI of this series[7] it was derived that, under the usual conditions, for a 10% accuracy θ should not exceed 1000 Ωcm^2; this means (*cf.* the Randles equation[11]) that for measurements at the equilibrium potential, $n^2k_{sh}(C_O^*)^\alpha(C_R^*)^\beta > 10^{-10}$ should hold. With concentrations in the usual order of 10^{-5} mole/cm^3, it follows that $k_{sh} > 10^{-5}/n^2$ cm sec^{-1}; therefore k_{sh}-values lower than 10^{-5} cm sec^{-1} cannot be determined in this way. Higher concentrations could be used, because migration besides diffusion has no influence on the cell impedance for these irreversible reactions, decreasing this limit to perhaps 10^{-7} cm sec^{-1}. From (12a) it follows that θ may be smaller at potentials away from the equilibrium potential (*cf.* θ-curves in Figs. 1 and 2.) and it could therefore be possible to extend the attainable k_{sh}-range by measurements at non-equilibrium potentials. In the following, this will be examined more closely.

In Figs. 1 and 2, values of θ and $\sigma\omega^{-\frac{1}{2}}$ are represented as a function of potential; these values have been calculated numerically, using the data: $n=2$, $\alpha=0.7$, $D_O = \frac{1}{2}D_R = 8 \cdot 10^{-6}$ cm^2 sec^{-1}, $\delta_O = \delta_R/\sqrt{2} = 5 \cdot 10^{-3}$ cm, $\sqrt{\omega} = 80$ sec$^{-\frac{1}{2}}$ and several k_{sh}-values, for $C_O^* = 10^{-6}$ mole/cm^3 and $C_O^* = C_R^* = 10^{-6}$ mole/cm^3, respectively. These data correspond to the values normally found for the $Zn^{2+}/Zn(Hg)$ reaction at a D.M.E. For a D.M.E. the best expression for δ is

$$\delta = \sqrt{\frac{3}{7}\pi Dt} \tag{14}$$

For a S.M.E. the results will be qualitatively the same, the difference with a D.M.E. is caused only by the different value of δ. Obviously $\sigma\omega^{-\frac{1}{2}}$ is not negligibly small at any potential, even for very small k_{sh}-values. In addition, therefore, the quantity q has to be considered, which in practice is obtained easily from the impedance measurements[7] with $Z = Z' - jZ''$

$$\frac{(Z - R_\Omega)^2 + (Z'')^2}{Z' - R_\Omega} = q = \theta + \sigma\omega^{-\frac{1}{2}} + \frac{\sigma^2\omega^{-1}}{\theta + \sigma\omega^{-\frac{1}{2}}} \tag{15}$$

In Figs. 1 and 2, values of $1/q$, corresponding with θ and $\sigma\omega^{-\frac{1}{2}}$, are plotted against potential. If q is determined at different frequencies, θ and σ can be evaluated (frequency variation method). The accuracy of the results will depend on the accuracy of q and on the ratio $p = \theta/\sigma\omega^{-\frac{1}{2}}$: if p is large, the error in σ is large; if p is small, θ contains a large error. At a fixed potential this ratio is independent of concentration

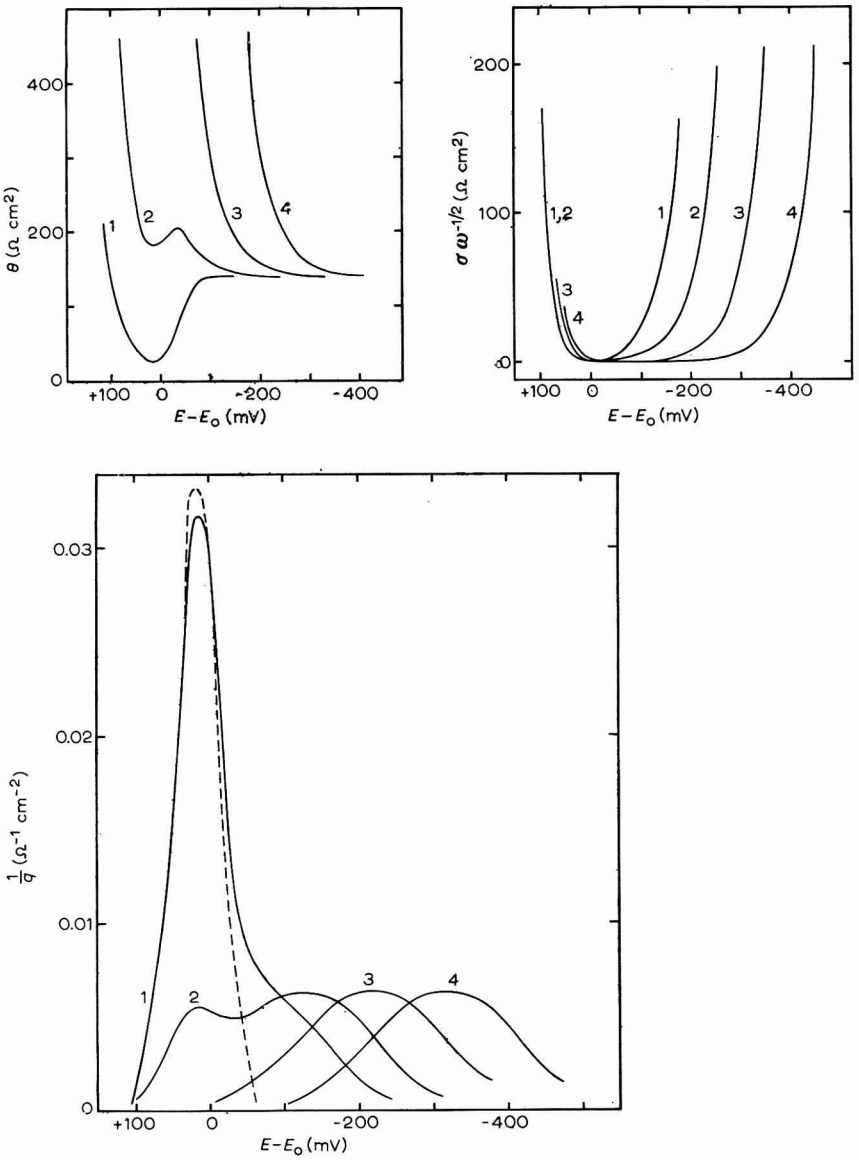

Fig. 1. Plots of $\theta, \sigma\omega^{-\frac{1}{2}}$ and $1/q$ against d.c. potential for $C_R^* = 0$, according to eqns. (12) and (15). Value of k_{sh} in cm/sec: (1), $5 \cdot 10^{-3}$; (2) 10^{-3}; (3) 10^{-4}; (4) 10^{-5}; For other data see text. (- - -), Plot of $1/q$ against d.c. potential for $C_R^* = 0$, according to the *reversible* eqn. (13) for $k_{sh} = 5 \cdot 10^{-3}$ cm/sec.

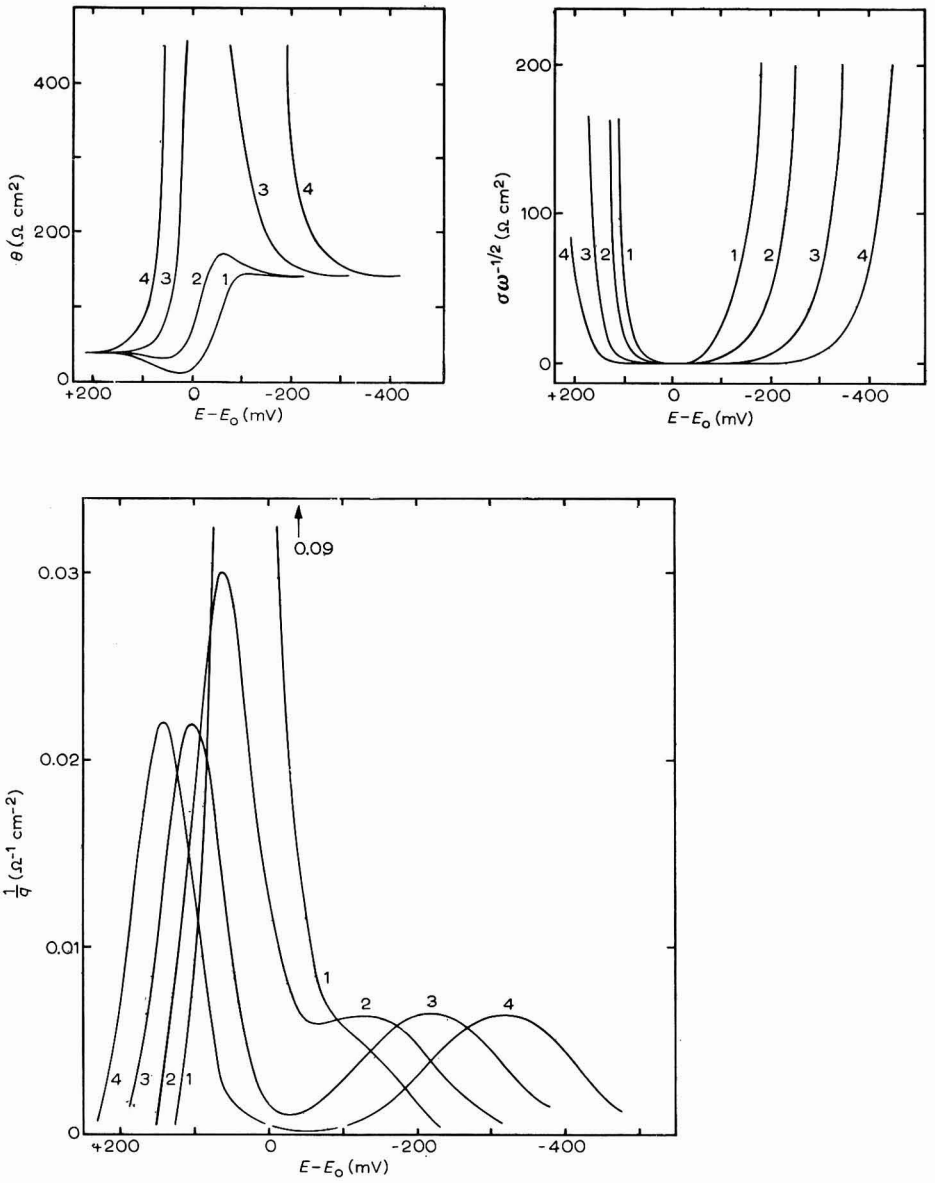

Fig. 2. Plots of $\theta, \sigma\omega^{-\frac{1}{2}}$ and $1/q$ against d.c. potential for $C_O^* = C_R^* = 10^{-6}$ mole/cm³ according to eqns. (12) and (15).
Value of k_{sh} in cm/sec: (1) $5 \cdot 10^{-3}$; (2) 10^{-3}; (3) 10^{-4}; (4) 10^{-5}. For other data see text.

$$p = \frac{\sqrt{2\omega}}{k_{sh}} \cdot \frac{1}{D_R^{-\frac{1}{2}} \exp(\alpha\varphi) + D_O^{-\frac{1}{2}} \exp(-\beta\varphi)} \tag{16}$$

If the double-layer capacitance is independent of the concentration of the reactant, the value of p itself can be determined (as was pointed out in part VI[7]) from impedance

measurements for varying concentration, at fixed potential and frequency (concentration variation method). This is done most easily from a plot of $Z''/[(Z'')^2+(Z'-R_\Omega)^2]$ against $(Z'-R_\Omega)/[(Z'')^2+(Z'-R_\Omega)^2]$, which should be a straight line with slope, $1/p+1$, and intercept, ωC_d. In this case, θ and σ can be evaluated from q at a single frequency.

From Figs. 1 and 2 it can be concluded that, in fact, q may be relatively small at certain potentials, so that θ may be accessible for small k_{sh}-values. If, however, the interpretation of the results has to be based on the general equation (12a), only a numerical calculation, probably by trial and error, of k_{sh} (and α) seems to be possible. In special cases, however, simplified versions of (12) can be applied.

Possible simplifications

(i) a_O and a_R can be neglected. If $\alpha a_O \ll \exp(-\beta\varphi)$, and $\beta a_R \ll \exp(\alpha\varphi)$, eqn. (12) reduces to the *reversible* eqns. (13). It is common use to suppose that this is the case for $k_{sh} > 10^{-2}$ cm sec^{-1} (system reversible to d.c. current[10]). It follows, however, from Table 1 that this is not true for the whole potential region of the $1/q$ *wave*. For $k_{sh} = 10^{-2}$ cm sec^{-1}, the approximation is sufficiently close only at potentials near to E_O (compare also the broken curve in Fig. 1).

TABLE 1

Difference between the $1/q$-values, for different d.c. potentials, calcd. from (13) and the general eqns. (12) for $k_{sh} = 10^{-2}$ cm sec^{-1}. $C_O^* = C_R^* = 1$ mM, other data as in Fig. 1.

φ	$(1/q)_{rev.}$	$(1/q)_{gen.}$	*Difference (%)*
+6	0.017	0.025	32
+4	0.073	0.087	16
+2	0.150	0.165	9
0	0.143	0.143	0
−2	0.055	0.057	4
−4	0.014	0.020	30
−6	0.003	0.009	66

TABLE 2

Error in k_{sh}, if k_{sh} is calcd. from experiments at the peak-potential, by application of (13a) instead of the general expression (12a).

k_{sh} *(cm sec^{-1})*	*Difference at peak (%)*
10^{-2}	4
$6 \cdot 10^{-3}$	7
$4 \cdot 10^{-3}$	9
$2 \cdot 10^{-3}$	15
10^{-3}	20

In part VI of this series[7] it was proposed to determine k_{sh}-values from the peak value $(1/q_m)$ of $(1/q)$. If the *reversible* eqn. (13a) for θ is used, the result will be correct only for $k_{sh} \gg 2 \cdot 10^{-3}$ cm sec^{-1}, as can be calculated from the inequalities given before, inserting normal values for a D.M.E. and[7] $\varphi_{peak} = \ln(\alpha a_R/\beta a_O)$. The error in the k_{sh}-value, calculated from (13a) instead of from the general eqn. (12a), increases with the irreversibility of the reaction (Table 2) and at the peak-potential only for $k_{sh} > 10^{-2}$ cm sec^{-1} is (13a) a good approximation for (12a).

(ii) a_O is large compared to $\exp(-\beta\varphi)$ for $\varphi \ll 0$. Only this case will be treated here, as for $\varphi \gg 0$ a similar reasoning holds. If $\exp(\alpha\varphi)$ is negligibly small compared to $\exp(-\beta\varphi)$, βa_O and $\beta a_O C_O^*/C_R^*$, which is fulfilled for $\varphi < -10$ if $k_{sh} < 10^{-2}$ cm sec^{-1} and $C_O^*/C_R^* > 0.1$ with α not too extreme, (12a) reduces to

$$\theta = \frac{RT}{n^2F^2k_{sh}} \cdot \frac{a_O + \exp(-\beta\varphi)}{a_O\beta C_O^* \exp(-\beta\varphi)} \qquad (17)$$

For $a_0 \gg \exp(-\beta\varphi)$ this reduces further to

$$\theta = \frac{RT}{n^2F^2k_{sh}} \cdot \frac{\exp(+\beta\varphi)}{\beta C_0^*} \tag{18}$$

Simultaneously $\sigma = RT/n^2F^2\beta C_0^* \sqrt{2D_0} = \text{constant}$. The total faradaic impedance, however, is almost equal to θ ($p = \theta/\sigma\omega^{-\frac{1}{2}} = (\sqrt{2\omega D_0}/k_{sh}) \exp(\beta\varphi) \approx a_0 \exp(\beta\varphi) \gg 1$).

The descending branches of θ in Figs. 1 and 2 for $\varphi \ll 0$ can be described by (18). Plotting log θ against φ under these conditions gives a straight line, the slope yielding the value of β, and the intercept at $\varphi = 0$ the value of k_{sh}. In part X of this series[1], eqn. (18) was applied intuitively to the hydrogen reduction on mercury, without proof of its validity. This procedure is correct, if $\varphi < -10$, $a_0 > 10 \exp(-\beta\varphi)$ and $\theta < 10^3\ \Omega\text{cm}^2$ (higher values of θ cannot be measured accurately[7]). The latter two conditions yield

$$\frac{5 \cdot 10^{-10}}{n^2C_0^*} < k_{sh} \exp(-\beta\varphi) < 2 \cdot 10^{-4} \tag{19}$$

The extrapolation of the log θ *vs* φ plot, for obtaining a correct k_{sh}-value, requires that the curve is a straight line for a sufficiently large potential region *e.g.*, 100 mV.

If $n^2C_0^*$ is chosen $= 5 \cdot 10^{-5}$ mole cm^{-3}, (19) reduces to

$$10^{-5} < k_{sh} \exp(-\beta\varphi) < 2 \cdot 10^{-4}$$

For $k_{sh} = 10^{-5}$ cm sec^{-1} this inequality is fulfilled for $-4 < \varphi < 0$, which is, as a rule, a too limited potential region. Moreover $\varphi < -10$ is not fulfilled. For $k_{sh} \leqslant 10^{-10}$ cm sec^{-1} the proposed procedure can be used (for $k_{sh} = 10^{-10}$ cm sec^{-1} $-24 < \varphi < -15$ holds). If C_0^* is chosen larger than 10^{-5} mole/cm^3, even larger k_{sh}-values can be measured. It can be concluded that very low k_{sh}-values can be measured with this a.c. technique and that it is therefore possible to make a comparison between the results of a.c. and d.c. methods.

(iii) a_0 is small compared to $\exp(-\beta\varphi)$ for $\varphi \ll 0$. Again only $\varphi \ll 0$ will be treated here. Starting from (17) and postulating $a_0 \ll \exp(-\beta\varphi)$, or $\exp(-\beta\varphi) > 2 \cdot 10^{-2}/k_{sh}$, one obtains

$$\theta_- = \frac{RT}{n^2F^2} \cdot \frac{\delta_0}{C_0^*D_0\beta} \tag{20}$$

$$\sigma = \frac{RT}{n^2F^2\sqrt{2D_0}} \cdot \frac{\exp(-\beta\varphi)}{a_0\beta C_0^*}$$

Thus, θ becomes constant, independent of k_{sh} and potential, for $\varphi \ll 0$ (*cf.* the θ-curves in Figs. 1 and 2 for $\varphi \ll 0$).

Surprisingly, $1/q$ reaches a maximum in this potential region, the value of which is approximately equal to $1/\theta_-$, given by (20). The *peak-potential* of this wave is given by

$$(\varphi_-)_m = -\frac{1}{\beta} \ln\left[\frac{1}{k_{sh}}\left(\frac{2\omega D_0^3}{\delta_0^2}\right)^{\frac{1}{4}}\right] \tag{21}$$

As $1/q$ is proportional to C_0^* even for very low k_{sh}-values, a straight calibration line will be obtained on plotting $(1/q)_m$ against concentration. For a 10% accuracy,

$C_O^* > 10^{-7}/n^2$ mole cm^{-3} should hold, which can be derived in an analogous way as in ref. 7. It is worthwhile to stress that this limit is independent of k_{sh}.

For $\varphi \gg 0$, another peak appears in the $1/q$-plot, the height of which is approximately equal to the reciprocal of the limiting value of θ on the anodic side

$$\theta_+ = \frac{RT}{n^2F^2} \cdot \frac{\delta_R}{C_R^* D_R \alpha} \tag{22}$$

Thus, this peak height is proportional to C_R^* and this concentration can be evaluated from it, if $C_R^* > 10^{-7}/n^2$ mole/cm^3.

THE A.C. POLAROGRAPHY OF IRREVERSIBLE ELECTRODE REACTIONS

From the definition (15) of q it follows that $1/q$ is identical to Y_F', the real component of the faradaic admittance. Consequently, the $1/q$–E plot represents the theoretical *in-phase a.c. polarogram*. The absolute value of the faradaic admittance is equal to $Y_F' \sqrt{1+1/(p+1)^2}$, which means that the theoretical *normal a.c. polarogram* is approximately identical with the $1/q$–E plot if $p > 2$.

According to the *reversible* eqns. (13), the maximum value of $1/q$ would decrease for decreasing k_{sh}-values, so that a very irreversible reaction would not exhibit a detectable peak in an a.c. polarogram, as is generally assumed. DELMASTRO AND SMITH[13], for example, make this supposition, although in our opinion their calculated a.c. polarograms disprove their own assumption. From the general eqns. (12), however, it follows that, in fact, for small k_{sh} the faradaic alternating current is very small at potentials near to E_0, but increases on cathodic polarization forming a substantial peak (Fig. 1). As pointed out in the preceding section, the peak height is proportional to C_O^* and with increasing irreversibility reaches a limiting value, independent of k_{sh}. The peak width also becomes constant. The peak potential shifts away from E_0 to more negative values for decreasing k_{sh} (*cf.* (21)).

The question then arises, whether the peak current is large enough to be detectable, compared to the capacity current. For normal polarographic conditions (*e.g.*, $C_O^* = 5$ mM, $n = 2$, $\alpha = 0.5$, $C_d = 25$ μF cm^{-2}, frequency 100 Hz) $1/q_m = 0.04$ Ω^{-1} cm^{-2} and $\omega C_d = 0.01$ Ω^{-1} cm^{-2}, so that the a.c. wave can be detected easily.

Another striking conclusion is, that with both O and R present, two very distinct peaks occur in the a.c. polarogram, even for moderately irreversible electrode reactions. The occurrence of two peaks could be interpreted as indicating that two different electrode reactions take place (*cf.* ref. 18). Evidently, for irreversible reactions this is not necessarily true. Curve 2 in Fig. 1 also shows two maxima although $C_R^* = 0$, similar to the curve published by MATSUDA[4] for the same conditions. This splitting up of the a.c. wave is quite accidental because it appears only for $k_{sh} \sim 10^{-3}$ cm sec^{-1}. For other k_{sh}-values only one peak appears for $C_R^* = 0$ and therefore these two maxima are of different nature from the two peaks occurring in an a.c. polarogram for low k_{sh}-values with both O and R present. Therefore, even the occurrence of two peaks with only O present, does not prove unequivocally that two reactions take place.

A number of authors[5,14–17] have reported theoretical and experimental studies concerning the drop-time dependence of a.c. polarographic currents. If in addition to diffusion, some process influences kinetically the d.c. current, the surface concentra-

tions and hence the a.c. current are time-dependent. For irreversible reactions the slow electron transfer is such a process.

From (14) and (20) it follows that for very irreversible electrode reactions $(1/q_-)_m$ is proportional to $t^{-\frac{1}{2}}$. This is verified by the data of AYLWARD AND HAYES[14] for the quasi-reversible reduction of the cadmium–EDTA complex. If the peak heights from their Table 1 are plotted against $t^{-\frac{1}{2}}$, a straight line is obtained, Fig. 3 (note that there exists also a pre-wave in the reduction of the cadmium–EDTA complex which is an electrode reaction preceded by a chemical reaction and shows also a time-dependency, their Table 3). AYLWARD AND HAYES[14] assume that the time-dependence of the peak height for the oxidation of an amalgam is caused by streaming at the mercury surface. Streaming will certainly influence the time-dependence of an a.c. current, but

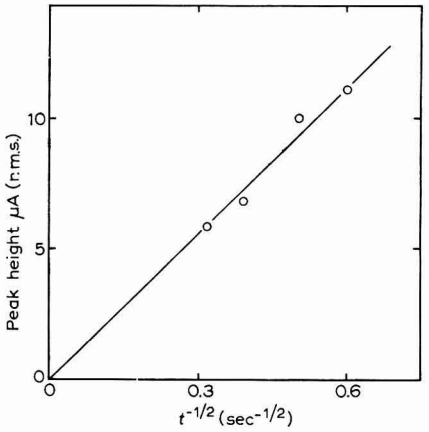

Fig. 3. The a.c. peak height for the reduction of the cadmium–EDTA complex as a function of $t^{-\frac{1}{2}}$ from data published by AYLWARD AND HAYES[14].

even if there is no streaming, the currents will be time-dependent for irreversible reactions (*cf.* (22) together with (14)).

DISCUSSION

As was mentioned in the introduction, general theories on a.c. polarography (valid for reversible and irreversible systems) are given by MATSUDA[4] and AYLWARD *et al.*[5], but only for $C_R^* = 0$, so that a comparison with our results can be made only for this case. AYLWARD *et al.* made the same approximations as in this paper and showed that the resulting a.c. current compares favourably with the more rigorous, but still not exact expressions for a D.M.E. of MATSUDA. According to DELMASTRO AND SMITH[13], the latter lie closest to their more correct expressions for a D.M.E., so that it can be concluded that our expressions, which are more accessible, are a good approximation for a D.M.E.

The numerically calculated polarograms of MATSUDA[4] and AYLWARD *et al.*[5] are similar to the curves in Fig. 1. It can be calculated that for their curves the peaks are proportional to β for low k_{sh}-values, as predicted by (20). The curves given by MATSUDA also show that the peak reaches a limiting value for decreasing k_{sh}-values,

although he did not state both facts explicitly, perhaps because of the complexity of his equations.

To our knowledge, it has not been stated before in the literature that (i) even very irreversible systems still exhibit peaks in an a.c. polarogram, the peak height being independent of k_{sh} and proportional to α or β (eqns. (20) and (22)) and (ii) that two distinct peaks occur in an a.c. polarogram for irreversible systems with both O and R of the reactant present.

In a recent publication[3] we reported the occurrence of at least two peaks in the a.c. polarograms of the $Zn^{2+}/Zn(Hg)$ reaction in 1 M KCl in the presence of a surface-active substance; this was thought to give further evidence for the hypothesis, that the reaction proceeds *via* univalent zinc. The present results suggest that this hypothesis is untenable.

We shall communicate on the mechanism of the zinc reaction more extensively in a further paper and describe experimental results supporting the theory presented here.

ACKNOWLEDGEMENT

This investigation was supported in part by the Netherlands Foundation for Chemical Research (SON) with financial aid from the Netherlands Organisation for the Advancement of Pure Research (ZWO).

SUMMARY

A theoretical treatment for the potential dependence of the faradaic impedance, in the case that the electrode reaction behaves irreversibly with respect to the direct current, using the steady-state concept, is presented. An analysis of the expressions obtained in the complex impedance plane is given and a method is described to measure even a very small rate constant, k_{sh}. The consequences for a.c. polarography are discussed. It has been found that even very irreversible electrode reactions exhibit substantial peaks in an a.c. polarogram. If only the oxidized form of the reactant is present, one peak appears even for very small k_{sh}-values. For decreasing k_{sh}, the peak height decreases to a limiting value, independent of k_{sh} and sufficiently large to be detectable in an a.c. polarogram. If both the oxidized and reduced form are present, two peaks occur for irreversible systems, the peak heights again being independent of the k_{sh}-value.

REFERENCES

1 M. SLUYTERS-REHBACH AND J. H. SLUYTERS, *Rec. Trav. Chim.*, 83 (1964) 581.
2 A. B. IJZERMANS, M. SLUYTERS-REHBACH AND J. H. SLUYTERS, *Rec. Trav. Chim.*, 84 (1965) 764.
3 M. SLUYTERS-REHBACH, A. B. IJZERMANS, B. TIMMER, J. B. GRIFFIOEN AND J. H. SLUYTERS, *Electrochim. Acta*, 11 (1966) 483.
4 H. MATSUDA, *Z. Elektrochem.*, 62 (1958) 977.
5 G. H. AYLWARD, J. W. HAYES AND R. TAMAMUSHI, *Proceedings 1st Australian Conference on Electrochemistry, 1963*, Pergamon Press, Oxford, 1964, p. 323.
6 M. REHBACH AND J. H. SLUYTERS, *Rec. Trav. Chim.*, 80 (1961) 469.
7 M. SLUYTERS-REHBACH AND J. H. SLUYTERS, *Rec. Trav. Chim.*, 82 (1963) 525.
8 E. WARBURG, *Ann. Physik*, 67 (1899) 493; 6 (1901) 125.
9 H. EYRING, L. MARKER AND T. C. KWOH, *J. Phys. Colloid Chem.*, 53 (1949) 1453.

10 P. DELAHAY, *New Instrumental Methods in Electrochemistry*, Interscience, New York, 1954.
11 J. E. B. RANDLES, *Discussions Faraday Soc.*, 1 (1947) 11.
12 J. H. SLUYTERS, *Rec. Trav. Chim.*, 79 (1960) 1092.
13 J. R. DELMASTRO AND D. E. SMITH, *J. Electroanal. Chem.*, 9 (1965) 192.
14 G. H. AYLWARD AND J. W. HAYES, *J. Electroanal. Chem.*, 8 (1964) 442.
15 H. L. HUNG AND D. E. SMITH, *Anal. Chem.*, 36 (1964) 922.
16 G. H. AYLWARD AND J. W. HAYES, *Anal. Chem.*, 36 (1964) 2218.
17 D. E. SMITH AND H. L. HUNG, *Anal. Chem.*, 36 (1964) 2219.
18 H. L. HUNG AND D. E. SMITH, *J. Electroanal. Chem.*, 11 (1966) 237, 425.

ELECTROANALYTICAL CHEMISTRY AND INTERFACIAL ELECTROCHEMISTRY
Elsevier Publishing Company, Amsterdam – Printed in The Netherlands

ON THE IMPEDANCE OF GALVANIC CELLS

XIX. THE POTENTIAL DEPENDENCE OF THE FARADAIC IMPEDANCE IN THE CASE OF AN IRREVERSIBLE ELECTRODE REACTION; EXPERIMENTAL VERIFICATION FOR THE REDOX COUPLE Eu^{3+}/Eu^{2+} IN 1 *M* $NaClO_4$ AND THE MECHANISM OF THE $Zn^{2+}/Zn(Hg)$ REACTION IN KCl

B. TIMMER, M. SLUYTERS-REHBACH AND J. H. SLUYTERS
Laboratory of Analytical Chemistry, State University, Utrecht (The Netherlands)
(Received June 18th, 1966)

INTRODUCTION

In a previous paper[1], a theoretical treatment for the potential dependence of the faradaic impedance in the case that the electrode reaction behaves irreversibly with respect to d.c. current (irreversible electrode reaction) was presented. The system, Eu^{3+}/Eu^{2+} in 1 *M* $NaClO_4$, has been chosen to verify this theory. The rate constant of this redox couple is known to be $k_{sh} \approx 10^{-4}$ cm sec^{-1}, so that it is suitable as an example of an irreversible system. Moreover, since both Eu^{3+} and Eu^{2+} exist in the solution, there is no need of amalgams. From the theoretical expressions[1] it is predicted that two peaks occur in an a.c. polarogram if Eu^{3+} and Eu^{2+} are present at sufficiently large concentrations; this will be verified in this paper. Only one electron is involved in the reaction and therefore it is unlikely that an intermediate exists that could also give rise to more peaks[3] (see, however, ref. 4 and comments on this reference by GIERST AND CORNELISSEN[2]).

For the $Zn^{2+}/Zn(Hg)$ reaction in 1 *M* KCl also, more peaks were observed in the a.c. polarogram[5,6]. This was explained by assuming that the reaction proceeds *via* univalent zinc. This assumption will be reconsidered in the light of the new theoretical expressions[1] and of additional experimental data described in this paper.

EXPERIMENTAL

Europium

Solutions of 20 m*M* Eu^{3+} in 1 *M* $NaClO_4$ (pH 3) were prepared by dissolving Eu_2O_3 (Fluka, "puriss") in a small excess of $HClO_4$ and adding the appropriate amount of $NaClO_4 \cdot H_2O$ (Fluka, p.a.). Eu^{2+} was generated in the measuring cell by electrolysis, using a mercury pool at the bottom of the cell as a cathode, and another mercury pool in 1 *M* KCl (connected to the cell *via* a $NaNO_3$–agar salt bridge) as anode. The concentrations of Eu^{3+} and Eu^{2+} were determined polarographically.

The experiments were performed at 25°, using a dropping mercury electrode

(D.M.E.); the drop was knocked off mechanically every 4.6 sec. The solutions were de-aerated with tank nitrogen.

The a.c. polarograms were obtained by the complex plane method[7], which means that the real and imaginary components, Z' and Z'', of the cell impedance are measured as a function of d.c. potential. The impedance measurements were performed with the a.c. bridge described previously[7]. The potential of the D.M.E. was measured against a S.C.E. by means of a potentiometer with high input resistance. The ohmic resistance, R_Ω, of the cell was found either by extrapolation of Z' to infinite frequency or from the value of Z' at d.c. potentials where the faradaic impedance is infinite.

Zinc

The $Zn^{2+}/Zn(Hg)$ couple was studied at a Heyrovsky-type streaming mercury or zinc amalgam electrode (S.M.E.) in a solution of Zn^{2+} in 1 M KCl (pH 3). In this case, cell admittances were measured as a function of d.c. potential (as described previously[8]) instead of cell impedances, because in an impedance circuit the charging current causes a d.c. potential shift[8,9] which disturbs the measurements. The ohmic resistance was found by extrapolation of the cell admittance to infinite frequency.

RESULTS AND DISCUSSION

Europium

D.c. polarograms were recorded for different ratios Eu^{3+}/Eu^{2+} with a total concentration of 20 mM in 1 M $NaClO_4$ (pH 3). By plotting the diffusion limiting currents, i_{1a}, against i_{1c} for different ratios, a straight line is obtained (Fig. 1), from which the diffusion constants for Eu^{3+} and Eu^{2+} can be calculated using the Ilkovic

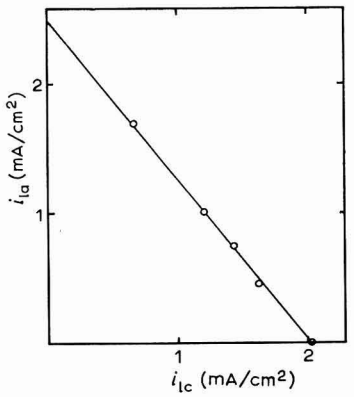

Fig. 1. Plot of the anodic limiting current, i_{1a}, *vs.* the cathodic limiting current, i_{1c}, for different ratios Eu^{3+}/Eu^{2+} at a total concn. of 20 mM. Drop time, 4.6 sec.

equation, *i.e.*, $D_{Eu^{3+}} = 7.0 \times 10^{-6}$ cm^2 sec^{-1} and $D_{Eu^{2+}} = 10.0 \times 10^{-6}$ cm^2 sec^{-1}. A plot of log $i/[(1-i/i_{1c})-(1+i/i_{1a})\ \exp(F\eta/RT)]$ against $\eta = E - E_{eq}$ (ref. 10; p. 171) calculated from a d.c. polarogram, yields log i_0 and $\beta = 1-\alpha$ (i is the current at the end of drop-life, i_0 the exchange current density and α the transfer coefficient).

The results are summarized in Table 1.

The average value of β is 0.57 $\pm$0.04. It is possible to calculate the rate constant, k_{sh}, from the log i_0-values. However, this is not very accurate, due to the uncertainty in β. Better results are obtained by plotting log $i_0/C_{Eu^{3+}}$ against log $C_{Eu^{2+}}/C_{Eu^{3+}}$ (ref. 10; p. 167) yielding $\beta = 0.60 \pm 0.05$ and $k_{sh} = (2.5 \pm 0.5) \cdot 10^{-4}$ cm sec^{-1}. It is also possible to make such a plot from i_0-values calculated from the measured impedances at the equilibrium potential[7,11] for different ratios of Eu^{3+} and Eu^{2+}. This plot yields

TABLE 1

VALUES OF β AND LOG i_0, OBTAINED FROM D.C. POLAROGRAMS

Concn. Eu^{2+} (mM)	*Concn. Eu^{3+} (mM)*	β	*log i_0*
5.1	14.9	0.53	—3.70
10.1	9.9	0.60	—3.65
11.2	8.8	0.56	—3.62
13.5	6.5	0.61	—3.56

$\beta = 0.59$ and $k_{sh} = (2.9 \pm 0.2) \cdot 10^{-4}$ cm sec^{-1}, in good agreement with the result from the d.c. polarograms. These β- and k_{sh}-values are apparent values, as no double-layer correction has been made. The standard potential, $E_0 = -605 \pm 5$ mV (SCE), was determined from the equilibrium potentials at different ratios Eu^{3+}/Eu^{2+}.

GIERST AND CORNELISSEN[2] have studied the Eu^{3+}/Eu^{2+} reaction in various concentrations of $NaClO_4$ and reported $D_{Eu^{3+}} = 7.1 \times 10^{-6}$ cm^2 sec^{-1}, $D_{Eu^{2+}} = 8.3 \times 10^{-6}$ cm^2 sec^{-1} and $E_0 = -600$ mV (SCE). From their Tafel plot for 1 M $NaClO_4$, it can be calculated that $\alpha = 0.49$, $\beta = 0.56$ and $k_{sh} = 1.5 \times 10^{-4}$ cm sec^{-1}. All these values are in reasonable or good agreement with the values reported in this paper.

The impedance measurements were analysed according to the complex plane method by calculating the quantity $1/q = Y_F'$ (real component of the faradaic admittance) as a function of the electrode potential, q being defined by[1,7]

$$q = \theta + \sigma\omega^{-\frac{1}{2}} + \frac{\sigma^2\omega^{-1}}{\theta + \sigma\omega^{-\frac{1}{2}}} \qquad (1)$$

in which θ is the activation polarization resistance and σ the Warburg coefficient. It has been pointed out that a plot of $1/q$ against E is essentially an ideal *real component a.c. polarogram*[1].

These plots are given in Fig. 2 for different concentrations of Eu^{3+} and Eu^{2+}. It can be seen that even an irreversible electrode reaction as that for europium yields substantial peaks in such a polarogram, as was predicted theoretically[1]. From Fig. 3 it follows that the anodic peak height depends linearly on the Eu^{2+} concentration and the cathodic peak height on the Eu^{3+} concentration, as both θ and σ should be inversely proportional to concentration[7].

For 20 mM Eu^{3+}, θ and σ were evaluated from the frequency-dependence of $1/q$[1,7] determined at frequencies between 320 and 2000 Hz. The results are represented in Fig. 4a.

Another method of obtaining θ and σ is by the *method of concentration variation*[1,7], which is carried out in the following way. After subtraction of R_Ω from Z', the remainder is combined with Z'' to calculate Y_{el}', and Y_{el}'', the real and imaginary compo-

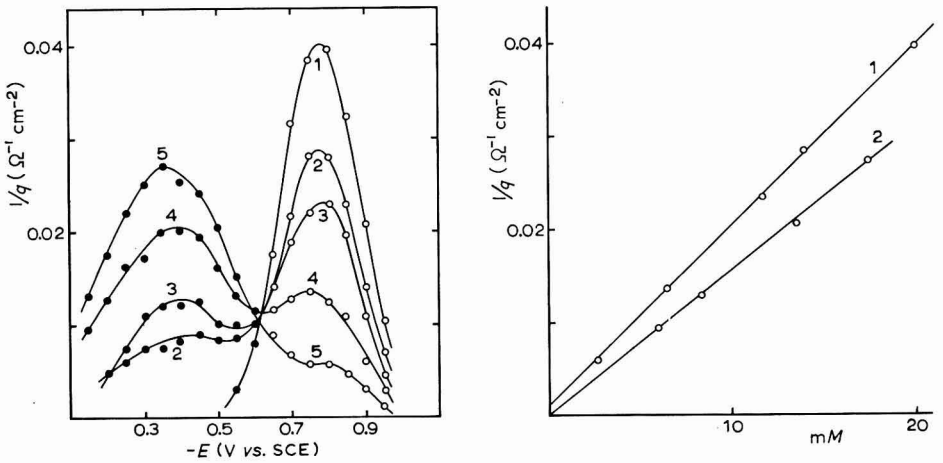

Fig. 2. The real component of the faradaic admittance ($1/q$) as a function of potential at 480 Hz (D.M.E.). (●), potentials anodic to E_0; (○), cathodic potentials. Concns.: (1), 20 mM Eu^{3+}; (2), 14 mM Eu^{3+} + 6 mM Eu^{2+}; (3), 11.7 mM Eu^{3+} + 8.3 mM Eu^{2+}; (4), 6.5 mM Eu^{3+} + 13.5 mM Eu^{2+}; (5), 2.6 mM Eu^{3+} + 17.4 mM Eu^{2+}.

Fig. 3. Calibration lines: (1), Eu^{3+}; (2), Eu^{2+}.

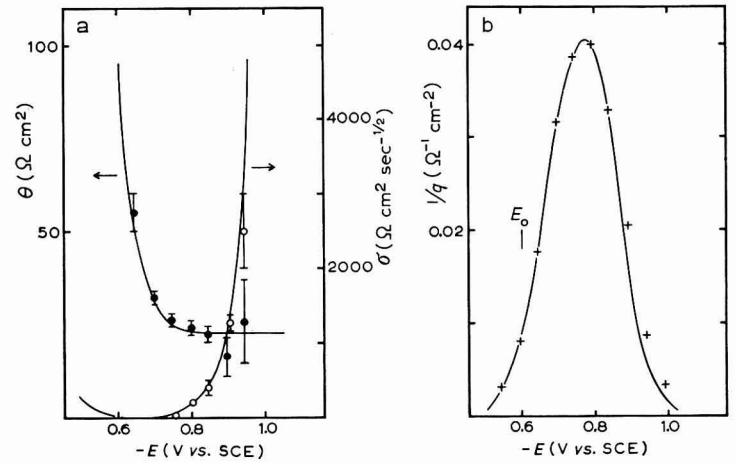

Fig. 4 (a). The activation polarization resistance θ (●) and the Warburg coefficient σ (○) as a function of potential for 20 mM Eu^{3+} obtained with the frequency variation method (D.M.E.). Theoretical curves (full lines) are calcd. from eqn. 4.
(b) Plot of $1/q$ *vs.* potential (+) for 20 mM Eu^{3+} at 480 Hz. Theoretical curve (full line) is calcd. from (1) and (4).

nents of the admittance of the electrode–solution interface (electrode admittance):

$$Y_{el}' = \frac{Z' - R_\Omega}{(Z' - R_\Omega)^2 + (Z'')^2} \tag{2}$$

$$Y_{el}'' = \frac{Z''}{(Z' - R_\Omega)^2 + (Z'')^2} \tag{3}$$

(note that $Y_{el}' = 1/q$). If $p = \theta/\sigma\omega^{-\frac{1}{2}}$ and C_d is the double-layer capacity, $Y_{el}'' = \omega C_d + Y_{el}'/(p+1)$ holds; if at a certain potential, therefore, Y_{el}' and Y_{el}'' are varied, a plot of Y_{el}'' against Y_{el}' will be a straight line if C_d remains constant. Normally, the variation of Y_{el}' and Y_{el}'' is effected by varying the total concentration of the electroactive species. In the case of an irreversible reaction, the procedure is also possible for sufficiently anodic or cathodic potentials, by varying the Ox/Red ratio, keeping the total concentration constant. The latter procedure has been followed in our case and indeed straight lines were obtained at different potentials. The p-values obtained in this way were in accordance with those of the frequency variation and were used to calculate θ and σ from the $1/q$-curve in Fig. 1 for 6.5 mM Eu^{3+} and 13.5 mM Eu^{2+} (Fig. 5a).

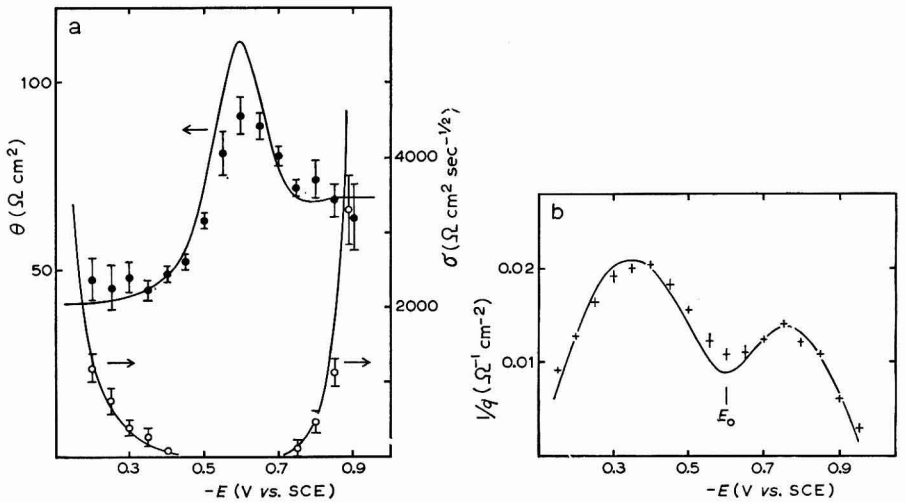

Fig. 5 (a). The activation polarization resistance θ (●) and the Warburg coefficient σ (○) as a function of potential for 6.5 mM Eu^{3+} + 13.5 mM Eu^{2+} obtained with the concn. variation method (D.M.E.). Theoretical curves (full lines) are calcd. from eqn. 4.
(b) Plot of $1/q$ *vs.* potential (+) for 6.5 mM Eu^{3+} + 13.5 mM Eu^{2+} at 480 Hz. Theoretical curve (full line) is calcd. from (1) and (4).

In Figs. 4 and 5, theoretical curves also have been drawn for comparison with the experimental results. The curves were calculated from the theoretical expressions[1] for θ and σ:

$$\theta = \frac{RT}{n^2F^2k_{sh}} \cdot \frac{a_O + (a_O/a_R)\exp(\alpha\varphi) + \exp(-\beta\varphi)}{a_O\exp(-\beta\varphi)[\beta + (1/a_R)\exp(\alpha\varphi)]C_O^* + \exp(\alpha\varphi)[\alpha a_O + \exp(-\beta\varphi)]C_R^*} \tag{4a}$$

$$\sigma = \frac{RT}{n^2F^2\sqrt{2}} \{D_R^{-\frac{1}{2}}\exp(\alpha\varphi) + D_O^{-\frac{1}{2}}\exp(-\beta\varphi)\} \cdot \frac{a_O + (a_O/a_R)\exp(\alpha\varphi) + \exp(-\beta\varphi)}{a_O\exp(-\beta\varphi)[\beta + (1/a_R)\exp(\alpha\varphi)]C_O^* + \exp(\alpha\varphi)[\alpha a_O + \exp(-\beta\varphi)]C_R^*} \tag{4b}$$

in which $a = D/\delta k_{sh}$ where δ is the thickness of the diffusion layer ($\delta = \sqrt{3/7\pi Dt}$ for a D.M.E.) and $\varphi = nF/RT\ (E - E_0)$. The necessary data for the calculation of the a.c.

curves were obtained from the d.c. measurements. The following values have been used: $E_0 = -605$ mV (S.C.E.), $\alpha = 0.4$, $k_{sh} = 2.5 \times 10^{-4}$ cm sec^{-1}, $D_O = 7.0 \times 10^{-6}$ cm^2 sec^{-1}, $D_R = 10.0 \times 10^{-6}$ cm^2 sec^{-1}, $\sqrt{\omega} = 54.9$ sec$^{-\frac{1}{2}}$ (480 Hz), $a_O = 3.9$ and $a_R = 4.7$.

The agreement between the experimental and theoretical results is very good for 20 mM Eu^{3+} (Fig. 4). This is somewhat beyond expectation, in view of the fact that some data (especially α) used in the calculations are not accurately known. The curves in Fig. 5 for 6.5 mM Eu^{3+} and 13.5 mM Eu^{2+} do not agree well for potentials in the vicinity of E_0, but the agreement is still reasonable. At these potentials the theoretical curves are sensitive for errors in the k_{sh}-value inserted. If $k_{sh} = 2.9 \times 10^{-4}$ cm sec^{-1} is inserted, as was calculated from the a.c. measurements, a better fit of the theoretical and experimental curves is obtained. At potentials more remote from E_0, θ and σ are not very sensitive to the k_{sh}-value (*cf.* eqn. (20) and (22) of ref. 1) so that the calculated curves of Fig. 4 do not change at all, or only slightly, if the k_{sh}-value is varied.

Figure 3 shows that the $1/q$(peak) against concentration plot passes through the origin for Eu^{2+}, whereas the plot for Eu^{3+} has a (small) positive intercept. This is explained by the fact that at the cathodic peak potential (-775 mV) the contribution of C_R^* ($=20$ mM if $C_O^* = 0$) in the denominator of the expressions for θ and σ (4) is not negligible, as can be calculated theoretically using the data given above. The experimental intercept is of the same magnitude as the theoretical one. At the anodic peak potential (-350 mV), the contribution of the term in C_O^* is too small to be detected.

Summarizing, it can be concluded that the experimental results for the faradaic impedance of the Eu^{3+}/Eu^{2+} system are in good accordance with the theory for the potential dependence of the faradaic impedance in the case of irreversible electrode reactions[1].

Zinc

Recently[6] we communicated on the mechanism of the $Zn^{2+}/Zn(Hg)$ reaction. The occurrence of more than one peak in the $1/q$-plot was thought to prove that the reaction proceeds *via* univalent zinc. Theoretical calculations were made to show that for a one-step electrode reaction only one peak could occur. However, the theoretical expressions used were incorrect and a better treatment[1] shows that two peaks can occur.

The theoretical a.c. polarograms ($1/q$-plots) in ref. 1 (Figs. 1 and 2) have been calculated with parameters that are known to pertain to the $Zn^{2+}/Zn(Hg)$ reaction (α, D_O, D_R) at a D.M.E. (δ_O and δ_R). The experimental $1/q$-plots for a D.M.E. with varying concentration of surfactant BRY 35 (Figs. 8 and 9 of ref. 6) agree qualitatively with the theoretical curves calculated for different k_{sh}-values. The experimental cathodic (Zn^{2+}) wave has the same height and shape as the corresponding theoretical one. The experimental anodic (zinc amalgam) wave is considerably lower than theory predicts. This could be caused by the fact that $\delta_R \sim 2.10^{-2}$ cm is too large with respect to the radius of the droplet, $r \sim 5 \cdot 10^{-2}$ cm, so that the assumption of linear diffusion no longer holds. The *shoulder* in the anodic range at -0.45 V (S.C.E.) (peak Ia in Fig. 8 of ref. 6) is not in accordance with the theory[1] presented. Probably, the potential dependence of the adsorption of the surfactant and therefore of the rate constant k_{sh}, has to be taken into account[12].

Since this complication does not occur if the reaction is made more *irreversible* by using a S.M.E., a comparison of experiment and theory in this case seems worthwile. For this purpose we measured the admittances of a streaming 3-mM zinc amalgam electrode in a 1 M KCl (pH 3) solution of 3 mM Zn^{2+} at different potentials for frequencies between 320 and 2500 Hz. From these measurements, θ and σ were calculated as for europium (Fig. 6). The solution was adjusted to pH 3 because the small peak at -1330 mV (S.C.E.)[5], earlier ascribed to the $Zn(OH)_2/Zn$ reaction[13], does not then appear.

For the calculation of the theoretical θ- and σ-curves in Fig. 6, we inserted in (4) the following data[7,14] which are relevant to the zinc couple at a S.M.E.:

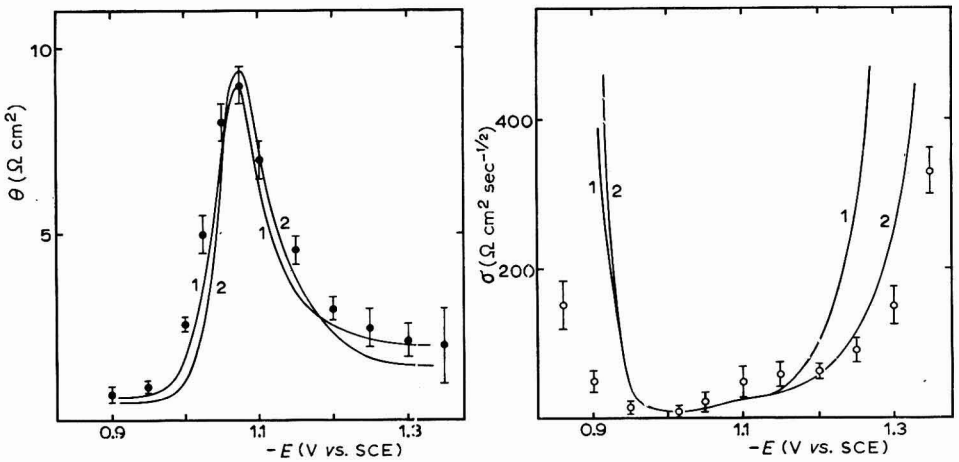

Fig. 6. The activation polarization resistance θ (●) and the Warburg coefficient σ (○) as a function of potential for 3 mM Zn(Hg) + 3 mM Zn^{2+} in 1 M KCl (pH 3) obtained with the frequency variation method (S.M.E.). Theoretical curves (full lines) are calcd. from eqn. 4; (1), $\alpha = 0.70$; (2), $\alpha = 0.75$. For other data see text.

$D_{Zn} = 2\ D_{Zn^{2+}} = 1.6 \times 10^{-5}$ cm² sec^{-1}, $n = 2$, $E_0 = -1025$ mV (S.C.E.) and for curve 1 $\alpha = 0.7$, $a_O/a_R = 0.8$, $a_O = 10$, $k_{sh} = 3.8 \times 10^{-3}$ cm sec^{-1} and for curve 2, $\alpha = 0.75$, $a_O = a_R = 15$, $k_{sh} = 4.2 \times 10^{-3}$ cm sec^{-1}†. The main difference between the two curves is caused by α; the other data are chosen to obtain the best fit with the experimental results. It should be noted that, strictly speaking, (4) may not be used for a S.M.E.[5], but in this case the more rigorous expression[5] reduces to (4) since the frequencies used are sufficiently high[8]. The agreement between experimental and theoretical results is reasonable, considering that the d.c. potential is not corrected for the ohmic drop in the solution ($R \sim 30\ \Omega$ and the direct current of the order of milliamperes).

The same data have been used to calculate theoretical $1/q$-plots for the S.M.E.; these can be compared with the experimental plots already published[6]. Again, the agreement is good and even the *shoulder* in the $1/q$-plot for $C_{Zn}^* = 0$ appears in the theoretical curve; this shoulder does not prove, therefore, that two electrode reactions are taking place.

We also measured admittances of a S.M.E. in 0.1 M and 1 M KCl solutions

† Theoretically $\delta = \frac{1}{2}\sqrt{\pi D t}$ for a S.M.E., if t is the contact time, as can be derived from the limiting current expression for a S.M.E.

(pH 3) with varying concentration of BRY 35 up to 1 g/l. The $1/q$-plots obtained from these measurements have, qualitatively, the same form as the curves for a D.M.E. in the presence of BRY 35[6]. They are not represented here, as it is difficult to interpret them quantitatively. The unknown potential dependence of k_{sh} has to be taken into account[12]; moreover, the concentration profiles of the electroactive species and BRY 35 at a S.M.E. are not known exactly[5] and it would be difficult to obtain for this case even simplified expressions for the faradaic impedance.

It may be concluded that the a.c. measurements at the D.M.E. and the S.M.E. for the zinc redox couple in 1 *M* KCl give no definite evidence of an intermediate Zn^+ as was thought in a previous paper[6].

Some investigators[7,13] have reported the occurrence of a small second peak in the a.c. polarograms of zinc in 1 *M* KCl at a D.M.E. In *normal a.c. polarograms* this peak was found to disappear on lowering the pH or de-aerating the solution[13] and therefore it was ascribed to the formation of $Zn(OH)_2$ on the electrode surface due to OH^- arising from the reduction of O_2. According to our experience the second peak becomes smaller in acidic solutions, but does not disappear (*cf.* dashed curve in Fig. 9 of ref. 6). This is fully in accordance with the theoretical polarogram, given in ref. 1 (curve 1 in Fig. 1) and it must therefore be concluded that the second peak found for acid solutions is due to the $Zn^{2+}/Zn(Hg)$ reaction as is the first peak. The enhancement in neutral solution may be explained in two ways: either by the assumption that $Zn(OH)_2$ is formed, or by the assumption that k_{sh} decreases slightly resulting in a lowering of the first peak and an increase in the second.

Existence of univalent zinc

The mechanism of the $Zn^{2+}/Zn(Hg)$ reaction has been the subject of many investigations and the existence of the Zn^+ ion as an intermediate is postulated in a number of publications. We comment below on these papers in the light of our own findings.

DIRKSE[15] concluded that the electrode reaction of zinc in KOH solutions proceeds *via* Zn^+, erroneously supposing that the reaction is reversible, as he noticed in a later paper[16]. His experimental data can be explained fully by the assumption that the irreversible electrode reaction

$$ZnO_2^{2-} + 2\ H_2O + 2\ e \rightleftarrows Zn + 4\ OH^-$$

proceeds with $\alpha = 0.48$.

HUSH AND BLACKLEDGE[14] measured k_{sh} and α of the zinc couple in $NaClO_4$ solutions of different ionic strength. They concluded from the concentration dependence of k_{sh} and α that there is some evidence for the consecutive-step mechanism. However, it should be noted that the corrections for the double-layer structure (*Frumkin theory*, ref. 10, chap. 7) in the case of a single charge-transfer step should be made in the calculation of k_{sh} and α before drawing conclusions from a concentration dependence.

The Frumkin correction for k_{sh} can be made according to[10]

$$(k_{sh})_{app} = (k_{sh})_t \exp(\beta n - Z_O) F\varphi_2/RT \qquad (5)$$

in which $(k_{sh})_{app}$ and $(k_{sh})_t$ are the rate constants without and with the double-layer correction, Z_O is the ionic valence with sign of the oxidized form of the electroactive

nspecies and φ_2 is the potential i the outer plane of closest approach. Unfortunately, we have no data for φ_2 for $NaClO_4$ solutions, but at potentials close to E_0 of the zinc couple, specific adsorption of ClO_4^- is small[17] and data for NaF[18] or KCl[19] may be used as an approximation. With these data it can be calculated from (5) that in the concentration range 0.1–1 M, $(k_{sh})_{app}$ for a simultaneous two-electron transfer behaves similarly to that observed by HUSH AND BLACKLEDGE. Moreover, a correction should be made for the change in activity coefficients. If the reasonable assumption is made that the activity coefficients increase for decreasing concentration, the apparent k_{sh}-values will increase, in accordance with experiment.

From the current–voltage relation with double-layer correction[10], it can be derived in our notation that

$$1-\alpha_{app} = (\beta_{app}) = 1-\alpha_t+(\alpha_t-1+Z_0/n)\ (\varphi_2-\varphi_2^{eq})/(E-E_{eq}) \qquad (6)$$

If $\alpha_t = 0.70$ and $Z_0 = n = 2$ are inserted, this expression yields, with the φ_2-data of NaF, that β_{app} changes from 0.32 to 0.35 for 1 to 0.1 M solutions. For the φ_2-values of KCl, β_{app} ranges from 0.33 to 0.36. It can be seen that an increase in β_{app} can be explained in this way. The increase in β observed by HUSH AND BLACKLEDGE is, however, larger than was calculated from (6) with approximate data for φ_2, and should be otherwise explained. On the other hand, KORYTA[20] has made an analogous investigation of the zinc reaction in $NaNO_3$ solutions which shows that k_{sh} and α are independent of the $NaNO_3$ concentration if the proper double-layer corrections are made. Thus from the concentration dependence of k_{sh} and α found by HUSH AND BLACKLEDGE[14] little evidence remains for the existence of the Zn^+ ion.

The high value of β at anodic overpotentials, calculated by these authors from the amalgam dissolution currents, could indicate the existence of Zn^+. However, it should be noted that, frequently, a maximum occurs in the anodic Zn(Hg) current (*cf.* dashed curve in Fig. 6 of ref. 6), which possibly could lead to an erroneous value of β. This is supported by the rather large inaccuracy in β found by HUSH AND BLACKLEDGE.

To explain the irreversibility of the zinc electrode reaction apparent from the oscillopolarograms, HEYROVSKY[21,22] assumed that the Zn^+ intermediate exists. This is said to be indicated by the dependence of the oscillopolarograms on temperature, frequency and the presence of gelatine. In our opinion, HEYROVSKÝ has presented a possible theoretical explanation for the irreversibility of the zinc reaction but has given no conclusive experimental proof for the existence of Zn^+. The different positions of the anodic and cathodic incisions only prove the irreversible character of a reaction, (*cf.* in the voltage sweep method[23], even for reversible reactions, the anodic and cathodic peak are 2.2 RT/nF apart) but do not necessarily imply the existence of an intermediate. The dependence on temperature, frequency and gelatine cannot be interpreted in terms of any mechanism until theoretical expressions are available for the oscillopolarograms of irreversible electrode reactions.

Finally, if the Zn^+ ion is an intermediate in the zinc reaction, the most acceptable fate of Zn^+ is the dismutation[5,6]

$$2\ Zn^+ \rightarrow Zn + Zn^{2+}$$

We have made a chronopotentiometric study to obtain, if possible, the value of the dismutation rate constant, k. Transition times, τ, of 20 sec–10 msec were measured

at a hanging mercury drop in 5 mM and 10 mM Zn^{2+} solutions in 1 M KCl (pH 3) with 20 and 50 mg/l of the surfactant, BRY 35. For $\tau > 1$ sec, a correction was made for the sphericity of the drop[24]. From a plot of $i/\sqrt{\tau}$ against $i^{\frac{2}{3}}$, the rate constant, k, can be calculated[25]. These plots showed that the dismutation, if present, is very fast ($k > 10^9$ l/mole sec). It is, therefore, unlikely that Zn^+ could be detected experimentally.

In our opinion, no definite proof for the existence of the Zn^+ ion as an intermediate in the zinc electrode reaction has so far been presented in literature. The experimental data can be explained by the one-step electrode reaction

$$Zn^{2+} + 2\,e \rightleftarrows Zn(Hg)$$

ACKNOWLEDGEMENT

This investigation was supported in part by the Netherlands Foundation for Chemical Research (SON) with financial aid from the Netherlands Organisation for the Advancement of Pure Research (ZWO).

SUMMARY

An experimental verification of the theory for the potential dependence of the faradaic impedance in the case of irreversible electrode reactions, described in part XVIII, is presented for the Eu^{3+}/Eu^{2+} couple in 1 M $NaClO_4$ at a D.M.E. It is shown that two peaks occur in an a.c. polarogram, if both Eu^{3+} and Eu^{2+} are present. A good quantitative agreement exists between the experimentally found- and theoretically calculated-faradaic impedance as a function of electrode potential.

The consequences of the theoretical treatment in part XVIII are discussed for the zinc couple in the presence of surfactants. The a.c. measurements do not prove that the reaction proceeds *via* univalent zinc, as was concluded earlier. The evidence for the existence of the Zn^+ ion, published by a number of authors, is discussed and it is concluded that no definite proof for the existence of Zn^+ has so far been presented.

REFERENCES

1 B. TIMMER, M. SLUYTERS-REHBACH AND J. H. SLUYTERS, *J. Electroanal. Chem.*, 14 (1967) 169.
2 L. GIERST AND R. CORNELISSEN, *Collection Czech. Chem. Commun.*, 25 (1960) 3004.
3 H. L. HUNG AND D. E. SMITH, *J. Electroanal. Chem.*, 11 (1966) 237, 425.
4 A. A. VLCEK, *Collection Czech. Chem. Commun.*, 24 (1959) 181.
5 A. B. IJZERMANS, M. SLUYTERS-REHBACH AND J. H. SLUYTERS, *Rec. Trav. Chim.*, 84 (1965) 729, 764.
6 M. SLUYTERS-REHBACH, A. B. IJZERMANS, B. TIMMER, J. B. GRIFFIOEN AND J. H. SLUYTERS, *Electrochim. Acta*, 11 (1966) 483.
7 M. SLUYTERS-REHBACH AND J. H. SLUYTERS, *Rec. Trav. Chim.*, 82 (1963) 525, 535.
8 A. B. IJZERMANS AND J. H. SLUYTERS, *Rec. Trav. Chim.*, 84 (1965) 740, 751.
9 P. DELAHAY, *J. Electroanal. Chem.*, 10 (1965) 1, 165.
10 P. DELAHAY, *Double-layer and Electrode Kinetics*, Interscience, New York, 1965.
11 J. E. B. RANDLES, *Discussions Faraday Soc.*, 1 (1947) 11.
12 M. SLUYTERS-REHBACH, B. TIMMER AND J. H. SLUYTERS, *Z. Physik. Chem.*, 52 (1967) 89.
13 T. TAKAHASHI AND H. SHIRAI, *J. Electroanal. Chem.*, 1 (1959) 331.
14 N. S. HUSH AND J. BLACKLEDGE, *J. Electroanal. Chem.*, 5 (1963) 420.
15 T. P. DIRKSE, *Z. Physik. Chem. N.F.*, 5 (1955) 1.
16 T. P. DIRKSE, *Z. Physik. Chem.*, 33 (1962) 387.

17 R. PAYNE, *J. Phys. Chem.*, 70 (1966) 204.
18 C. D. RUSSELL, *J. Electroanal. Chem.*, 6 (1963) 486.
19 R. PARSONS, private communication.
20 J. KORYTA, *Electrochim. Acta*, 6 (1962) 67.
21 J. HEYROVSKÝ, *Discussions Faraday Soc.*, 1 (1947) 212.
22 J. HEYROVSKÝ, *Z. Elektrochem.*, 59 (1955) 802.
23 P. DELAHAY, *New Instrumental Methods in Electrochemistry*, Interscience, New York, 1954, chap. 6.
24 M. G. MCKEON, *J. Electroanal. Chem.*, 4 (1962) 93.
25 O. FISCHER AND O. DRAČKA, *Collection Czech. Chem. Commun.*, 24 (1959) 3046.

ELECTROANALYTICAL CHEMISTRY AND INTERFACIAL ELECTROCHEMISTRY
Elsevier Publishing Company, Amsterdam – Printed in The Netherlands

ÜBER DEN MECHANISMUS DES KATALYTISCHEN WASSERSTOFF-PEROXIDZERFALLS AN AKTIVEN BLANKEN PLATINELEKTRODEN IN ALKALISCHER LÖSUNG

L. MÜLLER
Physikalisch-Chemisches Institut, Humboldt Universität, 108 Berlin
(Eingegangen am 18. Juni 1966)

Die von uns durchgeführten Untersuchungen der kathodischen Reduktion von H_2O_2 in alkalischen Lösungen zeigten[1,2], dass an aktiven glatten Platinelektroden der katalytische heterogene Zerfall von H_2O_2 einen wesentlichen Einfluss auf die Geschwindigkeit des kathodischen Prozesses hat. So konnte von uns mit Hilfe der rotierenden Scheibenelektrode mit Ring nachgewiesen werden[1,2], dass an einer mit chemisorbiertem Sauerstoff bedeckten Pt-Elektrode H_2O_2 quantitativ unter Bildung von molekularem Sauerstoff und Wasser zerfällt, während an einer oxidfreien Pt-Elektrode der katalytische heterogene Zerfall von H_2O_2 stark gehemmt ist.

Der Mechanismus der katalytischen Wirkung der Platinoxide und demzufolge auch der Mechanismus des katalytischen Zerfalls von H_2O_2 an Pt ist gegenwärtig noch nicht aufgeklärt. In der Literatur werden zu dieser Frage verschiedene Standpunkte vertreten. So betrachten GERISCHER[3] und WINKELMANN[4] den Zerfall von H_2O_2 an Pt als einen elektrochemischen Prozess, bestehend aus einem anodischen und kathodischen Teilprozess, während BIANCHI u.a.[5] und VIELSTICH[6] die Zwischenbildung von Pt-oxiden und nachfolgende elektrochemische Reduktion derselben nach

$$Pt + H_2O_2 \rightarrow PtO + H_2O$$
$$PtO + 2e^- + 2H^+ \rightarrow Pt + H_2O$$

annehmen.

In unseren Arbeiten, in denen der stark beschleunigende Einfluss der Pt-Oberflächenoxide auf den katalytischen Zerfall von H_2O_2 untersucht wurde[1,2], wurde dagegen angenommen, dass sich die Versuchsergebnisse am besten mit Hilfe des von HABER UND GRINBERG[7] aufgestellten Zerfallmechanismus erklären liessen. Eine direkte experimentelle Bestätigung eines der oben genannten Mechanismen konnte für alkalische Lösungen bisher nicht gegeben werden. An Hand der von uns durchgeführten Untersuchungen des beschleunigenden Einflusses von Pt-Oberflächenoxiden auf die Reduktion von $S_2O_8^{2-}$ in 0.1 *M* KOH an Pt[8] ist es jedoch möglich geworden, neue Aussagen über den Mechanismus des katalytischen Zerfalls von H_2O_2 an aktiven Platinelektroden in alkalischen Lösungen zu machen.

Bei der Reduktion von $S_2O_8^{2-}$ an Pt zeigte sich nämlich, dass, wie auch im Falle[1] der kathodischen Reduktion von H_2O_2, an der Pt-Oberfläche chemisorbierter Sauerstoff ($\varphi > 0.65$ V) die Geschwindigkeit des kathodischen Prozesses stark be-

schleunigt. Der Einfluss von Platinoberflächenoxiden auf die kathodische Reduktion von $S_2O_8^{2-}$ konnte von uns darauf zurückgeführt werden[8], dass an einer oxidierten Platinelektrode die dissoziative Chemisorption unter Sprengung der O–O-Bindung sehr schnell verläuft, während diese Reaktion an einer reduzierten Pt-Oberfläche stark gehemmt ist. Da $S_2O_8^{2-}$ einerseits die gleiche molekulare Struktur wie H_2O_2 besitzt, und in beiden Fällen die kathodische Reduktion auf eine Spaltung der O–O-Bindung hinausläuft, andererseits aber in beiden Fällen der gleiche beschleunigende Einfluss von Pt-Sauerstoffverbindungen beobachtet wurde, scheint es gerechtfertigt, die an Hand der Reduktion von $S_2O_8^{2-}$ gewonnenen Erkenntnisse über die beschleunigende Wirkung von Platinsauerstoffverbindungen auf die Wirkung derselben beim katalytischen Zerfall von H_2O_2 an glatten aktiven Pt-Elektroden auszudehnen.

Im Falle des katalytischen Zerfalls von H_2O_2 würde das bedeuten, dass die beschleunigende Wirkung von Platinoberflächenoxiden beim katalytischen H_2O_2-Zerfall darauf zurückzuführen ist, dass sie die Einstellung des dissoziativen Chemisorptionsgleichgewichtes von H_2O_2 nach

$$H_2O_2 \rightleftarrows 2\ OH^{\cdot}{}_{chem} \qquad (1)$$

stark beschleunigen, während an einer sauerstofffreien Pt-Oberfläche die Reaktion der dissoziativen Chemisorption von H_2O_2 unter Bildung von OH·-Radikalen stark gehemmt ist.

Um den beschleunigenden Einfluss von Platinoberflächenoxiden auf den katalytischen Zerfall von H_2O_2 an Pt zu erklären, ist es naheliegend, anzunehmen, dass die nach Reaktion (1) an oxidbedeckter Pt-Oberfläche entstandenen OH·-Radikale nicht wie im Falle der Reduktion von $S_2O_8^{2-}$ elektrochemisch reduziert werden, sondern ähnlich wie freie OH·-Radikale in Lösungen[9] mit weiteren H_2O_2-Molekülen reagieren und so den Zerfall von H_2O_2 bewirken.

$$HO_2^- \rightleftarrows OH^{\cdot}{}_{chem} + O^{\cdot-}{}_{chem}$$

$$O^{\cdot-}{}_{chem} + H_2O \rightleftarrows OH^{\cdot}{}_{chem} + OH^-$$

$$OH^{\cdot}{}_{chem} + HO_2^- \rightarrow HO_2^{\cdot} + OH^-$$

$$OH^{\cdot}{}_{chem} + HO_2^{\cdot} \rightarrow H_2O + O_2$$

.....

$$2\ HO_2^- \rightarrow 2\ OH^- + O_2$$

Da an einer reduzierten Pt-Oberfläche die Reaktion der OH·-Radikalbildung nach (1) mit sehr geringer Geschwindigkeit verläuft, sollte man erwarten, dass an oxidfreiem Pt auch die Geschwindigkeit des katalytischen Zerfalls von H_2O_2 wesentlich kleiner ist.

Diese Überlegungen stehen in gutem Einklang mit den von uns früher gefundenen Versuchsergebnissen[1,2], dass an einer reduzierten Pt-Oberfläche die Geschwindigkeit des katalytischen Zerfalls von H_2O_2 sehr klein oder null gegenüber einer oxidbedeckten Pt-Oberfläche ist, an der die Geschwindigkeit des katalytischen Zerfalls von H_2O_2 in 10^{-3} *M* alkalischer H_2O_2-Lösung allein durch die Geschwindigkeit der Zudiffusion bestimmt war. Man kann deshalb sagen, dass der heterogene katalytische Zerfall von H_2O_2 an Pt nach einem Mechanismus verläuft, der durch $OH^{\cdot}{}_{chem}$-

Radikale ausgelöst wird, die sich an einer oxidbedeckten Platinelektrode mit grosser Geschwindigkeit durch dissoziative Chemisorption von H_2O_2 bilden.

ZUSAMMENFASSUNG

Der katalytische Zerfall von H_2O_2 verläuft nach einem Mechanismus, der durch chemisorbierte OH·-Radikale ausgelöst wird, die sich an einer oxidbedeckten Pt-Elektrode mit grosser Geschwindigkeit durch dissoziative Chemisorption von H_2O_2 bilden.

SUMMARY

The catalytic decomposition of H_2O_2 proceeds according to a mechanism in which chemisorbed OH· radicals are produced and which are formed with a greater velocity at an oxide-covered Pt electrode by dissociative chemisorption of H_2O_2.

LITERATUR

1 L. MÜLLER UND L. N. NEKRASSOW, *Dokl. Akad. Nauk SSSR*, 157 (1964) 416.
2 L. MÜLLER UND L. N. NEKRASSOW, *J. Electroanal. Chem.*, 9 (1965) 282.
3 R. GERISCHER UND H. GERISCHER, *Z. Physik. Chem. (Frankfurt)*, 6 (1956) 178.
4 D. WINKELMANN, *Z. Elektrochem.*, 60 (1956) 731.
5 G. BIANCHI, F. MAZZA UND T. MUSSINI, *Electrochim. Acta*, 7 (1962) 457.
6 W. VIELSTICH, *Z. Physik. Chem. (Frankfurt)*, 15 (1958) 409.
7 F. HABER UND S. GRINBERG, *Z. Anorg. Allgem. Chem.*, 18 (1898) 37.
8 L. MÜLLER, *J. Electroanal. Chem.*, 13 (1967) 275.
9 I. A. KASARNOWSKI UND N. P. LIPICHIN, *Izv. Akad. Nauk. SSSR Ser. Khim.*, (1965) 1312.

ELECTROANALYTICAL CHEMISTRY AND INTERFACIAL ELECTROCHEMISTRY
Elsevier Publishing Company, Amsterdam – Printed in The Netherlands

UNE NOUVELLE METHODE DE DOSAGE OSCILLOPOLAROGRAPHIQUE DU COBALT DANS LES MATIERES VEGETALES

PAUL NANGNIOT
Faculté des Sciences Agronomiques de l'Etat, Gembloux (Belgique)
(Reçu le 14 juin, 1966)

1. INTRODUCTION

Dans un article précédent consacré au dosage des oligoéléments métalliques dans les végétaux, nous faisions état de la découverte d'une méthode nouvelle et extrêmement sensible de dosage du cobalt[1].

En examinant le comportement oscillopolarographique des composés formés par le cobalt avec différents complexants organiques, nous avions remarqué que les complexants chélatés obtenus étaient souvent adsorbés à la surface de l'électrode à gouttes de mercure et donnaient lieu à la formation de pics d'adsorption aigus et très intenses.

Parmi les différents complexants mis en oeuvre nous avions retenu la diméthylglyoxime qui fournit en milieu NH_4OH–NH_4Cl un complexe brun soluble permettant d'atteindre la sensibilité limite de 0.004 μg/ml.

Nous nous proposons au cours de cette étude de compléter les informations recueillies précédemment et de comparer les résultats obtenus avec la diméthylglyoxime aux résultats nouveaux provenant de la mise en oeuvre d'autres dioximes, à savoir: la benzyldioxime, la diacétyldioxime et l'α-furyldioxime.

2. APPAREILLAGE ET CONDITIONS EXPÉRIMENTALES

(a) oscillopolarographe différentiel de Davis, A. 1660 (Southern Analytical, Angleterre)
— cellules à électrode de référence interne (nappe de mercure de grande surface) thermostatisées à 25°.

(b) polarographe Amel modèle 462 à 3 électrodes
— cellules à électrode de référence interne saturées au calomel.

Les polarogrammes sont enregistrés à la température ambiante.

L'utilisation d'un oscillopolarographe différentiel n'est pas indispensable; nous avons utilisé précédemment un oscillopolarographe Amel modèle 451 (Milan) à une cellule pour doser le cobalt dans les fourrages. L'emploi d'un système différentiel est, pour un ensemble de motifs qui tombent sous le sens, préférable au système monocellulaire.

La solution stock de cobalt est obtenue par dissolution de cobalt pur dans l'acide sulfurique. Les dioximes utilisées proviennent des firmes suivantes:
diméthylglyoxime: May et Baker (solution alcoolique à 1%)
benzyldioxime: Carlo Erba (solution alcoolique saturée)
diacétyldioxime: Carlo Erba (solution alcoolique à 1%)
Furyldioxime: British Drug House (solution alcoolique à 1%)

3. VARIATIONS DE L'INTENSITÉ DU PIC D'ADSORPTION DU COBALT EN FONCTION DES VARIATIONS DE COMPOSITION DU MILIEU DE BASE

Le milieu de base comprenant de la diméthylglyoxime, du tampon NH_4OH–NH_4Cl et de l'alcool, nous avons étudié l'influence de la variation de concentration de ces trois constituants.

a. Influence de la concentration en diméthylglyoxime

Les chiffres du Tableau 1 montrent les résultats obtenus. Les valeurs des courants, situées dans la deuxième colonne, sont exprimées en unités arbitraires; elles correspondent à la multiplication de la sensibilité utilisée par le nombre de divisions lues sur l'écran de l'oscilloscope.

TABLEAU 1

Cobalt: 1.64 μg/ml; NH_4OH–NH_4Cl: 0.5 *M*

Diméthylglyoxime (%)	*$(i_p)_{Co}$ (unités arbitraires)*	*Diméthylglyoxime (%)*	*$(i_p)_{Co}$ (unités arbitraires)*
0.005	42	0.10	160
0.01	93	0.12	160
0.02	114	0.14	150
0.04	138		
0.08	158		
0.16	150		

La concentration en diméthylglyoxime doit être comprise entre 0.08 et 0.12% pour obtenir le maximum de sensibilité et de stabilité. Dans la pratique, lorsque les solutions à analyser sont portées à 25 ml, on utilise de 2–3 ml de diméthylglyoxime à 1%.

b. Influence de la concentration en alcool

Le Tableau 2 montre qu'il est désavantageux d'ajouter de l'alcool à la solution

TABLEAU 2

Cobalt: 1.64 μg/ml; NH_4OH–NH_4Cl: 0.5 *M*; diméthylglyoxime: 0.08%

Alcool (%)	*$(i_p)_{Co}$ (unités arbitraires)*	*Alcool (%)*	*(unités arbitraires) $(i_p)_{Co}$*
8	158	32	75
16	129	40	57
24	96		

à polarographier. Les pics d'adsorption sont plus sensibles que les pics de diffusion normaux aux variations de composition du milieu de base, notamment aux modifications de la viscosité du solvant dues aux additions d'alcool.

c. Influence de la concentration du tampon NH_4OH–NH_4Cl

Comme le Tableau 2, le Tableau 3 met en évidence la sensibilité du pic d'adsorption du cobalt aux variations de composition du milieu.

TABLEAU 3

Cobalt: 1.64 μg/ml; diméthylglyoxime: 0.08%

NH_4OH–NH_4Cl (M)	*$(i_p)_{Co}$ (unités arbitraires)*	*E_p (V Hg interne)*
0.1	122	−1.18
0.2	138	−1.15
0.3	145	−1.15
0.4	150	−1.15
0.44	155	−1.13

TABLEAU 4

Cobalt: 0.82 μg/ml; diméthylglyoxime: 0.08%

Nature du milieu	*pH*	*$(i_p)_{Co}$ (unités arbitraires)*	*E_p (V Hg interne)*
NH_4Cl–HCl	1.60	0.0	—
NH_4Cl–HCl	1.90	0.0	—
NH_4Cl–HCl	2.50	74	−1.10
NH_4Cl–HCl	3.00	73	−1.10
NH_4Cl–HCl	3.35	74	−1.10
NH_4Cl–HCl	3.75	74	−1.11
NH_4Cl–HCl	4.70	74	−1.11
NH_4Cl	5.50	76	−1.12
NH_4OH–NH_4Cl	7.45	72	−1.12
NH_4OH–NH_4Cl	8.25	70	−1.13
NH_4OH–NH_4Cl	8.40	74	−1.14
NH_4OH–NH_4Cl	9.10	78	−1.16
NH_4OH–NH_4Cl	9.55	49	−1.19
NH_4OH	10.50	0	—
NaOH	13	0	—

d. Influence du pH sur la hauteur du pic d'adsorption

Les valeurs de l'intensité du pic en fonction du pH sont représentées dans le Tableau 4.

La zone de pH utilisable est comprise entre 2.50 et 9.10. En pratique, les valeurs de pH situés entre 5 et 9 sont les plus favorables; rappelons, en effet, qu'avant l'addition de la diméthylglyoxime, on mesure la hauteur des pics dûs au cuivre, au nickel et au zinc et que ces deux derniers ions ne sont déterminables qu'en milieu faiblement acide, neutre ou alcalin.

Cette étude des différents facteurs qui peuvent influencer l'intensité du pic du cobalt ou sa situation sur l'axe des potentiels prouve que le choix effectué an-

térieurement du tampon NH_4OH, 0.5 M–NH_4Cl, 0.5 M peut être maintenu sans réserves.

Indépendamment du pH, le choix des constituants du milieu de base joue un rôle considérable dans l'intensité du pic d'adsorption. Par exemple, dans le tampon acide acétique, 0.5 M–acétate de soude, 0.5 M le pic se situe à -1.06 V et son intensité ne vaut que le sixième de celle qui est observée au même pH, dans le milieu NH_4Cl–HCl. Lorsque l'acide acétique est remplacé par le thiocyanate de potassium, la hauteur du pic est quasi quadruplée, bien que la valeur du pH n'ait subi aucune modification.

Il faut encore signaler que le phénomène d'adsorption du cobalt, si aisément observable en oscillopolarographie à tension imposée, est tout aussi facilement détecté en polarographie classique. La Fig. 1 permet de comparer les polarogrammes obtenus avant et après l'addition de diméthylglyoxime et de se rendre compte de

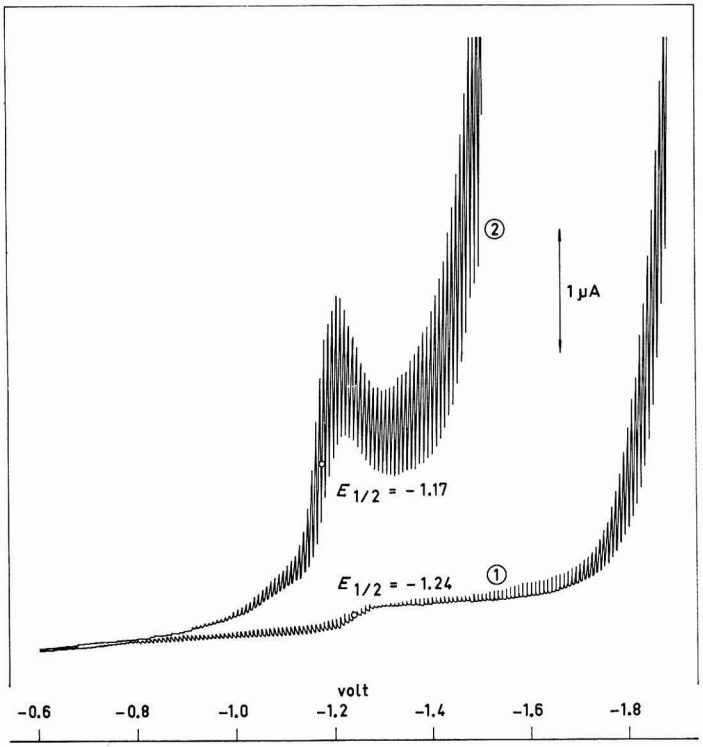

Fig. 1. (1) 1.63 µg Co^{2+}/ml dans NH_4OH–NH_4Cl 0.5 M; (2) idem + diméthylglyoxime 0.08%.

l'important gain de sensibilité qui résulte de l'adsorption du complexe à la surface de l'électrode.

Une autre manière de mettre en évidence l'adsorption consiste à relever point par point la courbe électrocapillaire.

La Fig. 2 montre les courbes obtenues en présence et en absence de cobalt; le déplacement du maximum et surtout la stabilisation de la durée de vie des gouttes de mercure au-delà de -0.8 V sont dûs à l'adsorption du chélate.

L'emploi de la polarographie classique n'est cependent pas à conseiller dans le cas particulier du dosage du cobalt dans les végétaux en raison de l'insuffisance du pouvoir résolutif de cette méthode.

4. POSSIBILITÉ D'INTERFÉRENCE PAR LES MÉTAUX EXTRAITS PAR LA DITHIZONE À pH 9

Avant d'être examiné par oscillopolarographie, le cobalt est préalablement extrait par la dithizone à pH 9, en présence de citrate ammonique qui s'oppose à la précipitation du fer et des phosphates. Le cuivre, le plomb, le cadmium, le nickel, l'étain, le bismuth, le thallium et le zinc sont extraits concomitamment. Vu la proximité de leur potentiel de pic, seules les interférences dues au nickel ($E_p = -0.95$ V) et au zinc ($E_p = -1.25$ V) sont à redouter.

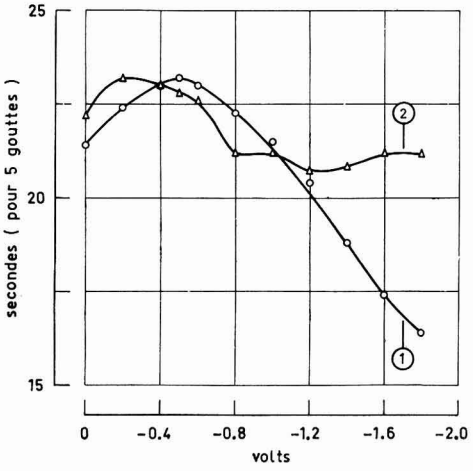

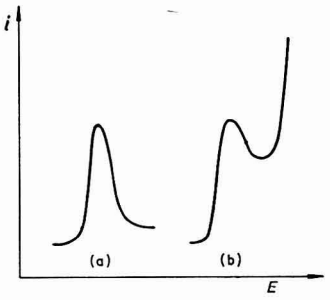

Fig. 2. Courbes de vie des gouttes de mercure. (1) milieu de base seul: NH_4OH–NH_4Cl 0.5 M, diméthylglyoxime 0.1%; (2) milieu de base + 4.085 μg Co^{2+}/ml.

Fig. 3. Influence du zinc sur la morphologie du pic d'absorption du complexe cobalt–diméthylglyoxime. (a) cobalt seul; (b) cobalt + zinc.

L'étain, le bismuth et le plomb ne sont pas réductibles dans le milieu utilisé; les potentiels de demi-vague du cuivre, du cadmium et du thallium sont beaucoup plus positifs que celui du cobalt et ne peuvent interférer que s'ils se trouvent présents dans les végétaux à une concentration supérieure à 100 p.p.m. Il va sans dire que ces trois métaux ne peuvent se rencontrer qu'exceptionnellement en telle quantité dans les végétaux. En l'occurence, il est d'ailleurs toujours possible d'éliminer les interférences en mettant à profit les possibilités de la méthode différentielle.

La valeur du rapport A/B toléré (A = concentration en nickel ou en zinc; B = concentration en cobalt) est obtenue en ajoutant à une solution de concentration déterminée en cobalt, des concentrations croissantes de l'élément interférent; on mesure, après chaque addition, la hauteur du pic du cobalt. La variation maximum de hauteur ne doit pas dépasser 5%.

(*a*) *Influence du zinc*

La présence de fortes quantités de zinc se traduit par une déformation du versant droit du pic du cobalt et par une augmentation de la hauteur du pic (voir Fig. 3). En oscillopolarographie ordinaire, le rapport A/B toléré vaut environ 60. Or, dans la plupart des fourrages que nous avons analysés, la teneur en zinc est environ 100 fois plus forte que celle du cobalt. Il est néanmoins possible de doser le cobalt avec précision en ajoutant aux solutions de cobalt destinées à l'étalonnage un sel de zinc dans un rapport approximativement égal à celui qui se rencontre dans le végétal examiné. L'emploi de cet artifice se justifie car les variations de la teneur en zinc d'une espèce végétale déterminée sont généralement faibles. En oscillopolarographie différentielle, le rapport A/B toléré est beaucoup plus favorable; il atteint en effet la valeur très largement suffisante de 400.

(*b*) *Influence du nickel*

Le nickel fournit avec la diméthylglyoxime un pic d'adsorption situé à -0.95 V et comparable à celui qui est obtenu avec le cobalt; le nickel n'interfère pas directement avec le cobalt, les pics de ces deux métaux étant suffisamment séparés. On

TABLEAU 5

INFLUENCE DE LA CONCENTRATION EN NICKEL SUR LA HAUTEUR DU PIC DU COBALT

Cobalt: 1.64 μg/ml NH_4OH–NH_4 0.5 M; diméthylglyoxime: 0.04%

Concn. en nickel (μg/ml)	*$(i_p)_{Co}$ (unités arbitraires)*	*Ni/Co*	*Concn. en nickel (μg/ml)*	*$(i_p)_{Co}$ (unités arbitraires)*	*Ni/Co*
0	138	—	11.50	82	6.0
1.15	138	0.6	23.0	69	12.0
2.26	138	1.2	36.4	64	19.0
3.32	130	1.8	71.5	58	37.3
5.75	118.0	3.0			

TABLEAU 6

INFLUENCE DE LA CONCENTRATION EN NICKEL SUR LA HAUTEUR DU PIC DU COBALT

Cobalt: 0.164 μg/ml; NH_4OH–NH_4Cl: 0.5 M; diméthylglyoxime: 0.04%

Concn. en nickel (μg/ml)	*$(i_p)_{Co}$ (unités arbitraires)*	*Ni/Co*
0	16.5	—
1.15	16.5	6
2.26	16.1	12
3.32	14.9	19
4.35	12.0	37.3

constate néanmoins que lorsque la concentration en nickel de la solution à analyser est telle qu'il apparaît un précipité rouge, la hauteur du pic du cobalt diminue en raison directe de l'augmentation de la concentration en nickel.

Dans le Tableau 5 sont rassemblées les valeurs expérimentales observées en présence de concentrations croissantes en nickel.

On voit, d'après les chiffres du Tableau 5 que la hauteur du pic du cobalt diminue d'une manière significative lorsque le rapport nickel/cobalt est égal à 3. Or, cette diminution coïncide avec l'apparition nette du précipité rouge de diméthylglyoxime de nickel.

La diminution observée est par conséquent imputable à l'adsorption du cobalt sur le précipité. Le même effet est d'ailleurs observé si on remplace le nickel par du fer.

Dans les végétaux que nous avons examinés, le rapport nickel/cobalt est le plus souvent supérieur à 3. Il faut donc, pour éviter des pertes par adsorption, que la prise d'essai sur laquelle le dosage du cobalt est effectué, soit telle qu'il ne se produise aucun précipité au moment de l'addition de la diméthylglyoxime. Cette condition est habituellement réalisée lorsque la prise d'essai est de l'ordre de 1 g. Le Tableau 6 montre que lorsque la teneur en cobalt est absissée à 0.164 μg/ml, le rapport nickel/cobalt toléré devient égal à 12.

L'oxydation de Co^{2+} en Co^{3+} et de Ni^{2+} en Ni^{3+} par l'eau de brome donne de mauvais résultats; le pic d'adsorption du cobalt est plus fortement influencé par le nickel qu'avant l'oxydation.

5. ESSAIS D'AUTRES DIOXIMES

(a) La benzyldioxime

Les pics d'adsorption observés avec le cobalt ($E_p = -0.99$ V) en présence de benzyldioxime ne sont ni reproductibles, ni proportionnels à la concentration. Ce complexant a donc été abandonné.

(b) La diacétyldioxime

Le complexe cobalt–diacétyldioxime se manifeste par un pic d'adsorption très intense, situé à -1.15 V. Le nickel, par contre, ne fournit qu'un pic insignifiant. Le précipité rouge dû à la formation du complexe nickel–diacétyldioxime possède un pouvoir adsorbant vis-à-vis du cobalt beaucoup plus faible que la diméthylglyoxime.

Des essais analogues à ceux qui sont repris dans les Tableaux 5 et 6 montrent que le rapport nickel/cobalt toléré vaut respectivement 25 et 250 selon que la concentration en cobalt est égale à 1.64–0.164 μg/ml.

La zone de pH utilisable est la même que pour la diméthylglyoxime. La limite de sensibilité atteinte est voisine de 0.005 μg/ml. La hauteur des pics est proportionnelle à la concentration depuis la limite inférieure jusque 0.16 μg/ml. Avec la diméthylglyoxime, la linéarité de la courbe d'étalonnage se vérifie jusque 2 μg/ml. Signalons également que la morphologie du pic d'adsorption obtenu avec le cobalt en présence de diacétylglyoxime ne présente pas le parfait caractère de netteté qui est observé avec la diméthylglyoxime.

Dans les conditions de la pratique du dosage correspondant à une prise d'essai de 1 g de matière sèche, on utilisera la diméthylglyoxime lorsque le rapport nickel/cobalt est inférieur à 12; lorsque ce rapport est supérieur à 12, on donnera la préférence à la diacétyldioxime.

(c) L'α-furyldioxime

Comme les autres complexants appartenant à la même famille, cette dioxime

fournit, en présence du cobalt, un pic d'adsorption; elle s'en distingue cependant par l'intensité exceptionnelle de l'adsorption observée.

Dans le tampon ammoniaque–chlorure ammonique, 0.5 *M* contenant de la furyldioxime à la concentration de 0.04%, 0.407 μg/ml de cobalt produit un pic valant 690 unités arbitraires et situé à -1.04 V. L'effet obtenu est plus de vingt fois supérieur à celui qui est observé avec les différentes dioximes examinées.

La courbe d'étalonnage est une droite jusque 2 μg de cobalt/ml. La limite de sensibilité est inférieure à 0.001 μg/ml. Malheureusement, la forte altération de ce pic d'adsorption par le zinc et surtout par le nickel ne permet pas d'en tirer parti dans le cas du dosage du cobalt dans les matières végétales.

RÉSUMÉ

Une nouvelle méthode de dosage oscillopolarographique du cobalt dans les végétaux est décrite. Elle est basée sur l'adsorption à la surface de l'électrode du complexe qui est formé par la diméthylglyoxime avec le cobalt. Les différents facteurs qui contrôlent l'apparition du pic d'adsorption sont étudiés systématiquement (concentration en alcool et en diméthylglyoxime, concentration du tampon, pH).

Les possibilités d'emploi des dioximes les plus courantes sont également discutées.

SUMMARY

A new method for the oscillopolarographic determination of cobalt in vegetable matter is described. It is based on the adsorption on the electrode surface of the complex formed between dimethylglyoxime and cobalt. The different factors controlling the appearance of the adsorption peak (concentration of dimethylglyoxime, alcohol, buffer and pH) are systematically studied. The possibilities of using commoner dioximes are also discussed

BIBLIOGRAPHIE

1 P. NANGNIOT, *J. Electroanal. Chem.*, 7 (1964) 50.

ELECTROANALYTICAL CHEMISTRY AND INTERFACIAL ELECTROCHEMISTRY
Elsevier Publishing Company, Amsterdam – Printed in The Netherlands

DETERMINATION OF TELLURIUM IN EVAPORATED THIN FILMS OF MERCURY, CADMIUM, AND TELLURIUM BY SINGLE-SWEEP POLAROGRAPHY

GERALD C. WHITNACK, T. M. DONOVAN AND MILTON H. RITCHIE
U.S. Naval Ordnance Test Station, China Lake, California 93555 (U.S.A.)
(Received September 19th, 1966)

INTRODUCTION

$Hg_{1-x}Cd_xTe$ is an alloy semiconductor the energy gap of which is a function of X, ranging from 1.5 eV for $X=1$ to 0 eV for $X=0$. Although the properties of this system are being studied extensively in the case of melt-grown crystals[1-3], very little has been published concerning the properties of evaporated alloy films. In order to study the properties of evaporated films it is essential that a reliable analytical technique be available for determining the separate elements in the presence of each other, using a limited sample size that is associated with the analysis of thin films.

Cadmium and mercury can be determined photometrically by extraction with dithizone at different acidities[4]. Tellurium can also be determined photometrically by the bismuthiol method[5]; however, this method requires two critical pH adjustments and a time delay for color development. The bismuthiol reagent deteriorates with time and fresh solutions are necessary for reliable results. In addition, extremely pure water is needed to avoid metal ion interference.

Tellurium has been determined polarographically in selenium metal[6] and produces well-defined polarograms in ammoniacal media. MAIENTHAL AND TAYLOR[7] recently determined p.p.m. of tellurium in cartridge brass and white cast iron by cathode-ray polarography. They reported that in 1.5 M phosphoric acid solution, the tellurium results are linear between about 0.05 and 0.7 p.p.m. in the final solution analyzed polarographically. However, they reported no data on the effect of mercury on the analysis, and the method requires chemical separation of the tellurium from the matrix material prior to the polarographic analysis.

A preliminary investigation with single-sweep polarography of solutions containing cadmium, mercury, and tellurium in nitric acid indicated that the tellurium peak is sufficiently separated from the cadmium peak to allow a quantitative measurement of the tellurium. Neither cadmium nor mercury seemed to interfere with the tellurium peak.

It is the purpose of this paper to describe the single-sweep polarographic method that was finally developed in this laboratory for the rapid analysis of tellurium in evaporated alloy films of mercury–cadmium telluride.

EXPERIMENTAL

Apparatus and materials

A linear sweep cathode-ray polarotrace manufactured by Southern Instruments, in England, was used throughout this work. The dropping mercury electrode had a drop time of 7 sec in distilled water and $m=4.4$ mg/drop. All polarographic measurements were made at 25° ±0.10°. Redistilled mercury C.P. was used as the anode and all current peak potentials and heights are referred to the mercury pool. A Moseley Model 2-D X-Y recorder, manufactured by F. L. Moseley Co., Pasadena, Calif., U.S.A. was used to record the polarograms.

Tellurium used in this work was obtained from Kern Chemical Corporation, Los Angeles, Calif.; HgTe and CdTe came from K and K Laboratories, Plainview, N.Y., and $Hg_{1-x}Cd_xTe$ alloys were supplied through the courtesy of Dr. D. MOREY of Eastman Kodak Cy., Rochester, N.Y., U.S.A.

Standard solutions of tellurium were prepared by dissolving 0.1 g pure tellurium (99.999%) in 5 ml of conc. H_2SO_4 by heating, and fuming to evaporate off most of the acid. The tellurous acid precipitate was treated with 100 ml of distilled water and then dissolved by adding a minimum amount of 4 *N* KOH. This solution was then diluted so that the final concentration of tellurium was 5 μg/ml.

Evaporated thin films

The films were deposited in a conventional vacuum system similar to that described previously[8]. A resistance-heated tantalum boat was used as a source, and microscope slides as substrates. Because of the instability of HgTe at evaporation temperatures, a liquid nitrogen trap was placed between the pumping port and source in the system to prevent free mercury from entering the diffusion pump.

Photometric measurements

The absorption of test solutions of tellurium in HgCdTe alloys was measured at room temperature with a Beckman DB spectrophotometer. Test solutions were prepared by the bismuthiol II extraction procedure of CHENG[5]. Interference by cadmium was suppressed by using 0.25 ml of 0.1 *M* EDTA in the color development solution. The method produces good data as long as a precaution is taken to use separatory funnels with Teflon stopcocks.

PROCEDURE

Solutions of the thin films were prepared by removing the film from the glass slide with a razor blade and dissolving the sample in 1 ml of conc. HNO_3 plus 2 drops of conc. HCl. Each solution was then diluted to a final volume of 100 ml with deionized-distilled water for both photometric and polarographic analysis. For polarographic analysis, 10 ml of the above solution was diluted to 100 ml with 0.01 *N* HNO_3. Two ml of this solution was then placed in a 5-ml capacity polarographic cell and pure nitrogen passed through the solution for 5 min. The single-sweep polarogram was then recorded with a start potential of −1.00 V and the peak height was referred to a standard graph for the tellurium concentration. If the standard addition technique is used, aliquots of 0.01–0.05 ml of a standard tellurium solution about $1 \cdot 10^{-5}$ g/ml

are added to the 2-ml solution in the cell and the tellurium concentration in the sample is determined from a ratio of two wave heights.

RESULTS AND DISCUSSION

The tellurium concentration in several alloy films of cadmium, mercury, and tellurium was determined by both the photometric procedure of CHENG and the single-sweep polarographic procedure described in this paper. The results are shown in Table 1; the data is in fair agreement. The polarographic analyses appear to be a little higher, which may be indicative of loss of tellurium in the extraction with dithizone in the photometric procedure.

TABLE 1

TELLURIUM IN HgTe AND CdTe THIN FILMS

Sample	*Type*	*Tellurium found (μg/ml)*		*Sample*	*Type*	*Tellurium found (μg/ml)*	
		Polarographic	*Photometric**			*Polarographic*	*Photometric**
A	CdTe	34.0	33.5	I	HgTe	43.0	41.5
B	CdTe	34.0	34.1	J	HgTe	36.5	35.2
C	CdTe	35.0	35.0	K	HgTe	30.7	28.0
D	CdTe	31.7	34.0	L	HgTe	26.6	23.0
E	CdTe	32.3	30.2	M	HgTe	20.7	16.4
F	CdTe	25.4	28.4	N	HgTe	13.8	9.2
G	CdTe	19.2	18.4				
H	CdTe	13.1	15.0				

* Procedure of CHENG.

Tellurium produces a sharply-defined peak around −1.2 V in 0.01 *N* HNO_3. The peak voltage varies slightly with concentration, becoming more positive with more concentrated solutions of tellurium. The peak height was found to remain linear in the range 0.05–2 μg/ml, and this range of concentration was used to obtain the final data in the analysis of the thin films reported in this work. The peak voltage for a 0.2 μg/ml-solution of tellurium in 0.01 *N* HNO_3 is −1.25 V *vs.* a Hg pool. If cadmium or mercury is present no effect on the tellurium peak height is observed up to 30 μg/ml of either element. CdTe film solutions produce two well-defined peaks in 0.01 *N* HNO_3 at −0.84 V and −0.98 V, respectively, with the height of the first peak about twice that of the second peak when about equivalent concentrations of cadmium and tellurium are present in the film; however, these pre-waves do not seem to affect the tellurium wave that follows at −1.25 V. Either the method of standard addition or the use of a standard graph may be employed in the analysis for tellurium. If the thin films that are being analyzed have a tellurium concentration that falls within about a ten-fold range in concentration below 2 μg/ml, the standard graph method is reliable; however, if a wide range of tellurium concentration is expected or a concentration above 2 μg/ml, then the method of standard addition should be used for reliable results. One can make, and then use, several standard graphs if a wide range in tellurium concentration is expected, but at concentrations above 2 μg/ml a sharp decline in linearity appears. This is in agreement with MAIENTHAL who reported this effect above 1 p.p.m. in phosphoric acid solution with a cathodic scan.

SUMMARY

A rapid and reliable single-sweep polarographic method of analysis is described for tellurium in evaporated HgTe and CdTe thin films and in evaporated alloy films of mercury–cadmium telluride. The procedure is simple and should be applicable to a large number of alloy films and other materials containing tellurium, with only slight modification. A comparison of polarographic and photometric results for tellurium are presented.

REFERENCES

1 P. W. KRUSE, *Appl. Opt.*, 4 (1965) 687.
2 A. J. STRAUSS, T. C. HARMAN, J. G. MAVROIDES, D. H. DICKEY AND M. S. DRESSELHAUS, *Report of the International Conference on the Physics of Semiconductors, Exeter, 1962.*
3 W. D. LAWSON, S NIELSEN, E. H. PUTLEY AND A. S. YOUNG, *J. Phys. Chem. Solids*, 9 (1959) 325.
4 E. B. SANDELL, *Colorimetric Determination of Traces of Metals*, Interscience Publishers, New York, 3rd ed., 1959.
5 K. L. CHENG, *Talanta*, 8 (1961) 301.
6 G. H. OSBORN AND J. G. C. COBB, *Analyst*, 78 (1953) 267.
7 E. J. MAIENTHAL AND J. K. TAYLOR, *Anal. Chem.*, 37 (1965) 1516.
8 T. M. DONOVAN AND E. J. ASHLEY, *J. Opt. Soc. Am.*, 54 (1964) 1141.

ELECTROANALYTICAL CHEMISTRY AND INTERFACIAL ELECTROCHEMISTRY
Elsevier Publishing Company, Amsterdam – Printed in The Netherlands

POLAROGRAPHY OF THE CADMIUM AND ZINC XANTHATE COMPLEXES

HIROSHI KODAMA AND KENJIRO HAYASHI
Department of Chemistry, Faculty of Science, Hokkaido University, Sapporo (Japan)
(Received June 10th, 1966)

INTRODUCTION

Bivalent cadmium and zinc form sparingly-soluble precipitates with ethyl xanthate in aqueous solution[1,3]. It has been found, however, that the precipitates dissolve in the presence of excess xanthate. For example, $5 \cdot 10^{-3}$ *M* cadmium and zinc form water-soluble complexes in 0.1 *M* and 0.3 *M* ethyl xanthate, respectively.

In the present study, the nature of the water-soluble complex formed between cadmium or zinc and xanthate has been investigated by the polarographic method and the over-all formation constants derived.

EXPERIMENTAL

Reagents

The potassium ethyl xanthate stock solution (Tanaka Chemicals G.R.) was freshly prepared every few days and stored in a stoppered bottle protected from light. The concentration of this solution was determined gravimetrically as copper xanthate.

Cadmium and zinc solutions were prepared from their nitrates and standardized by titration with EDTA.

Gelatin, at a concentration of 0.01% in the final solution, was found satisfactory as maximum suppressor.

Apparatus

Polarographic waves were recorded with a polarograph (Shimazu Type R-P-2) using an H-type cell in conjunction with a saturated calomel electrode as the reference electrode. Current–voltage measurements were made on a manual set-up under air-free conditions. The experiments were carried out at 25.00 ± 0.01°.

Reduction of cadmium complex

(1) In aqueous solution. Experiments were performed with $5 \cdot 10^{-4}$ *M* cadmium. The concentration of potassium ethyl xanthate was varied from 0.06 to 1 *M*, keeping the ionic strength at 1.0 by addition of the requisite amount of potassium nitrate. The half-wave potentials were not affected by pH.

The plot of $\log i/(i_d - i)$ against potential is shown in Fig. 1. Thir curve indicates that the polarographic reduction process of cadmium in xanthate medium is a quasi-reversible system.

The "half-wave potential" which is defined in reversible wave can be evaluated from these data by applying the MATSUDA–AYABE equation[4] (Fig. 2).

The plot of the half-wave potential against log of the xanthate concentration gives a straight line (Fig. 3). It is, therefore, reasonable to conclude that the complex

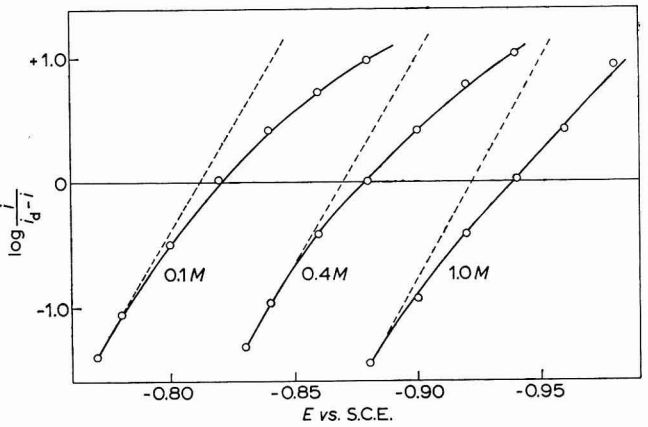

Fig. 1. The relation between $\log i/(i_d - i)$ and potential for cadmium xanthate complex in aqueous solns.; xanthate concn. 0.1, 0.4 and 1.0 M.

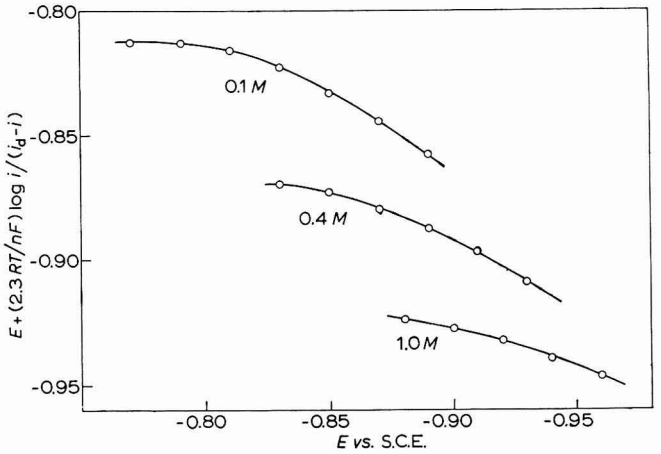

Fig. 2. The relation between potential and $E + (2.3\,RT/nF) \log i/(i_d - i)$ for cadmium xanthate complex in aqueous soln.[4]; xanthate concn. 0.1, 0.4 and 1.0 M.

being reduced is composed of only one species. The number of ligands/cadmium ion can thus be estimated by using the expression[5]

$$p = -\frac{\mathrm{d}(E_{\frac{1}{2}})_c}{\mathrm{d}\log[\mathrm{X}]} \Big/ \frac{RT}{0.4343\,nF}$$

where $(E_{\frac{1}{2}})_c$ is the half-wave potential when the concentration of xanthate is [X], and p is the number of co-ordinated ligands.

The slope of the curve in Fig. 3 is 120 mV, which gives a value of 4 for p in the equation, *i.e.*, four xanthate ions/cadmium ion in the complex.

The expression[5]

$$(E_{\frac{1}{2}})_c - (E_{\frac{1}{2}})_s = -\frac{RT}{nF} \ln \frac{I_c}{I_s} f_M K_p [X]^p / f_{MX_p}$$

gave a value of 1.13×10^{11} for the over-all formation constant for the cadmium xanthate complex, $Cd(C_2H_5OCS_2)_4^{2-}$.

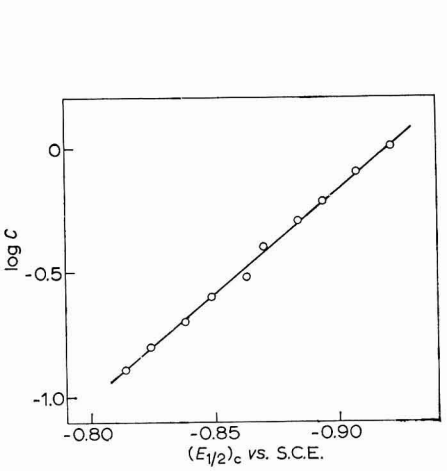

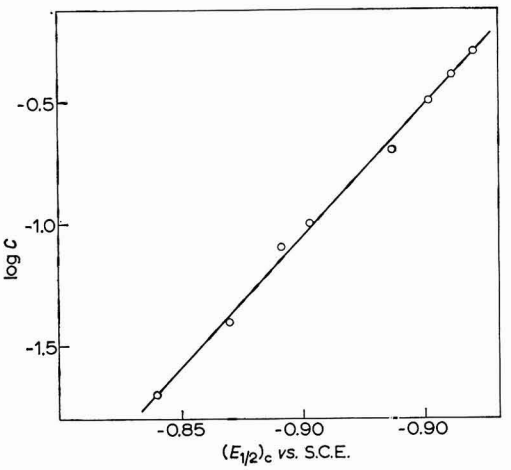

Figs. 3–4. Plot of $(E_{\frac{1}{2}})_c$ as a function of xanthate concn. for cadmium xanthate complex; (3) in aqueous soln., (4) in non-aqueous soln.

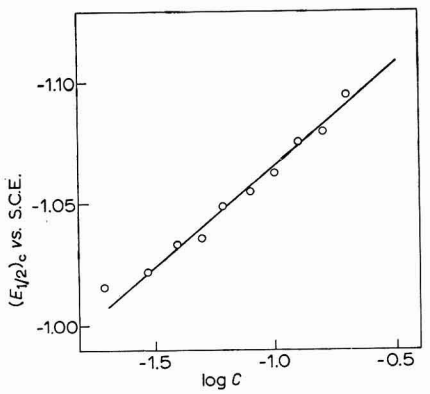

Fig. 5. Plot of $(E_{\frac{1}{2}})_c$ as a function of xanthate concn. for zinc xanthate complex in non-aqueous soln.

(2) In non-aqueous solution. The polarographic reduction of cadmium in a 1:1 (v/v) mixture of water and dimethylformamide (DMF) was carried out in 0.5 M lithium perchlorate as a supporting electrolyte. The concentration of potassium ethyl xanthate was varied from 0.02 to 0.5 M, keeping the ionic strength at 2 by the addition of potassium nitrate.

Evidence for the reversibility of the polarographic reduction of cadmium in the mixed solvent was obtained from the following experimental facts: (i) the temperature coefficient for the diffusion current was 2%/degree; (ii) plots of $\log i/(i_d - i)$ *vs.* E gave well-defined straight lines with a slope of 22 ± 2 mV.

The over-all formation constant and the value of p were evaluated by the method described above.

A plot of $(E_{\frac{1}{2}})_c$ against log [xanthate] gives a well-defined straight line with a slope of 93 mV, which leads to a value of 3.1 (= 3) for p (Fig. 4).

The over-all formation constant was estimated to be 2.5×10^{14}.

Reduction of zinc complex

Experiments were performed with $5.0 \times 10^{-4} M$ zinc in lithium chloride supporting electrolyte. The concentration of potassium ethyl xanthate was varied from 0.02 to 0.5 M, keeping the ionic strength at 1.0 by addition of the requisite amount of lithium chloride.

The polarographic reduction of zinc in xanthate medium was quasi-reversible. The "half-wave potentials", $(E_{\frac{1}{2}})_c$, were obtained by the method described above.

A plot of $(E_{\frac{1}{2}})_c$ against log [xanthate] gives a straight line with a slope of 86 mV (Fig. 5). The values of p and the over-all formation constant were estimated to be 2.9 (= 3) and 4.26×10^4, respectively.

REFERENCES

1 J. STARY, *The Solvent Extraction of Chelates*, Pergamon Press, London, 1964.
2 A. T. PILIPENKO AND N. V. UL'KO, *Zh. Analit. Khim.*, 10 (1955) 299.
3 A. L. ZAGYANSKII, *Tsvetn. Metal.*, 37 (1964) 25.
4 H. MATSUDA AND Y. AYABE, *Z. Elektrochem.*, 63 (1959) 1164.
5 D. D. DEFORD AND D. N. HUME, *Z. Elektrochem.*, 63 (1951) 1164.

ELECTROANALYTICAL CHEMISTRY AND INTERFACIAL ELECTROCHEMISTRY
Elsevier Publishing Company, Amsterdam – Printed in The Netherlands

COMPLEXES OF COPPER(I) AND SILVER(I) WITH ACETONITRILE IN WATER, THE LOWER ALCOHOLS, ACETONE, AND NITROETHANE

STANLEY E. MANAHAN
Department of Chemistry, University of Missouri, Columbia, Missouri (U.S.A.)
REYNOLD T. IWAMOTO
Department of Chemistry, University of Kansas, Lawrence, Kansas (U.S.A.)
(Received July 6th, 1966)

Complexes of copper(I) and silver(I) ions with acetonitrile have been known for some time. The copper salts[1] $[Cu(CH_3CN)_4]NO_3$ and[2] $[Cu(CH_3CN)_4]ClO_4$ have been prepared by the reaction of solid copper with acetonitrile solutions of silver nitrate and of silver perchlorate, respectively. Polarographic investigation shows that copper(I) ion is stable with respect to disproportionation in acetonitrile, a behavior attributed partly to the relatively strong solvation of copper(I) ion in acetonitrile[3]. The formation of silver(I) complexes of acetonitrile in aqueous solution has been demonstrated by potentiometry at the silver electrode. Assuming that only the mono-ligand complex exists in aqueous solution, PAWELKA has reported[4] a value of 4 for the stability constant of $AgCH_3CN^+$. In another potentiometric investigation of the complexes of silver ion with acetonitrile in water, the formation of $Ag(CH_3CN)_2^+$ was reported[5]. The stability constant of the di-acetonitrile complex determined at different ligand concentrations, however, varies by a factor of over 30. Undoubtedly, other silver complexes besides $Ag(CH_3CN)_2^+$ were present in solution.

We have examined the effect of solvent on the acetonitrile complexes of copper (I) and silver (I). The copper(I) complexes were studied by voltammetry at the dropping copper-amalgam electrode, and the silver(I) complexes by potentiometry at the silver electrode.

EXPERIMENTAL

Reagent-grade acetonitrile was distilled twice from phosphorus pentoxide, the fraction boiling at $81.0 \pm 0.5°$ was collected. Methanol and ethanol were dried by treatment with magnesium activated by iodine[6]. 2-Butanol was refluxed over calcium hydride and a small quantity of sodium borohydride, prior to distillation. 2-Propanol and acetone were allowed to stand over Drierite for a week, and were then decanted and distilled. Nitromethane was passed through a column consisting of a layer of basic alumina on top of a section of acidic alumina.

Lithium perchlorate was prepared by adding a slight excess of 70% reagent-grade perchloric acid to reagent-grade lithium carbonate, followed by three recrystallizations from water; the product was dried in an oven at 200° for several

days. Tetraethylammonium perchlorate was prepared by neutralization of Eastman aqueous 10% tetraethylammonium hydroxide with 70% reagent-grade perchloric acid. The tetraalkylammonium perchlorate was recrystallized twice from water and dried *in vacuo* at 80° for 48 h. Hydrated silver perchlorate, G. F. Smith Co., was dried *in vacuo* at 700° for 48 h.

The acetonitrile complexes of copper(I) were examined in methanol, ethanol, 2-propanol, 2-butanol, acetone, nitroethane and water. The complexes of silver(I) were investigated in all these solvents except ethanol and 2-propanol. Nitroethane solutions were 0.1 *M* in tetraethylammonium perchlorate; all other solutions were 0.1 *M* in lithium perchlorate. The polarographic curves were obtained with a controlled-potential polarograph of the Kelly-Jones-Fisher type[7]. A dropping amalgam electrode of simple design was used[8]. The polarographic solutions were de-oxygenated with purified nitrogen and maintained at 25 ± 1°. For the potentiometric study of the silver–acetonitrile complexes, a Leeds and Northrup Model 7401 pH-meter was used.

The formation constants of the copper(I)–acetonitrile complexes were calculated from the current–potential data obtained with the dropping copper-amalgam electrode (D.A.E.) for solutions 10^{-3}–1 *M* in acetonitrile. In all solvents, well-defined, essentially reversible polarographic waves were obtained for the copper(I), copper(Hg) couple. In several cases, copper(I) was added as $Cu(CH_3CN)_4ClO_4$. The composite anodic–cathodic curves for these solutions passed through zero-current without inflection, indicating a reversible system.

Plots of $(E_{\frac{1}{2}})_c-(E_{\frac{1}{2}})_s$ *vs.* $-\log [CH_3CN]$ of the copper(I) complex-formation data are smooth curves with rapidly increasing slope at high acetonitrile concentrations. Formation constants of the copper(I)–acetonitrile complexes were evaluated by the method used by LARSON AND IWAMOTO[9]. The equation for the half-wave potential *vs.* $-\log [CH_3CN]$ curve is:

$$(E_{\frac{1}{2}})_c-(E_{\frac{1}{2}})_s = -0.059 \log (1+\beta_1 L+\beta_2 L^2+ \ldots +\beta_p L^p)$$

where L represents the concentration of unbound acetonitrile, β_n is the overall formation constant of the complex species with n acetonitrile molecules, $(E_{\frac{1}{2}})_s$ is the half-wave potential of the copper(I), copper(Hg) couple in the absence of complexing agent, and $(E_{\frac{1}{2}})_c$ is the half-wave potential of the copper(I), copper(Hg) couple in a medium of ligand concentration L. The $(E_{\frac{1}{2}})_c-(E_{\frac{1}{2}})_s$ *vs.* $-\log [CH_3CN]$ curves for the case of copper(I) have been analyzed on the assumption that a maximum of four acetonitrile molecules coordinate to copper(I) ion. This assumption appears valid because the portion of the curves with slope 0.059×4 falls near the half-wave potential for the copper(I), copper(Hg) step in pure acetonitrile, from which salts with the composition $Cu(CH_3CN)_4ClO_4$ and $Cu(CH_3CN)_4NO_3$ have been isolated. Temporary β-values were obtained first, by extrapolation of the points on the curve at which the slopes are 0.059, 0.059×2, etc., to $\log [CH_3CN] = 0$. Because of the closeness of the individual formation constants, the temporary β-values vary somewhat from the true values, and it is necessary to recalculate successively each individual formation constant, until values are found that fit the experimental data precisely. Iterations were continued until two successive cycles produced less than $10^{0.05}$ change in each of the individual constants. In most cases, the concentration of copper in the amalgam was much less than the concentration of ligand in solution. Therefore, it was not necessary in these cases to correct the ligand concentration for bound

acetonitrile. For solutions of low ligand concentration, the half-wave potentials were obtained by extrapolation from the low-current section of the polarographic waves. With no copper(I) originally present in solution, also it was not necessary, in these cases, to correct the ligand concentration.

Data for the plots of $E_c - E_s$ *vs.* $-\log [CH_3CN]$, to secure information on the nature and stability of silver–acetonitrile complexes, were obtained from potentiometric titration of solutions of silver perchlorate, 1.0×10^{-3} *F*, with solutions of acetonitrile also $1.0 \times 10^{-3} F$ in Ag(I). The titrations were followed with a silver–aqueous saturated calomel electrode pair, with the aqueous calomel electrode, an H-type, placed in a separate compartment which was connected to the titration vessel by a fine-porosity glass frit. The expression used and the approach taken to analyze the data on the acetonitrile complexes of silver(I) are similar to those described earlier for the analysis of the acetonitrile complexes of copper(I). As in the case of the copper(I) complexes, the $E_c - E_s$ *vs.* $-\log [CH_3CN]$ plots are smooth curves. From the limiting slopes in the region of *ca.* 2 *M* acetonitrile, the highest silver complex obtained appears to be $Ag(CH_3CN)_3^+$.

RESULTS AND DISCUSSION

The refined formation constants for the acetonitrile complexes of copper(I) and silver(I) are given in Table 1 (see ref. 8 for detailed data).

The stability of the acetonitrile complexes of copper(I) and of silver(I) generally does not vary greatly with solvent. This is not surprising in view of (i) the nearly

TABLE 1

FORMATION CONSTANTS (LOG β_n) OF ACETONITRILE COMPLEXES OF COPPER(I) AND SILVER(I) IN VARIOUS SOLVENTS[a] (25°)

Solvent	*Metal*	β_1	β_2	β_3	β_4
Methanol	Cu(I)	2.5	3.9	4.5	4.2
	Ag(I)	1.1	1.2	1.2	—
Ethanol	Cu(I)	3.7	5.4	5.9	5.9
2-Propanol	Cu(I)	3.2	5.3	5.9	6.1
2-Butanol	Cu(I)	3.1	4.6	5.7	6.4
	Ag(I)	1.0	1.4	1.3	—
Acetone	Cu(I)	4.4	6.3	6.7	7.2
	Ag(I)	1.0	1.5	1.6	—
Nitroethane[b]	Cu(I)	2.3	4.5	5.5	5.9
	Ag(I)	1.1	2.8	3.7	4.2
Water	Cu(I)	—	3.9	4.1	—
	Ag(I)	0.7	0.8	—	—

[a] 0.01 *M* $LiClO_4$ solutions, [b] 0.01 *M* Et_4NClO_4

similar potentials of the copper(I), copper(Hg) and of the silver(I), silver couples in the solvents studied, which suggest close to identical solvation energies for each of the ions in the solvents, and (ii) the high compatibility of acetonitrile and each of the seven solvents used in this study. $E_{Cu(I),Cu(Hg)}{}^{0'}$ values (*vs.* S.C.E.) are: −0.04 V, methanol; +0.02 V, ethanol; 0.00 V, 2-propanol; +0.06 V, 2-butanol; +0.06 V,

acetone; +0.04 V, nitroethane; +0.15 V, water. $E_{Ag(I),Ag}{}^{0'}$ values (*vs.* S.C.E.) are: +0.46 V, methanol; +0.44 V, 2-butanol; +0.51 V, acetone; +0.61 V, nitroethane; +0.55 V, water. Both series of potentials have been corrected for differences in junction potential between each solvent and the aqueous saturated calomel electrode[10,11].

The effect of acetonitrile on the electrochemical behavior of copper ions in water is of special interest. The standard potential for the copper(I), copper(Hg) couple in water is +0.15 V *vs.* S.C.E. and for the copper(II), copper(I) couple, −0.09 V *vs.* S.C.E.[12]. Consistent with these potentials, aqueous solutions of copper(II) ion give one-step two-electron polarographic waves. This wave is shown in Fig. 1, curve A (as the anodic wave for the oxidation of copper from the amalgam). Provided there is no complexation of copper(II) ion, the formation of copper(I) complexes should shift the potential of the copper(I), copper(Hg) couple negative and that of the copper(II), copper(Hg) couple positive, by equal amounts. In the case of water 1.0 *M* in acetonitrile, complexation of copper(I) is extensive enough that a split wave is obtained, as shown in Fig. 1, curve B. Curve B yields half-wave potentials of −0.12 V and +0.21 V *vs.* S.C.E. for the copper(I), copper(Hg) and copper(II),

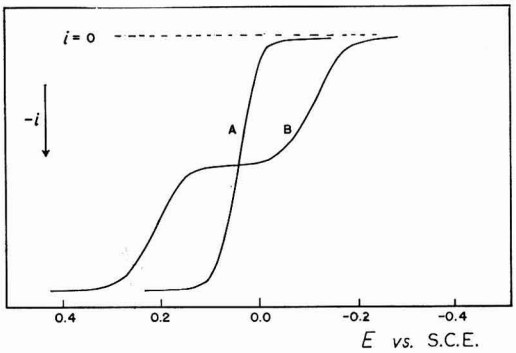

Fig. 1. Anodic waves at the dropping copper-amalgam electrode in water: (A), in the absence of acetonitrile; (B), in 1.0 *M* acetonitrile. Supporting electrolyte, 0.1 *M* $LiClO_4$.

copper(I) couples, respectively. The copper(I), copper(Hg) couple has been shifted negative by 0.27 V and the copper(II), copper(I) couple, positive by 0.29 V by approximately equal amounts.

The clearly greater stability of copper(I)–acetonitrile complexes over silver(I)–acetonitrile complexes is consistent with the stability data on ammonia, ethylenediamine, and olefinic complexes of the two metal ions in water[13]. This sort of difference in stability has been attributed to difference in the electronegativity of the metal ions, a good criterion of which, in this case, is the first ionization potential of the metals of the ions[14].

ACKNOWLEDGEMENT

The authors gratefully acknowledge the support of the General Research Fund, University of Kansas.

SUMMARY

The effect of solvent on the stability of acetonitrile complexes of copper(I) and silver(I) has been investigated. Small non-correlatable differences in stability are evident. Because of no major differences in the compatibility of the ligand, acetonitrile and the solvents, and the nearly identical potentials for the copper(I), copper(Hg) and for the silver(I), silver couples in the solvents examined, the general similarity of the stability constants of the copper(I) complexes and of the silver(I) complexes in the solvents used is not completely unexpected.

REFERENCES

1 H. H. MORGAN, *J. Chem. Soc.*, (1923) 2901.
2 G. BERGERHOFF, *Z. Anorg. Allgem. Chem.*, 327 (1964) 139.
3 I. M. KOLTHOFF AND J. COETZEE, *J. Am. Chem. Soc.*, 79 (1957) 1852.
4 F. PAWELKA, *Z. Elektrochem.*, 30 (1924) 180.
5 F. K. KOCH, *J. Chem. Soc.*, (1930) 2053.
6 A. I. VOGEL, *Practical Organic Chemistry*, Longmans, London, 3rd ed., 1956, p. 169.
7 M. T. KELLEY, H. C. JONES AND D. J. FISHER, *Anal. Chem.*, 31 (1959) 1475.
8 S. E. MANAHAN, Ph. D. Thesis, University of Kansas, 1966.
9 R. C. LARSON AND R. T. IWAMOTO, *Inorg. Chem.*, 1 (1962) 316.
10 I. V. NELSON AND R. T. IWAMOTO, *Anal. Chem.*, 35 (1963) 867.
11 F. FARHA, JR. AND R. T. IWAMOTO, *Anal. Chem.*, 38 (1966) 143.
12 I. M. KOLTHOFF AND J. J. LINGANE, *Polarography*, Vol. 1, Interscience, New York, 2nd ed. 1952, p. 227.
13 L. G. SILLÉN AND A. E. MARTELL, *Stability Constants of Metal-Ion Complexes*, The Chemical Society, London, 1964.
14 H. J. EMELEUS AND A. G. SHARPE, *Advances in Inorganic Chemistry and Radiochemistry*, Vol. 3, Academic Press, New York, 1961, p. 267.

ELECTROANALYTICAL CHEMISTRY AND INTERFACIAL ELECTROCHEMISTRY
Elsevier Publishing Company, Amsterdam – Printed in The Netherlands

POLAROGRAPHIC STUDY OF DICYCLOPENTADIENYLTITANIUM DICHLORIDE ($TiCp_2Cl_2$)

SERGIO VALCHER AND MARINA MASTRAGOSTINO
Polarographic Centre of the National Research Council, Institute of Chemistry "G. Ciamician", University of Bologna (Italy)
(Received June 16th, 1966)

In 1953, WILKINSON *et al.* prepared $TiCp_2Cl_2$ for the first time[1,2] and discussed the electrochemical behavior of the compound in aqueous solution. They found that in aqueous perchloric acid both $TiCp_2Br_2$ and $TiCp_2Cl_2$ gave a reduction wave with $E_{\frac{1}{2}} = -0.44$ V *vs.* S.C.E. The coincidence of the half-wave potentials for these compounds is in agreement with the fact that in water they hydrolyze to give the cation $TiCp_2OH^+$ which has been isolated and analyzed as the picrate by the above authors. By both electrochemical and chemical reduction of this cation, WILKINSON *et al.* obtained green solutions which showed an anodic wave with $E_{\frac{1}{2}} = -0.44$ V *vs.* S.C.E. From this solution a brown picrate was isolated, which according to the results of measurements of magnetic susceptibility, showed a single unpaired electron, as is seen for titanium(III) compounds.

Ten years later, KORSHUNOV AND MALYUGINA, considering the data on the electrochemical behavior of $TiCp_2Cl_2$ not sufficiently detailed, undertook a polarographic study on this compound. They found a main reduction wave with $E_{\frac{1}{2}} = -0.5$ V *vs.* S.C.E. in aqueous solutions of alkali chlorides and sulfates. On the basis of coulometric determinations they found that the reduction of the compound at a dropping mercury electrode (D.M.E.) takes place with the participation of two electrons. This is contrary to the facts deducible from the work of WILKINSON *et al.*

Two other waves were obtained at -1.2 and -1.7 V, respectively. They identified the first one as an absorption postwave and the other as an irreversible catalytic discharge of hydrogen.

Only HSIUNG AND BROWN[4] investigated the behavior of $TiCp_2Br_2$ in a non-aqueous solvent, formamide, where the compound is not hydrolyzed. They found an ill-defined cathodic wave with $E_{\frac{1}{2}} = -0.62$ V *vs.* aqueous S.C.E.

No other papers concerning the electrochemical behavior of dicyclopentadienyltitanium compounds have been found in the literature.

Since the interpretation of the reduction process of $TiCp_2Cl_2$ given by WILKINSON *et al.* is different from that of KORSHUNOV AND MALYUGINA, the problem warranted further consideration. Furthermore, the limited results obtained by HSIUNG AND BROWN for $TiCp_2Br_2$ in a non-aqueous solvent led us to examine the behavior of $TiCp_2Cl_2$ in dimethylformamide (DMF).

EXPERIMENTAL

Measurements were carried out with two Amel Polarographs, models 461 and 462. The first was employed for the measurements of average current because of the inertia of the potentiometric recorder (time for full-scale deflection = 18 sec). The second was employed for all other polarographic measurements relative to the determination of potentials in controlled-potential conditions. The latter instrument was also used as a recording coulometer and as a potentiostat for electrolysis.

The half-wave potentials were measured *versus* an aqueous saturated calomel electrode (S.C.E.). For the measurements in DMF, salt bridges with the same solvent were used in order to avoid the diffusion of water from the reference electrode to the cell. The junction potentials were generally neglected.

The DMF employed was obtained by dehydrating a commercial product (RP C. Erba) for 24 h with BaO and then distilling under a reduced pressure of nitrogen according to the method of THOMAS AND ROCHOW[5].

The supporting electrolytes employed for DMF solutions were anhydrous LiCl (Merck) and $(C_2H_5)_4NClO_4$ (Et_4NClO_4) (Erba special reagent for polarography).

For the experiments in aqueous solutions, phosphate–acetate buffers, LiCl, HCl and $HClO_4$ (pure reagents) were used.

Coulometric determinations were carried out in cells containing 50–60 ml of the solution with a mercury cathode at controlled potential and a counter-electrode separated by a sintered-glass disk. The concentration of the depolarizer after electrolysis was determined polarographically.

$TiCp_2Cl_2$ was prepared according to the method proposed by WILKINSON *et al.* using $TiCl_4$ and NaC_5H_5 and then recrystallizing from toluene.

RESULTS AND DISCUSSION

The polarographic behavior of $TiCp_2Cl_2$ in aqueous solution was examined only for the properties of the main wave indicated by KORSHUNOV AND MALYUGINA, about whose nature, as we have said, there is some disagreement.

With LiCl (1 *M*) as the supporting electrolyte, $TiCp_2Cl_2$ ($2.5 \cdot 10^{-3}$ *M*) gave a cathodic wave deformed by a maximum which was suppressed by the addition of gelatine (the wave still remained anomalous, probably because of the unbuffered solution).

The half-wave potential in the presence of gelatine was -0.5 V, in agreement with the value reported by KORSHUNOV AND MALYUGINA.

In HCl (1 *M*), the wave is well defined with a half-wave potential of -0.4 V. An electrolysis was then carried out under identical experimental conditions at a controlled potential of -0.6 V on a mercury cathode. 70% of the depolarizer was reduced and the cathanodic wave resulting showed the same half-wave potential as before. This demonstrates the reversibility of the electrode process. The number of electrons participating in the reaction is 1; this was found by an analysis of the two reversible waves shown in Fig. 1.

The number, n, of electrons participating in the electrode process for the first main wave was determined by coulometry for different experimental conditions; the data are reported in Table 1.

The average value of n was found to be 1.15 ± 0.18 which is very close to 1, as obtained with the above experiment.

The effect of pH on half-wave potential was examined in buffered solutions. The results are shown in Fig. 2. The slope of the line corresponds to a variation of -0.052 V/unit pH.

It can be concluded that the reaction involves one electron and one proton. Titanium therefore becomes trivalent and maintains a positive charge on the complex.

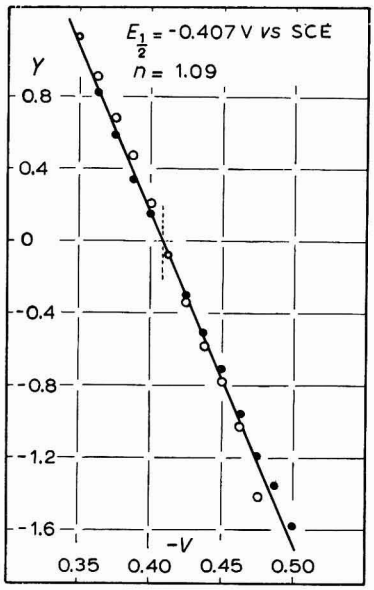

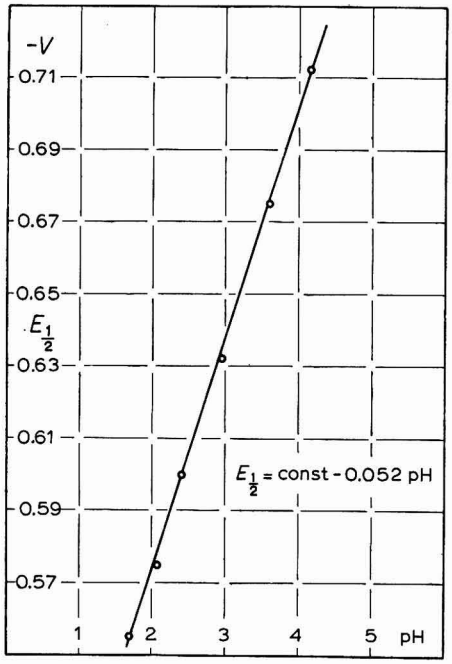

Fig. 1. Analysis of the polarographic waves obtained from titanium dicyclopentadiene complexes in HCl (1 M).
(○), cathodic wave for $Y = \log \frac{i_d - i}{i}$; (●), cathanodic wave for $Y = \log \frac{i_{dc} - i}{i - i_{ac}}$.

Fig. 2. Effect of pH on the half-wave potential. $TiCp_2Cl_2$ ($2 \cdot 10^{-3}$ M) in aqueous buffer soln.

This was demonstrated by WILKINSON *et al.* by the possibility of isolating titanium as a picrate. Since the results of these authors enable us to affirm that the complex of Ti(IV) is present in the form Cp_2TiOH^+, the mechanism of reduction can be expressed by:

$$Cp_2TiOH^+ + e^- + H^+ \rightleftarrows Cp_2Ti^+ + H_2O$$

The mechanism, proposed by KORSHUNOV AND MALYUGINA, is based on a coulometric determination performed by electrolysis at -1.7 V *vs.* S.C.E. in LiCl or HCl as the supporting electrolyte. Another reduction wave with $E_{\frac{1}{2}} = -1.7$ V appears using LiCl as the supporting electrolyte. This wave, which was attributed to the catalytic discharge of hydrogen, is masked in HCl by the discharge of the electrolyte. It follows that the two electrons found by these authors ought to be considered

TABLE 1
COULOMETRIC DETERMINATIONS ON $TiCp_2Cl_2$ IN WATER SOLUTIONS

	Half-wave potential	*Electrolysis potential*	*Moles initially* ($\times 10^4$)	*Moles consumed* ($\times 10^4$)	*Coulombs*	*Electrons/ molecule*
HCl 1 *M*	−0.41	−0.60	1.0	0.626	7.12	1.18
HCl 1 *M*	−0.41	−0.60	0.40	0.281	3.52	1.20
$HClO_4$ 1 *M*	−0.41	−0.60	0.40	0.210	2.60	1.28
$HClO_4$ 1 *M*	−0.41	−0.60	0.30	0.228	2.94	1.33
LiCl 1 *M** with gelatine	−0.47	−0.56	5.1	0.986	10.55	1.11
LiCl 1 *M** with gelatine	−0.49	−0.56	0.125	0.709	6.92	1.01
LiCl 1 *M** with gelatine	−0.52	−0.80	0.51	0.332	3.23	1.00
LiCl 1 *M** with gelatine	−0.45	−0.80	5.1	2.14	20.2	0.98
Buffer pH=2.15** with gelatine	−0.58	−0.80	0.80	0.506	5.80	1.18
Buffer pH=2.05** with gelatine	−0.57	−0.70	0.40	0.252	2.94	1.22

* The half-wave potentials are not constant in LiCl solns. because of the variation in the concn. of the depolarizer caused by the different volumes of the solns. which are unbuffered.
** For buffered solutions the half-wave potentials are quite in accord with the observed effect of pH.

relative to two reduction phenomena of which only one pertains to the complex. Also, the proposed mechanism does not explain the effect of pH on the half-wave potential. In addition, the reoxidation by oxygen, which they discuss, is also admissible to a complex of Ti(III).

$TiCp_2Cl_2$ is reduced reversibly in solution in DMF with LiCl as the supporting electrolyte. The half wave potential of cathodic and cathanodic or anodic waves obtained by electrolysis were in fact coincident. A concentration of $4.7 \cdot 10^{-3}$ *M* of LiCl is sufficient to make the reduction wave of the compound reversible (in concentration of $5 \cdot 10^{-3}$ *M*). The half-wave potential is affected by the concentration of Cl^- ion as can be seen in Fig. 3.

A salt bridge containing NH_4NO_3 saturated in DMF was used in order to keep the junction potential constant.

The slope of the line, $E_{\frac{1}{2}}/\log C_{Cl^-}$, has a value of 0.052 V which is close to the theoretical value for the difference of one chloride ion between the oxidized and the reduced form of the complex. This is in relation to the well-known equation[6]:

$$E_{\frac{1}{2}} = \text{const.} - \frac{p-q}{a} 0.059 \log C$$

Where a = number of exchanged electrons, $p-q$ = difference in the number of ligands in the oxidized and reduced forms and C = concentration of the ligand in solution.

The limiting current is a linear function of the concentration of the depolarizer and of the square root of the mercury pressure. The value and the characteristic of the

limiting current do not vary passing from LiCl to Et_4NClO_4 as supporting electrolyte ($I = 1.68\ \mu A\ l\ sec^{\frac{1}{2}}/mM\ mg^{\frac{2}{3}}$). The wave, however, becomes irreversible and the anodic wave that is formed by electrolysis in the solution presents a half-wave potential which is shifted in respect to that of the cathodic wave. In every case the product of the electrodic reduction has a green color.

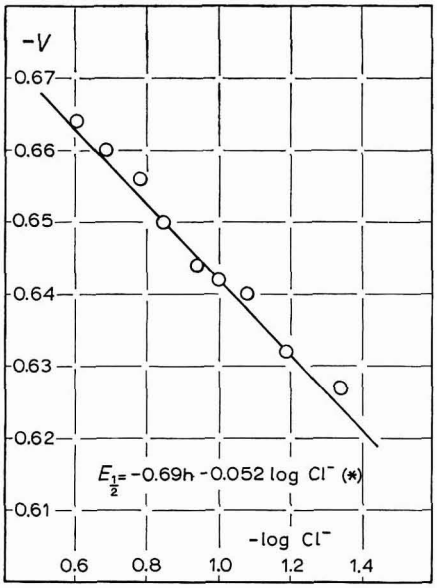

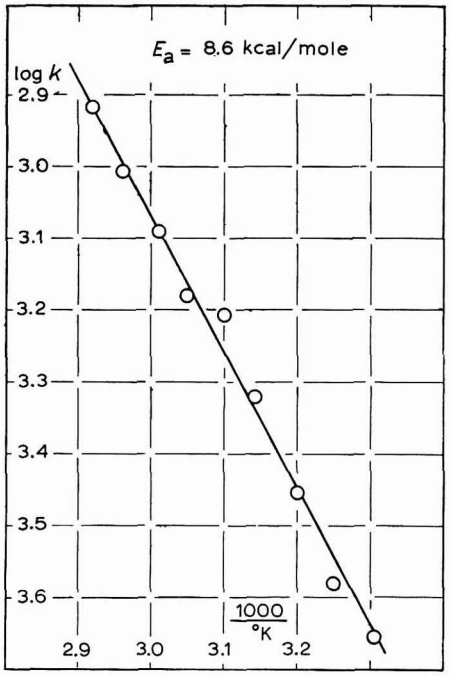

Fig. 3. Effect of Cl^- concn. on the half-wave potential. $TiCp_2Cl_2$ ($5 \cdot 10^{-3}$ M) in DMF; ($LiCl$) + (Et_4NClO_4) = 0.5 M; salt bridge: NH_4NO_3 saturated in DMF. (×) Values obtained by mean square calcns.

Fig. 4. Logarithms of the heterogeneous rate constants as a function of the reciprocal of the abs. temp. $TiCp_2Cl_2$ (6.82×10^{-3} M) in DMF; Et_4NClO_4 (1 M).

Having verified that one electron/molecule is involved in the electrodic reduction and that the reduced form of the complex differs from the oxidized one by one ligand, we may describe the mechanism of the reaction as follows:

$$TiCp_2Cl_2 + e^- \rightleftarrows TiCp_2Cl + Cl^-$$

which is valid with both supporting electrolytes.

With Et_4NClO_4 ($5 \cdot 10^{-1}$ M), also contained in the salt bridge, the reduction wave of $TiCp_2Cl_2$ ($5 \cdot 10^{-3}$ M) shows a half-wave potential of -0.63 V. Under these conditions two anodic waves appear besides the reduction wave. Their half-wave potentials are -0.22 and $+0.19$ V. The intensity of the limiting current of the first of these anodic waves is independent of the mercury pressure (see Table 2). The extreme irregularity of the second wave does not permit an accurate study. Such waves can be attributed to the chloride ion derived from the dissociation of the complex $TiCp_2Cl_2$.

In fact, two analogous waves have been obtained by us using LiCl as the depolarizer in DMF and with Et_4NClO_4 as the supporting electrolyte. The first wave given by LiCl produces a limiting current proportional to the square root of the mercury pressure, which is different from the limiting current given by the titanium complex.

TABLE 2

LIMITING CURRENTS AS A FUNCTION OF THE MERCURY PRESSURE FOR THE ANODIC WAVE OBTAINED FROM A DMF SOLUTION OF $TiCp_2Cl_2$ ($3.57 \cdot 10^{-3}$ M) WITH Et_4NClO_4 AS THE SUPPORTING ELECTROLYTE

h_{Hg}(cm)	i(μA)	h_{Hg}(cm)	i(μA)
59	2.20	74	2.25
64	2.20	79	2.20
69	2.20		

GIVEN AND PEOVER[7] have attributed this wave to the oxidation of the electrode mercury depolarized by the chloride ion according to the reaction

$$4\,Cl^- + Hg \rightleftarrows HgCl_4^{2-} + 2\,e^-$$

The independence of the limiting current of the mercury pressure for the first oxidation wave of the complex $TiCp_2Cl_2$ shows the kinetic character of this wave. This fact is confirmed by the relatively high temperature coefficient (2.85%/degree between 25 and 70°).

Since the complex is to be considered slightly dissociated in DMF it can be assumed that the reaction of dissociation:

$$TiCp_2Cl_2 \xrightarrow{k} TiCp_2^{2+} + 2\,Cl^- \qquad (1)$$

constitutes the slow step of the electrodic process.

This oxidation process as a whole can be described by the following equation:

$$TiCp_2Cl_2 + \tfrac{1}{2}\,Hg \rightarrow TiCp_2^{2+} + \tfrac{1}{2}\,HgCl_4^{2-} + e^- \qquad (2)$$

JENSEN AND BASOLO[8], who have studied the kinetics of substitution of the halogen ligand in complexes of the type $TiCp_2Cl_2$, spectrophotometrically, have demonstrated that in the absence of a sufficiently nucleophilic entering substituent, such reactions are first-order. Since ClO_4^-, which is present in our solution, is not a nucleophilic reagent we can assume that our dissociation reaction also should be first-order or pseudo-first-order if the solvent reacts. It is then possible to apply the theory of DELAHAY[9] on the polarographic current controlled by the rate of reaction and diffusion, and to evaluate the rate constant of the dissociation of the complex.

According to the above theory the average current of a kinetic wave is expressed by the equation:

$$\bar{i}_k = 1255\,\beta\,nm^{2/3}\,t^{2/3}\,Ck$$

in which k is the rate constant for reaction 1 expressed in cm sec^{-1}, m is the mercury flow rate, C is the concentration of the diffusing substance, *i.e.*, $TiCp_2Cl_2$, t is the drop time, n is the number of electrons involved in process 2 and β is a function of k, t and

of the diffusion coefficient, D, of $TiCp_2Cl_2$. D has been calculated from the reduction wave of the complex.

The evaluation of the product $\beta k D^{-\frac{1}{2}}$ necessary for the calculation of k is easily obtained by dividing the average limiting current, $\bar{i}_k$, by the current, $\bar{i}_d$, of the cathodic wave. One obtains:

$$\frac{\bar{i}_k}{\bar{i}_d} = \frac{1255\,\beta\, nm^{2/3}t^{2/3}Ck}{607\, nm^{2/3}t^{1/6}CD^{1/2}} = \frac{kt^{1/2}}{D^{1/2}0.484}$$

from which

$$\beta k \bar{D}^{-1/2} = \frac{\bar{i}_k}{\bar{i}_d}\, 0.484\, t^{-1/2}$$

The value of k is then obtained by means of graphical calculations as reported in DELAHAY's paper.

TABLE 3

CALCULATION DATA AND RATE CONSTANTS AT DIFFERENT TEMPERATURES

$TiCp_2Cl_2$ $6.82 \cdot 10^{-3}$ M, Et_4NClO_4 $5 \cdot 10^{-1}$ M in DMF, t = 1.30 sec (forced dropping).

T(°C)	i_d	i_k	$\beta k D^{-\frac{1}{2}} = (ik/i_d)\ 0.484\ t^{-\frac{1}{2}}$	$kD^{-\frac{1}{2}} \cdot 10^2$	$D^{\frac{1}{2}} \cdot 10^3$	$k \cdot 10^4$ (cm sec^{-1})
30	11.02	1.098	0.0417	7.50	2.94	2.20
35	12.70	1.374	0.0460	8.31	3.14	2.61
40	13.15	1.710	0.0552	10.45	3.34	3.49
45	13.51	2.150	0.0676	13.45	3.57	4.80
50	13.99	2.740	0.0833	16.27	3.81	6.20
55	14.50	2.810	0.0823	16.18	4.07	6.58
60	14.91	3.230	0.0922	18.63	4.34	8.08
65	15.45	3.600	0.0990	20.00	4.63	9.26
70	15.57	4.150	0.1170	24.59	4.94	12.14

The data needed for the calculation of the rate constant, and the results relative to the experiment carried out with $TiCp_2Cl_2$ $6.82 \cdot 10^{-3}$ M in DMF with Et_4NClO_4 ($5 \cdot 10^{-1}$ M) at different temperatures, are reported in Table 3.

The homogeneous rate constants can be calculated by dividing the heterogeneous constants by δ, which is the average distance between the depolarizer molecules in the solution.

In our case, δ was found to be 6.2×10^{-7} cm; the homogeneous rate constant resulting is 3.4×10^2 sec^{-1} at 30°.

The logarithms of the heterogeneous rate constants are reported in Fig. 4 as a function of the reciprocal of the absolute temperature.

An activation energy of 8.6 kcal/mole was calculated from the slope of the straight line.

ACKNOWLEDGEMENT

We are grateful to Professors ELIO VIANELLO and GIOVANNI SEMERANO for their valuable guidance and helpful discussions.

SUMMARY

The polarographic behavior of $TiCp_2Cl_2$ has been studied in water and dimethylformamide solutions.

In every case the complex is reduced, at the DME, to a compound of Ti(III).

In DMF, two anodic waves are also obtained; these waves enable the kinetics of dissociation of the complex: $TiCp_2Cl_2 \xrightarrow{k} TiCp_2^{2+} + 2\ Cl^-$, to be studied. The rate constant and the activation energy were evaluated by polarographic measurements.

REFERENCES

1 G. WILKINSON, P. L. PAUSON, J. M. BIRMINGHAM AND F. A. COTTON, *J. Am. Chem. Soc.*, 75 (1953) 1011.
2 G. WILKINSON AND J. M. BIRMINGHAM, *J. Am. Chem. Soc.*, 76 (1954) 4281.
3 I. A. KORSHUNOV AND N. I. MALYUGINA, *Zh. Obshch. Khim.*, 34 (1964) 734.
4 H.-S. HSIUNG AND G. H. BROWN, *J. Electrochem. Soc.*, 110 (1963) 1085.
5 A. B. THOMAS AND E. G. ROCHOW, *J. Am. Chem. Soc.*, 79 (1957) 1843.
6 I. M. KOLTHOFF AND J. J. LINGANE, *Polarography*, Vol. I, Interscience, New York, London, 2nd ed., 1952, p. 222.
7 P. H. GIVEN AND M. E. PEOVER, *J. Chem. Soc.*, (1959) 1602–7.
8 A. JENSEN AND F. BASOLO, *J. Am. Chem. Soc.*, 81 (1959) 3813.
9 P. DELAHAY, *J. Am. Chem. Soc.*, 73 (1951) 4944.

ELECTROANALYTICAL CHEMISTRY AND INTERFACIAL ELECTROCHEMISTRY
Elsevier Publishing Company, Amsterdam – Printed in The Netherlands

POLAROGRAPHISCHE UNTERSUCHUNGEN AN PHOSPHORORGANISCHEN VERBINDUNGEN

IV. ABHÄNGIGKEIT DER INHIBITIONSEFFEKTE VON DER DEPOLISATOR-KONZENTRATION

H. SOHR UND KH. LOHS
Institut für Verfahrenstechnik der organischen Chemie, Leipzig, der Deutschen Akademie der Wissenschaften zu Berlin, DDR
(Eingegangen am 14 Juni 1966)

Die Mehrzahl der Veröffentlichungen, in denen Inhibitionseffekte behandelt werden, sind dadurch gekennzeichnet, dass die gewählten Depolarisatorkonzentrationen etwa im Bereich von $10^{-3}\,M$ bis $5 \cdot 10^{-2}\,M$ liegen. Obwohl meistens nicht näher darauf eingegangen wird, ist jedoch bekannt, dass Inhibitionseffekte bei höheren Depolarisatorkonzentrationen im allgemeinen ausgeprägter erscheinen. Dies konnten wir auch bei den meisten der von uns untersuchten phosphororganischen Verbindungen feststellen.

Wir sind in der Beurteilung dieses Sachverhaltes bei phosphororganischen Verbindungen zunächst von der Voraussetzung ausgegangen, dass die Adsorptionsparameter der oberflächenaktiven Substanzen im Verlauf der Inhibition nicht wesentlich geändert werden und sie somit keine ausschlaggebenden Ursachen für die eingangs erwähnte Abhängigkeit der Inhibitionseffekte von Depolarisatorkonzentrationen darstellen. Eine derartige Annahme ist in dieser Form bei Neutralmolekülen vertretbar, während bei oberflächenaktiven Ladungsträgern bekanntlich mit zusätzlichen Komplikationen gerechnet werden muss.

Die Abhängigkeit der Inhibitionseffekte von der Depolarisatorkonzentration bei völlig bedeckter Hg-Oberfläche stellt einen Teil der viel diskutierten Frage nach dem Mechanismus des Durchtritts entsprechender Depolarisatoren durch die Adsorptionsschicht dar und kann nur im Zusammenhang damit eine Erklärung finden.

Es ist nicht unsere Aufgabe, die einzelnen Interpretationen verschiedener Autoren im Hinblick auf den Mechanismus der Depolarisation in Gegenwart oberflächenaktiver Substanzen darzustellen, da dies schon mehrfach erfolgt ist[1–7].

Die Inhibitionseffekte sind im allgemeinen durch grosse Vielfalt gekennzeichnet. Je nach Art der untersuchten Systeme (Hg-oberflächenaktive Substanz-Depolarisator) treten einzelne Aspekte besonders in den Vordergrund, was in Ermanglung einer einheitlichen Theorie zu unterschiedlichen Erklärungen führte.

Die begrenzte Gültigkeit dieser Erklärungen wurde besonders offensichtlich, als SCHMID UND REILLEY mehrere solcher Systeme und ihre theoretischen Erklärungen verglichen[2].

Trotz vielseitiger Anstrengungen und einer Fülle experimentellen Materials ist

es noch nicht gelungen, eine umfassende Theorie zu erarbeiten, die in der Lage ist, das Versuchsmaterial quantitativ in befriedigender Weise zu erklären, obgleich in den letzten Jahren grosse Fortschritte erzielt worden sind[8-12]. Dieser Zustand ist auch deshalb unzulänglich, da Inhibitionsprobleme von grosser praktischer Bedeutung sind.

Nach unserer Auffassung ist ein wichtiger Grund für die ungenügende Klärung dieser Probleme in der nicht genügenden Beachtung der chemischen Wechselwirkungskräfte zwischen den Depolarisatoren und den unter den Bedingungen der Adsorption an der Hg-Oberfläche vorliegenden oberflächenaktiven Substanzen zu suchen. Beim Studium des Reaktionsverhaltens phosphororganischer Verbindungen an der Hg-Elektrode treten solche chemischen Effekte in der Adsorptionsschicht besonders stark in Erscheinung.

Ziel dieser Arbeit ist, weitere Beweise für das Wirksamwerden chemischer Wechselwirkungskräfte in der Adsorptionsschicht darzulegen.

EXPERIMENTELLES

Die Polarogramme wurden mit einem Heyrovský-Polarographen vom Typ LP 55 A aufgenommen. Die verwendete Jenaer Tropfkapillare hatte eine Ausflussgeschwindigkeit von 4.12 mg sec^{-1} bei 50 cm Quecksilberhöhe. Gemessen wurde gegen eine gesättigte Kalomelelektrode. Die Grundlösung war 0.1 *N* an Na_2SO_4 (bidest. H_2O). Die zu polarographierenden Lösungen wurden 3 Stunden vor den Messungen angesetzt. Die Temperatur in der Zelle betrug bei allen Versuchen $25 \pm 0.2°$. Für die verwendeten Substanzen gelten die Angaben der vorangegangenen Mitteilung[13].

ERGEBNISSE UND DISKUSSIONEN

a) Der Komplexbildungsmechanismus in der Adsorptionsschicht

In vorangegangenen Veröffentlichungen wurden Inhibitionseffekte mitgeteilt, die darauf hindeuten, dass die Penetration des Depolarisators in dem bedeckten Teil der Oberfläche der Hg-Elektrode infolge chemischer Wechselwirkungskräfte zwischen dem Depolarisator und der adsorbierten oberflächenaktiven Substanz vonstatten geht[13,14]. Als geschwindigkeitsbestimmender Schritt dieses Elektrodenvorganges wurde für die Penetration des Depolarisators durch die Adsorptionsschicht eine Reaktionsgleichung vorgeschlagen.

Die Ursache dieser Annahme wird einerseits durch das Auftreten von kinetischen Strömen im Potentialbereich der Adsorption und andererseits durch die Vergrösserung der Inhibition infolge Anreichung sowohl von bestimmten Schwermetallionen als auch von H^+-Ionen in der Adsorptionsschicht gestützt. Weitere Untersuchungen ergaben nunmehr, dass die Inhibition nicht allein von der Konzentration bestimmter Fremdkationen, sondern gleichermassen von der Konzentration des Depolarisators selbst abhängt. Hierbei vergrössern sich die Inhibitionseffekte mit Zunahme der Depolarisatorkonzentration, woraus geschlussfolgert werden kann, dass sich die Depolarisatorionen beim Passieren der Adsorptionsschicht gegenseitig behindern. In den Abbildungen 1–5 sind Kurven bei konstanter Konzentration an oberflächenaktiver Substanz und veränderter Depolarisatorkonzentration dargestellt. Hierbei ist die Empfindlichkeit (*E*) des Galvanometers zusammen mit der Konzentration des Depolarisators so geändert worden, dass ähnliche Polarogramme

der Grundlösungen ohne oberflächenaktive Substanz zustande kamen. Aus diesen Abbildungen geht klar hervor, dass mit Zunahme der Depolarisatorkonzentration die Wellen stärker deformiert werden. Hierbei erfolgt ein Wiederanstieg der Stromstärke (i) der Cu-Welle auf den Wert i_D bei immer negativeren Potentialen, so dass der Potentialbereich der Inhibition mit zunehmender Depolarisatorkonzentration

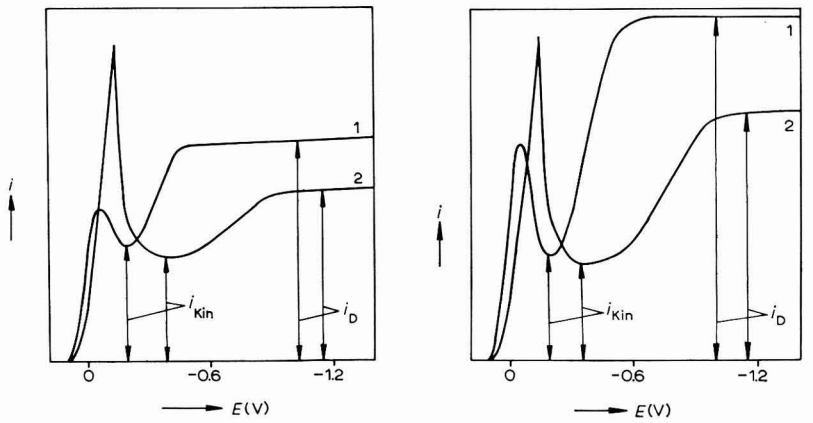

Abb. 1–2. Polarogramme von Cu^{2+} in Gegenwart von Tri-n-propylphosphat ($5 \cdot 10^{-3}$ M), pH 5. (1) Cu^{2+}, $2 \cdot 10^{-4}$ M; $E = 1/10$; (2) Cu^{2+}, $6 \cdot 10^{-3}$ M, $E = 1/300$.
Abb. 1, $t = 6.5$ sec; Abb. 2, $t = 3$ sec.

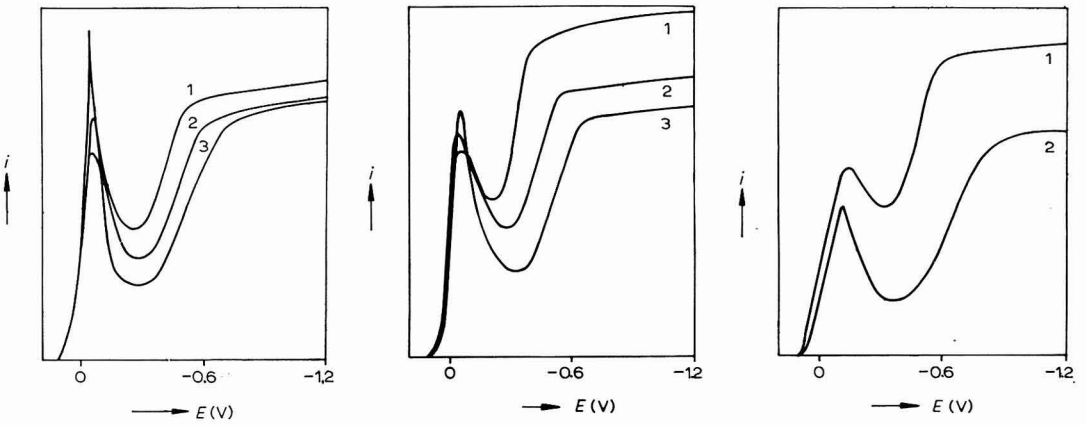

Abb. 3. Polarogramme von Cu^{2+} in Gegenwart von Tri-n-propylphosphat ($5 \cdot 10^{-3}$ M), pH 5; $t = 3$ sec. (1) Cu^{2+}, $6 \cdot 10^{-4}$ M; $E = 1/30$; (2) Cu^{2+}, 10^{-3} M; $E = 1/50$; (3) Cu^{2+}, $14 \cdot 10^{-3}$ M; $E = 1/70$.

Abb. 4. Polarogramme von Cu^{2+} in Gegenwart von Tri-iso-butylphosphat ($5 \cdot 10^{-4}$ M), pH 5, $t = 3$ sec. (1) Cu^{2+}, 10^{-4} M; $E = 1/5$; (2) Cu^{2+}, $4 \cdot 10^{-4}$ M; $E = 1/20$; (3) Cu^{2+}, 10^{-3} M; $E = 1/50$.

Abb. 5. Polarogramme von Cu^{2+} in Gegenwart von Triphenylphosphinoxid ($5 \cdot 10^{-4}$ M; Zusatz von 5% Methanol), pH 5, $t = 3$ sec. (1) Cu^{2+}, $2 \cdot 10^{-4}$ M; $E = 1/10$; (2) Cu^{2+}, $3 \cdot 10^{-3}$ M; $E = 1/150$.

breiter wird. Ausserdem wird mit zunehmender Depolarisatorkonzentration der Potentialbereich vom Kurvenminimum bis zum Erreichen des Wertes i_D zunehmend verzerrt. Man kann auch sagen, die Wellen des Wiederanstieges der Stromstärke werden mit zunehmender Depolarisatorkonzentration "irreversibler". Weiterhin sei erwähnt, dass die Stromstärke zwischen Abszisse und Kurvenminimum kinetisch bedingt ist, wie aus den Abbildungen 1 und 2 hervorgeht. Um für diese Ergebnisse eine Erklärung zu finden, muss man zunächst berücksichtigen, dass der Depolarisator als regelmässiger oktaedrischer Cu(II)–Aquo-Komplex in der angegebenen Grundlösung vorliegt. Die Wassermoleküle sind nach neueren Erkenntnissen in regelmässigen Abständen (2.18 Å) vom Zentralatom angeordnet[15]. Die an der Hg-Elektrode adsorbierten Moleküle der jeweils eingesetzten phosphororganischen Verbindung sind so ausgerichtet, dass die Phosphorylgruppen als stark hydrophyle Gruppen der Lösungsphase zugerichtet sind. Ausserdem handelt es sich bei den in Betracht kommenden phosphororganischen Verbindungen um tetraetrisch konfigurierte Substanzen, bei denen man auch infolge ihrer vergleichsweise geringen Grösse annehmen kann, dass sie sich in der Adsorptionsschicht regelmässig anordnen.

Unter diesen Voraussetzungen sind die Bedingungen für eine Substitution der Koordinationssphäre des Depolarisators durch die adsorbierten phosphororganischen Verbindungen durchaus gegeben. Bei geringen Depolarisatorkonzentrationen erfolgt eine stufenweise Substitution der Wassermoleküle des Cu(II)–Aquo-Komplexes durch die adsorbierten phosphororganischen Verbindungen nach folgendem Schema:

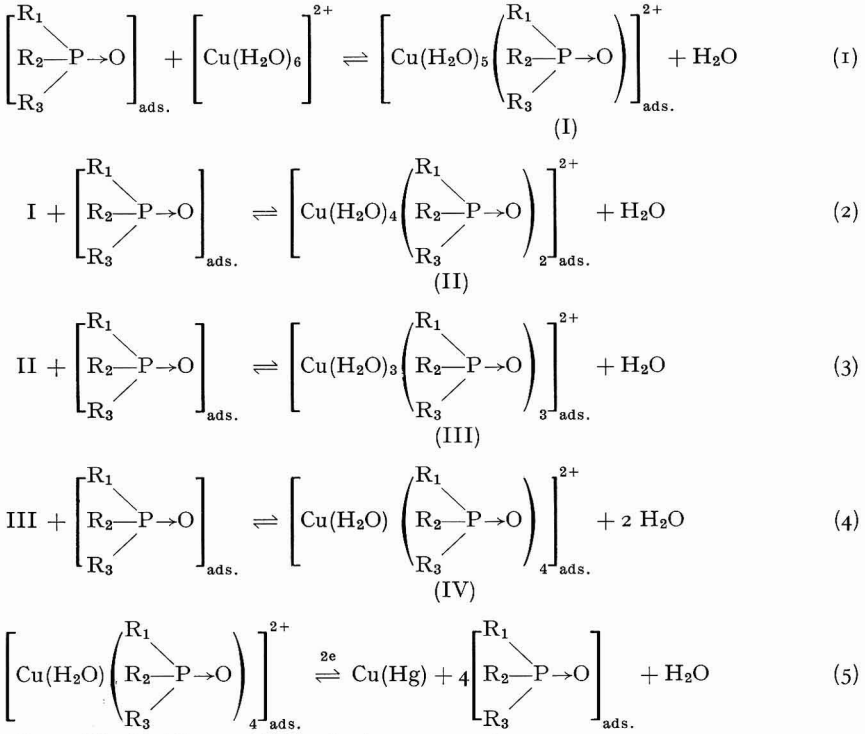

(R1, R2, R3 = Alkyl-, Alkoxy-, Aryl-, Aryloxygruppen)

Nach dem angegebenen Mechanismus wird zunächst durch ein adsorbiertes Phosphorsäureestermolekül eine Koordinationsstelle des oktaedrischen Cu(II)–Aquo-Komplexes besetzt (Gl. 1). Danach erfolgt die Substitution der Koordinationsstellen des Aquokomplexes durch die benachbarten adsorbierten Phosphorsäureestermoleküle, so dass bei (II) eine Kante und bei (III) eine Fläche des Oktaeders durch die adsorbierten Moleküle besetzt werden.

Durch diesen stufenweisen Substitutionsprozess gelangt das Cu(II)-Ion immer näher an die Hg-Elektrode heran. Im Komplex (IV) (Gl. 4) nimmt das Cu(II)-Ion die wahrscheinlich günstigste Lage für den Durchtrittsprozess ein, wobei es durch 4 planare Phosphorsäure-estermoleküle umgeben ist. Da die koordinative Phosphorylgruppe immer nur eine Koordinationsstelle eines Oktaeders betätigen kann, tritt mit zunehmender Depolarisatorkonzentration ein Mangel an Koordinationsstellen auf, so dass es fortschreitend mit der Erhöhung der Depolarisatorkonzentration zur Verzögerung des Eindringens der Depolarisatoren in die Adsorptionsschicht kommt, wodurch eine stärkere Verzerrung der polarographischen Kurven verursacht wird. Ausserdem können Abstossungskräfte zwischen den positiv geladenen Depolarisatorionen wirksam werden.

Gleichung (5) entspricht der Durchtrittsreaktion. Nach den allgemeinen Gesetzmässigkeiten der Komplexsubstitution dürfte Gl. (4) der geschwindigkeitsbestimmende Schritt des stufenweisen Ligandenaustausches und damit geschwindigkeitsbestimmend für den gesamten Elektrodenprozess sein[16–18]. Die durch Gleichung (4) bedingte Stromstärke entspricht i_{kin} (Abb. 1 und 2) im Minimum der polarographischen Kurven. Da die Stromstärke im Adsorptionsgebiet (siehe Abb. 1–5) den Wert i_D wieder erreicht, muss man annehmen, dass durch Änderung des Potentials nach negativeren Werten infolge Zunahme der elektrostatischen Kräfte die Abscheidung des Depolarisators schon aus Komplex (III) erfolgen kann. Die i_{kin}-bedingte Gleichung (4) spielt für die gesamte Elektrodenreaktion keine Rolle mehr und der geschwindigkeitsbestimmende Schritt ist in diesem Fall die Andiffusion des Depolarisators zur Hg-Oberfläche.

b) Durchtrittsreaktion und chemische Wechselwirkungskräfte als Ursachen der Penetration der Depolarisatoren durch die Adsorptionsschicht

Ausgehend von der Annahme der Komplexbildungstendenz in der Adsorptionsschicht als möglichen geschwindigkeitsbestimmenden Schritt des gesamten Elektrodenprozesses in einem bestimmten Potentialbereich kann man der bekannten Beziehung[2,8]:

$$k_{eff} = {}_0k_e(1-\theta) + {}_1k_e\theta \qquad (6)$$

(k_{eff} = effektive Geschwindigkeitskonstante der Durchtrittsreaktion;
${}_0k_e$ = Durchtrittsgeschwindigkeitskonstante auf dem nichtbedeckten Teil der Hg-Oberfläche;
${}_1k_e$ = Durchtrittsgeschwindigkeitskonstante auf dem bedeckten Teil der Hg-Oberfläche;
θ = Bedeckungsgrad)

einen erweiterten Sinn geben. Beim Auftreten von kinetischen Strömen im Potentialbereich der Adsorption kann ${}_1k_e$ auch die Grösse der Geschwindigkeitskonstante k_{kin} des geschwindigkeitsbestimmenden Schrittes der Ligandensubstitution darstel-

len. In unserem Fall wäre k_{eff} bei völlig bedeckter Hg-Oberfläche eine Funktion, die durch die Geschwindigkeit der Einstellung von Gl. (4) bedingt ist.

Wenn man demnach feststellt, dass bei einem bestimmten System ${}_1k_e > 0$, dann muss erst noch eine Klärung herbeigeführt werden, welcher Art ${}_1k_e$ ist.

Die Interpretation der Komplexbildung in der Adsorptionsschicht lässt sich auch auf andere Systeme anwenden. In direkter Beziehung zu unseren Ergebnissen stehen diejenigen von MARK UND REILLEY[19-21] sowie KŮTA[22]. Diese Autoren stellten fest, dass in Gegenwart oberflächenaktiver Substanzen (Amine und Aminosäuren) bei der Abscheidung von Schwermetallionen (Ni(II)) an der Hg-Elektrode katalytisch bedingte Vorwellen gemessen werden können, die kinetischen Charakter haben. Der von diesen Autoren angegebene Substitutionsmechanismus an der Hg-Elektrode entspricht im Prinzip dem von uns für die phosphororganischen Verbindungen vorgeschlagenen. HEYROVSKÝ UND MATYAS haben schon vor längerer Zeit darauf hingewiesen, dass die Ursache der Zunahme der Reversibilität bei Abscheidung von Cu(II), Sn(II) und Bi(III) in Anwesenheit bestimmter oberflächenaktiver Anionen in der Komplexbildungstendenz in der Adsorptionsschicht zu suchen sei[23].

Darüber hinaus kann man an Hand dieses Substitutionsmechanismus auch die Diskrepanzen zwischen Oberflächenaktivität und Inhibitionsaktivität qualitativ hinreichend erklären. ZAGANAOVA UND STROMBERG stellten beispielsweise zwischen der Inhibitionsaktivität und der Oberflächenaktivität von Kampfer und Gelatine eine solche Diskrepanz fest[24]. Obgleich Gelatine eine grössere Oberflächenaktivität als Kampfer besitzt, ist es mit der Inhibitionsaktivität in Gegenwart von Cd(II) als Depolarisator gerade umgekehrt. SCHMID UND REILLEY führten mehrere solcher Systeme an, bei denen Oberflächenaktivität und Inhibitionsaktivität grosse Unterschiede aufweisen[2].

Gelatine ist bekanntlich als Skleroprotein ein Polykondensat verschiedener Aminosäuren (hauptsächlich Prolin, Oxyprolin und Glykokoll) und besitzt demnach eine stärkeres Komplexbildungsvermögen für Schwermetallionen als Kampfer, wodurch es ionischen Schwermetallkomplexen leichter gelingt, durch Koordinationssubstitution in die Gelatineschicht einzudringen als in entsprechende Adsorptionsschichten, in denen Kampfermoleküle adsorbiert sind. Hierauf haben ZUMAN und Mitarbeiter schon in ähnlichem Zusammenhang hingewiesen[25].

Viel diskutiert wird die Bedeutung der Grösse des Depolarisators bezüglich der Überwindung der Adsorptionsschicht. Wir sind zu der Auffassung gelangt, dass die Grösse dabei nur scheinbar eine wichtige Rolle spielt. Die Inhibitionsaktivität ist, nach den bisherigen Darlegungen zu urteilen, einerseits thermodynamisch durch die Komplexstabilität des andiffundierenden Depolarisators und des möglicherweise in der Adsorptionsschicht entstehenden Komplexes sowie zum anderen durch kinetische Faktoren bedingt.

Es liegt also hier die Möglichkeit der Ligandensubstitution als Ursache des Eindringens des Depolarisators in die Adsorptionsschicht sowie eine daraus folgende Verringerung des Abstandes zwischen Depolarisator und Hg-Oberfläche vor. Dabei ist wichtig zu betonen, dass die kinetischen Faktoren der Komplexsubstitution und der Komplexstabilität nur wenig miteinander zu tun haben, bzw. dass die Theorie noch nicht in der Lage ist, diese Zusammenhänge richtig zu erklären[16].

In den vorangegangenen Mitteilungen wurde darauf hingewiesen, dass zwischen dem Eindringen des Depolarisators in die Adsorptionsschicht und der

flüssig–flüssig-Extraktion Parallelbeziehungen bestehen[13]. In diesem Sinne fungiert die Adsorptionsschicht als organische Phase. Eine solche Vorstellung ist durchaus diskutabel, da bekanntlich die Ableitung der Gibbs'schen Adsorptionsisotherme von dieser Voraussetzung ausgeht. Bei Inhibitionsvorgängen spielen aber zusätzlich die von der Hg-Elektrode ausgehenden und vom jeweils angelegten Potential bestimmten elektrostatischen Kräfte eine Rolle. Je nach den physikalischen und chemischen Eigenschaften der Moleküle in der Adsorptionsschicht und denen der Depolarisatoren treten unter den Bedingungen der Adsorption entweder Durchtrittseffekte oder chemische Wechselwirkungskräfte als Ursache der Penetration der Depolarisatoren durch die Adsorptionsschicht in Erscheinung. Hierbei können durchaus beide Ursachen für ein System in verschiedenen Potentialgebieten wirksam werden.

ZUSAMMENFASSUNG

Ausgehend von der Tatsache, dass die polarographischen Cu(II)-Kurven in Gegenwart einer konstanten Konzentration einiger als oberflächenaktive Substanzen fungierender phosphororganischer Verbindungen mit Vergrösserung der Depolarisatorkonzentration zunehmend deformiert werden, wurde ein stufenweiser Substitutionsmechanismus der Koordinationssphäre des Depolarisators vorgeschlagen. Die Ursache für diese zunehmende Deformation ist demnach in der Konkurrenz der Depolarisatoren um die Koordinationsstellen in der Adsorptionsschicht zu suchen. Die in dieser Schicht wirksam werdenden chemischen Wechselwirkungskräfte werden zusammen mit der Verzögerung der Durchtrittsreaktion als Ursache für den Grad der Inhibition diskutiert.

SUMMARY

Starting from the fact that the deformation of the polarographic waves for Cu(II), in the presence of a constant concentration of some organo-phosphorus compounds acting as surface-active agents, increases with increasing concentration of the depolarizer, a stepwise substitution mechanism of the depolarizer in the coordination sphere is proposed. The cause of this increasing deformation is accordingly to be sought in the competition of the depolarizer for the coordination sites in the adsorption layer. The chemical interaction forces acting in this layer, together with the retardation of the charge transfer reaction are the cause of the degree of inhibition discussed.

LITERATUR

1 A. N. FRUMKIN, *Nova Acta Leopoldina*, 19 (1957) 1.
2 R. W. SCHMID UND C. N. REILLEY, *J. Am. Chem. Soc.*, 80 (1958) 2087.
3 H. W. NÜRNBERG UND M. VON STACKELBERG, *J. Electroanal. Chem.*, 4 (1962) 1.
4 C. N. REILLEY UND W. STUMM, *Progr. Polarog.*, 1 (1962) 81.
5 A. N. FRUMKIN UND B. B. DAMASKIN, *Mod. Aspects Electro-Chem.*, 3 (1964) 149.
6 B. KASTENNING UND L. HOLLECK, *Talanta*, 12 (1965) 1259.
7 J. HEYROVSKÝ UND J. KŮTA, *Grundlagen der Polarographie*, Akademie-Verlag, Berlin, 1965, S. 252–306.
8 J. WEBER, J. KOUTECKY UND J. KORYTA, *Z. Elektrochem.*, 63 (1959) 583.
9 J. KŮTA UND J. SMOLER, *Z. Elektrochem.*, 64 (1960) 285.
10 J. KOUTECKY UND J. WEBER, *Collection Czech. Chem. Commun.*, 25 (1960) 1423.

11 J. KŮTA, J. WEBER UND J. KOUTECKY, *Collection Czech. Chem. Commun.*, 26 (1961) 224.
12 J. KŮTA UND J. WEBER, *Electrochim. Acta*, 9 (1964) 541.
13 H. SOHR UND KH. LOHS, *J. Electroanal. Chem.*, 13 (1967) 107.
14 H. SOHR UND KH. LOHS, *J. Electroanal. Chem.*, 13 (1967) 114.
15 SS. ANDREJEW UND O. W. SSAPOSHNIKOWA, *Dokl. Akad. Nauk. SSSR*, 156 (1964) 855.
16 H. TAUBE, *Chem. Rev.*, 50 (1952) 69.
17 H. TAUBE, *Advanc. Inorg. Chem. Radiochem.*, 1 (1959) 1.
18 F. BASOLO UND R. G. PEARSON, *Advanc. Inorg. Chem. Radiochem.*, 3 (1961) 1.
19 H. B. MARK JR. UND C. N. REILLEY, *J. Electroanal. Chem.*, 4 (1962) 189.
20 H. B. MARK JR., *J. Electroanal. Chem.*, 7 (1964) 276.
21 H. B. MARK JR., *J. Electroanal. Chem.*, 8 (1964) 253.
22 J. KŮTA, *Z. Anal. Chem.*, 216 (1966) 243.
23 J. HEYROVSKÝ UND M. MATYAS, *Collection Czech. Chem. Commun.*, 16 (1951) 455.
24 L. S. ZAGANAOVA UND A. G. STROMBERG, *Dokl. Akad. Nauk SSSR*, 105 (1955) 747.
25 R. ZUMANOVA, J. TEISINGER UND P. ZUMAN, *Chem. Zvesti*, 11 (1957) 517.

Elsevier Publishing Company, Amsterdam – Printed in The Netherlands

SHORT COMMUNICATIONS

The anodic formation of phosphates of mercury

The aim of this communication is to correlate potentiostatic and a.c. impedance measurements obtained in this laboratory with published polarographic data for anodic mercury salt formation in phosphate media.

A polarographic study of the phosphate system was carried out by ZUMAN[1] who found that the anodic wave of hydroquinone in phosphate buffer solutions showed a sharp decrease from the limiting current just prior to the final unlimited increase in current; he attributed this to the formation of a mercury–phosphate salt. CHRISTIAN AND PURDY[2] carried out a more extensive study of the residual current in orthophosphate medium, covering the pH range 3.0–10.6, and found as many as three waves in addition to the normal mercury dissolution wave. The height of the most anodic wave was proportional to the square root of the height of the mercury above the capillary, *i.e.*, a diffusion-controlled wave, while the others were adsorption pre-waves, their height being directly proportional to the head of the mercury above the capillary. They stated that at pH-values below 4.2 the half-wave potential of the diffusion-controlled wave corresponded well with the potential of the mercury–mercurous monohydrogen phosphate half-cell, but that at pH-values greater than 4.7 no simple relationship appeared to hold. More recently, LINGANE[3] has repeated ZUMAN's work but has reported only one pre-wave in a phosphate buffer of pH 7.23. A study of the characteristics of this anodic wave led him to believe that it was caused by the oxidation of mercury to form a monomolecular film of $(Hg_2)_3(PO_4)_2$. The final increase in current was attributed to the oxidation of mercury to Hg_2HPO_4. The formation of thin solid films on liquid electrodes has recently been discussed in relation to polarographic experiments[4] and it has been suggested that anodic polarographic pre-waves are due to the formation of monomolecular layers of the mercury salt at the electrode.

In the present work only one solution was used, *i.e.*, 0.1 *M* NaH_2PO_4 + 0.1 *M* Na_2HPO_4 + 0.6 *M* KNO_3. All reagents were AnalaR. The measured pH of this solution was 6.52. All measurements were made at 24° ± 1° and all potentials are given *versus* the saturated calomel electrode. The polarogram in Fig. 1 was obtained manually and shows two pre-waves which we attribute to the formation of two monomolecular layers of a mercury–phosphate salt. The first wave is almost a perfect step function but the second is not so well defined. The half-wave potentials of the first and second waves, $E_{\frac{1}{2}}^{I}$ and $E_{\frac{1}{2}}^{II}$, respectively, are given in Table 1; the potential of the final anodic rise, E^{III}, is also given. The impedance of a stationary mercury drop electrode was measured as a function of potential by the method described elsewhere[5]. The impedance was found to be purely capacitative at potentials cathodic to the half-wave potential of the second polarographic pre-wave and the form of this relationship is shown in Fig. 2. The two anodic discontinuities in the *C–E* curve are due to the formation of the first and second monomolecular layers, and the potentials at which these discontinuities occur, E^{I} and E^{II}, respectively, correspond well with the half-wave potentials from the polarogram (see Table 1). On first increasing and

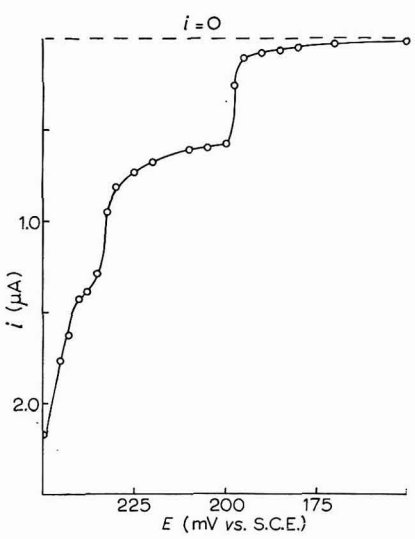

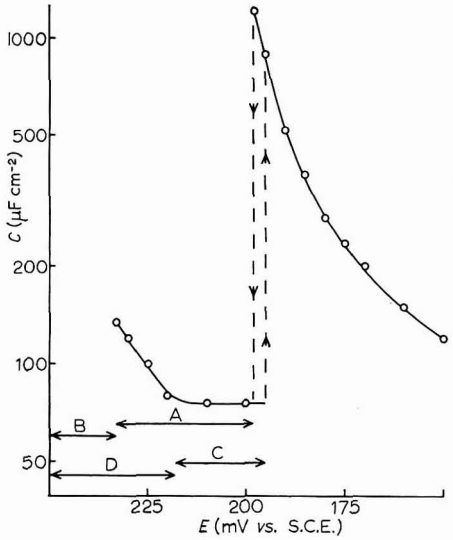

Fig. 1. Anodic polarogram of 0.1 *M* NaH_2PO_4, 0.1 *M* Na_2HPO_4, 0.6 *M* KNO_3.

Fig. 2. Capacity–potential curve for a static mercury electrode in 0.1 *M* NaH_2PO_4, 0.1 *M* Na_2HPO_4, 0.6 *M* KNO_3. A and B correspond to the regions of anodic stability of the first and second monomolecular layers, respectively. C and D correspond to the regions of cathodic stability.

TABLE 1

MONOMOLECULAR-LAYER AND MULTILAYER POTENTIALS

Polarographic results (mV)		*A.c. impedance results (mV)*		
			Formation	*Reduction*
$E_{\frac{1}{2}}^{I}$	198	E^{I}	198	195
$E_{\frac{1}{2}}^{II}$	234	E^{II}	233	218
E^{III}	242	E^{M}	250–260	235

then decreasing the potential hysteresis was observed at both discontinuities. The hysteresis was 3 mV and 15 mV for the first and second discontinuities, respectively, and these values give the difference between the formation and reduction potentials of the first and second monomolecular layers. The various regions of stability of the first and second monomolecular layers are shown in Fig. 2. Anodic current–time transients were obtained by using a potentiostat in conjunction with a rectangular pulse generator. The stationary mercury drop electrode was held cathodic to the monomolecular layer reversible potential, E_R, and the pulse height was such that on application to the electrode the potential became anodic with respect to E_R, resulting in the formation of the film. Some typical current–time transients are shown in Fig. 3, A–D. Figure 3, A and B, show the transients due to the formation of the first and second monomolecular layers, respectively. In both cases the base potential was cathodic with respect to E_R^I, the reversible potential of the first monomolecular layer. Figure 3C shows a transient for the second monomolecular layer formation with the base potential anodic with respect to E_R^I and cathodic with respect to E_R^{II}.

Figure 3D shows a transient for the formation of a multilayer, which begins to grow between +250 and +260 mV (E^{M}). The shape of the transients in Fig. 3, A–C, has been attributed to two-dimensional nucleation and subsequent growth. The current is therefore proportional to the length of the growing periphery and, due to overlap, a maximum in the current occurs[6]. This is the first system studied in which a second monomolecular layer can be formed and reduced without disturbing the first layer. The growth of this layer may result from nucleation at imperfections in the first layer, similarly holes may nucleate at imperfections on reduction. The rate of formation of the second layer is much slower than that of first and this results in the second polarographic pre-wave being less well defined than the first. The quantities of charge involved in forming the first and second monomolecular layers, q_{I} and q_{II}, respectively, were calculated from the current–time transients by graphical integration of the

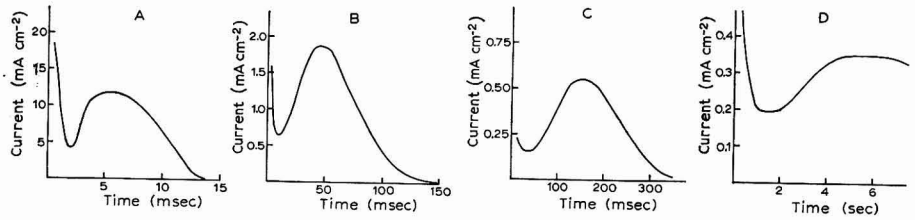

Fig. 3. Potentiostatic transients obtained in the formation of mercurous monohydrogen phosphate. Soln. composition: 0.1 M NaH_2PO_4, 0.1 M Na_2HPO_4, 0.6 M KNO_3. Final potentials: (A), 205; (B), 238; (C), 235; (D), 270 mV *vs.* S.C.E.

TABLE 2

MONOMOLECULAR-LAYER CHARGES

	From polarographic determination	*From potentiostatic determination*
q_{I}	140±10 μC cm^{-2}	100±10 μC cm^{-2}
q_{II}	170±40 μC cm^{-2}	125±10 μC cm^{-2}

peaks and compared (see Table 2), with those obtained from the polarogram using the equation

$$\bar{i} = (4\pi)^{\frac{1}{3}}(3/d)^{\frac{2}{3}} q m^{\frac{2}{3}} t_1^{-\frac{1}{3}}$$

where $\bar{i}$ is the average current (μA), m is the rate of flow of mercury (g sec^{-1}), t_1 is the drop time (sec), q is the charge (μCcm^{-2}) and d is the density of mercury (13.55 g/cm^3).

The difference between the potentiostatically and polarographically calculated values of q_{I} and q_{II} is attributed to the fact that the potentiostatic method involves only the area under the peak in the current–time transient whereas the polarographic method involves integration from the e.c.m. up to the potential of formation. The difference between q_{I} and q_{II} may be attributed to the different surface interactions causing a difference in structure in the first and second monomolecular layers, although they do agree within the limits of experimental error.

The half-cell reaction for the mercury–mercurous monohydrogen phosphate electrode is

$$2\,Hg + HPO_4^{2-} = Hg_2HPO_4 + 2\,e \qquad E^\circ = 180.5\ mV$$

The value of E° was determined from the results of DE VRIES AND COHEN[7], and LARSON[8] corrected for the most recent value of K_1[9] the first dissociation constant of phosphoric acid and combined with the second dissociation constant, $K_2 = 6.34 \times 10^{-8}$ mole l^{-1} [10]. In order to determine the bulk reversible potential of this half-cell reaction for the solution used in the present work, the activity of HPO_4^{2-} at unit ionic strength must be known. A value of this was estimated using two independent methods and both gave a value of 0.1. This leads to a bulk reversible potential of 240.5 mV. As this value concides with the final anodic rise on the polarogram, and as it lies between the formation and reduction potential of the multilayer, we may assume that the bulk phase is Hg_2HPO_4, in agreement with LINGANE[3]. Previous work in this laboratory[11] has shown that a plot of E^{II} against log $[HPO_4^{2-}]$ gives a straight line of slope -30 mV up to $[HPO_4^{2-}] = 10^{-3}\,M$, and from this we conclude that the second monomolecular layer is also Hg_2HPO_4. LINGANE[3] has stated that the anodic wave he observed, which corresponds to the formation of the first monomolecular layer, involves the anion PO_4^{3-}. However, if this were true it would be unlikely that two waves could be observed at low pH, yet CHRISTIAN AND PURDY*[2] have observed two anodic waves in a solution of pH 3, and one of us[11] has observed, potentiostatically, current–time transients showing two formation peaks in a solution of pH 2.2 From this we suggest that the anion HPO_4^{2-} is involved in the formation of the first monomolecular layer as well as the second. The monomolecular layers would then have the same stoichiometry, but a different structure, due to different surface interactions as only the first is formed on the bare mercury surface. The different surface interactions would account for the 35-mV difference between the formation potentials of the first and second monomolecular layers, although, as might be expected, the difference between E^{II} and E^{III} is small.

Department of Physical Chemistry,
University of Newcastle-upon-Tyne,
Newcastle-upon-Tyne, 1 (England)

R. D. ARMSTRONG
M. FLEISCHMANN
J. W. OLDFIELD

1 P. ZUMAN, *Collection Czech. Chem. Commun.*, 20 (1955) 876.
2 G. D. CHRISTIAN AND W. C. PURDY, *J. Electroanal. Chem.*, 3 (1962) 363.
3 J. J. LINGANE, *J. Electroanal. Chem.*, 12 (1966) 173.
4 R. D. ARMSTRONG AND M. FLEISCHMANN, *J. Polarog. Soc.*, 11 (1965) 31.
5 R. D. ARMSTRONG, D. F. PORTER AND H. R. THIRSK, *J. Electroanal. Chem.*, 14 (1967) 17.
6 M. FLEISCHMANN AND H. R. THIRSK, *Advan. Electrochem. Electrochem. Eng.*, 3 (1963) 123.
7 T. DE VRIES AND D. COHEN, *J. Am. Chem. Soc.*, 71 (1949) 114.
8 W. D. LARSON, *J. Phys. Chem.*, 54 (1950) 310.
9 D. J. G. IVES AND G. J. JANZ, *Reference Electrodes, Theory and Practice*, Academic Press, 1961, New York, p. 168.
10 R. G. BATES AND S. F. ACREE, *J. Res. Nat. Bur. Std.*, 30 (1943) 129.
11 J. OLDFIELD, unpublished work.

Received October 31st, 1966

* The potentials at which CHRISTIAN AND PURDY observe anodic polarographic waves do not agree with those of LINGANE or our own.

Polarographic estimation of uranium(VI) at the dropping mercury electrode in phosphoric acid

The reduction of uranium(VI) has been studied in various media[1-8]. In the work reported in this note, the polarographic wave in 1.0–4.0 *M* phosphoric acid containing about 0.3 *M* neutral salts was observed. The half-wave potential in the presence of the chlorides of the alkali metals and alkaline earths was about −0.14 V *vs.* S.C.E. and the values of $i_d/ct^{1/6}m^{2/3}$ were between 0.32 and 0.38. Similar results were obtained with KNO_3 and Na_2SO_4, but with NaF the wave height was smaller ($i_d/ct^{1/6}m^{2/3} = 0.26$ in the presence of 0.01 *M* cetyltrimethylammonium bromide for maximum suppression). In all these cases the wave shape corresponds to the equation for a reversible one-electron process. No further reduction steps were observed, probably because they were obscured by hydrogen evolution. In the presence of $KClO_3$, the irreversible wave shown in Fig. 1 (accompanied occasionally by a maximum) was not a strictly linear function of concentration. For the above mentioned electrolytes the limiting current was diffusion-controlled and proportional to uranyl nitrate concentration down to 10^{-5} *M*.

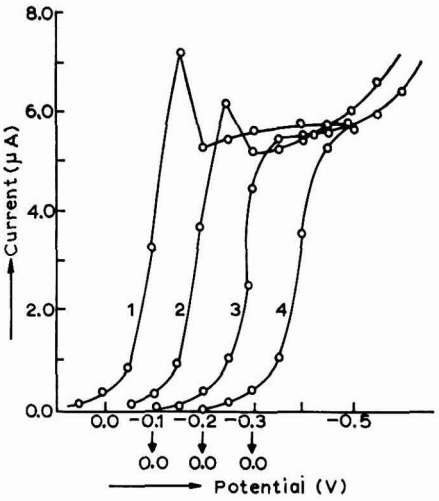

Fig. 1. Effect of $KClO_3$ concn. on the maxima in 2.0 *M* phosphoric acid, 1.334×10^{-3} *M* uranyl nitrate: (1), 0.1666; (2), 0.5; (3), 0.8334; (4), $1.0 \cdot 10^{-1}$ *M* $KClO_3$.

Equal concentrations of Tl(I), Ni(II), Co(II), Mn(II), Fe(II), Cd(II), Hg(II), Sn(II), Zn(II), Ce(III), Bi(III), Al(III), Cr(III), Zr(III), V(IV), Ce(IV), Sn(IV), Th(IV), Hf(IV), V(V) and Mn(VI) did not interfere. The reduction waves of Cu(II) and Ag(I) interfered seriously, but that of Fe(III), which results in a rise of current at more positive potentials, interfered only when present in an excess of greater than 5- or 10-fold. Cr(II) (recorded under a layer of kerosene oil) interfered, probably due to its oxidation to Cr(III) by U(VI) which was thus reduced to U(V). A well-defined step

of Pb(II) was obtained at potentials slightly more negative than the wave of U(V), but this caused no interference.

Chemical Laboratories,
University of Roorkee,
Roorkee (India)

WAHID U. MALIK
HARI OM GUPTA
CHOKHEY LAL SHARMA

1 P. HERASYMENKO, *Chem. Listy*, 19 (1925) 172; *Trans. Faraday Soc.*, 24 (1928) 272.
2 W. E. HARRIS AND I. M. KOLTHOFF, *J. Am. Chem. Soc.*, 67 (1945) 1484.
3 R. STRUBL, *Collection Czech. Chem. Commun.*, 10 (1938) 466.
4 I. M. KOLTHOFF, W. E. HARRIS AND G. MATSUYAMA, *J. Am. Chem. Soc.*, 66 (1944) 1782.
5 D. H. M. KERN AND E. F. ORLEMANN, *J. Am. Chem. Soc.*, 71 (1949) 2102.
6 K. A. KRAUS, F. NELSON AND G. L. JOHNSON, *J. Am. Chem. Soc.*, 71 (1949) 2510.
7 E. S. KRITCHEVSKY AND J. C. HINDMANN, *J. Am. Chem. Soc.*, 71 (1949) 2069.
8 H. F. BALLENGER, U.S. Government Pub. A.E.C.D. 2065.

Received August 22nd, 1966; in revised form November 10th, 1966

J. Electroanal. Chem., 14 (1967) 239–240

Zur Invers-Polarographie des Technetiums

Die inverse Polarographie wurde von uns erstmals auf ihre Eignung zur analytischen Bestimmung des Radioelements Technetium geprüft. Unter Verwendung der Kemula-Elektrode der Fa. Metrohm liessen sich an alkalischen $K^{99}TcO_4$-Lösungen nach Elektrolyse bei einem Abscheidungspotential von -1.0 V gut auswertbare Polarogramme aufnehmen; in neutralen Grundelektrolyten traten nur in Andeutungen Wellen auf, während sie in sauren Lösungen ganz ausblieben. Bei kathodischer Arbeitsweise (cathodic stripping) konnten keine Wellen beobachtet werden. Abb. 1 zeigt ein charakteristisches Invers-Polarogramm des TcO_4^- in alkalischer Grundlösung.

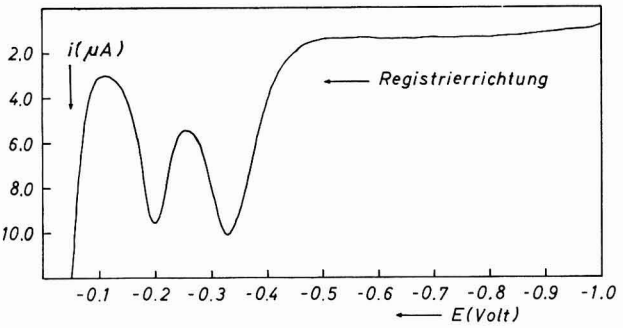

Abb. 1. Invers-Polarogramm von 20 ml $6.0 \cdot 10^{-5}$ *M* $KTcO_4$ in 1 *M* NaOH, Temp. 25°, Bezugselektrode ges. Ag/AgCl, Elektrolysedauer 4 min, Hg-Tropfendurchmesser $\simeq$ 0.8 mm, Spannungsvorschub 1 V min^{-1}.

Die beiden Wellen mit den Spitzenpotentialen $E_s \simeq -0.33$ V und $\simeq -0.20$ V liegen sehr viel positiver als die reversiblen TcO_4^--Reduktionsstufen des normalen Gleichstrom-Polarogramms[1]. Die den Wellen zugrunde liegenden Oxydationsvor-

gänge sind noch nicht geklärt. Der bei der Anreicherungselektrolyse am Hg-Tropfen beobachtete braunschwarze Belag deutet auf die Bildung des in alkalischem Medium bevorzugt entstehenden TcO_2 hin, so dass die Gesamtoxydation durch den Übergang Tc(IV)→Tc(VII) beschrieben werden könnte.

In 1 *M* Natronlauge wurde für die Welle bei −0.33 V im Konzentrationsbereich von 10^{-4} bis $3 \cdot 10^{-7}$ *M* Tc, für die Welle bei −0.20 V von 10^{-4} bis $4 \cdot 10^{-6}$ *M* Tc lineare Abhängigkeit des Spitzenstroms von der Konzentration nachgewiesen. Die Erfassungsgrenze lag bei 0.3 μg Tc. Die Messungen waren mit einem Fehler von ±4% reproduzierbar. Während in Gegenwart von UO_2^{2+} die Ausbildung der Wellen stark beeinträchtigt wird, konnten noch 0.5 μg Tc neben einem 10^4-fachen molaren MoO_4^{2-}-oder ReO_4^--Überschuss quantitativ bestimmt werden.

Die Untersuchungen wurden im Rahmen des Euratom-Forschungsvertrages Nr. 064-64 RISD durchgeführt. Prof. W. HERR danken wir für die freundliche Förderung dieser Arbeit.

Arbeitsgruppe "Institut für Radiochemie" der Kernforschungsanlage Jülich; L. ASTHEIMER
Institut für Kernchemie der Universität Köln K. SCHWOCHAU

Eingegangen 8. September 1966.

1 L. ASTHEIMER UND K. SCHWOCHAU, *J. Electroanal. Chem.*, 8 (1964) 382.

BOOK REVIEWS

The Glass Electrode, by G. EISENMAN, R. BATES, G. MATTOCK and S. M. FRIEDMAN, Interscience Publishers Inc., New York, London and Sydney, 1966, 330 pages, $7 or 53s.

This is a paperback reprint of articles by the four authors, respectively:

(i) *The Electrochemistry of Cation Sensitive Glass Electrodes* from *Advances in Analytical Chemistry and Instrumentation* edited by C. N. REILLEY, Vol. 4, (1965).

(ii) *The Glass Electrode in the Determination of pH* from *Determination of pH: Theory and Practice*, 1964.

(iii) *Laboratory pH Measurements* from *Advances in Analytical Chemistry and Instrumentation* edited by C. N. REILLEY, Vol. 2, 1963.

(iv) *Measurement of Sodium and Potassium by Glass Electrodes* from *Methods of Biochemical Analysis* edited by D. GLICK, Vol. 10, 1962.

Three of these articles were very well reviewed in this Journal: (i) 13 (1967) 468, (ii) 8 (1964) 493 and (iii) 8 (1964) 492. The only question is whether it is more useful to have them grouped in the present form rather than in the original. With the exception of (ii), there is little doubt that, being drawn from heterogeneous collections, they tend to be more useful in the newer grouping. However, the chapter from BATES' book is in a different category. It is designed as part of an integral work. Since this work is the

best book on pH, it seems unlikely that anyone wanting these articles could do without BATES' book. Of course the paperback is cheaper — about 47 pages/dollar as against an average of about 30 for the source books. On the other hand, there is no index and the articles are reprinted without any alteration; even the serious misprint noted in the earlier review of (iii) is still there.

ROGER PARSONS, University of Bristol

J. Electroanal. Chem., 14 (1967) 241–242

Advances in Magnetic Resonance, Vol. 1, edited by J. S. WAUGH, Academic Press, Inc., New York, 1966, £6, 413 pp.

A birth is always an important and exciting occasion, although this genus is now so prolific. Research in nuclear magnetic resonance and in electron spin resonance is now so diverse and widespread that this particular addition to the family is to be warmly welcomed; and the qualities and virility of the editorial father are such that we can look forward confidently to the future.

The Preface tells us that it was "with the insiders as well as the interested outsiders in mind that this serial publication was conceived... The subject matter ranges from original theoretical contributions, through syntheses of points of view toward series of phenomena, to critical and painstaking tabulations of experimental data."

This first volume contains six articles and they cover theoretical and experimental aspects of N.M.R., and, to a lesser extent, of E.S.R. REDFIELD has written an advanced, authoritative account of the theory of relaxation processes (32 pages). There is a timely review by JOHNSON (70 pages) of the concepts and methods of magnetic resonance techniques for the study of the rates of chemical changes. There is an excellent article (46 pages) by EATON AND PHILLIPS on the N.M.R. of paramagnetic molecules, a subject which is of special interest to inorganic chemists. The theory of nuclear spin–spin coupling is treated by BARFIELD AND GRANT (45 pages); it is a critical account and deals with directly-bonded and longer-range interactions. The authors rightly concentrate on the Fermi-contact contribution but point out that the other effects have not been shown to be negligible for heavy nuclei. Actually, Ramsey's original calculation that the dipole–dipole interaction *via* the electron spins contributes about 7% of the coupling constant in hydrogen is in error, and the effect is much less important. BOTHNER-BY has compiled (122 pages) geminal and vicinal proton–proton coupling constants and longer-range couplings in aromatic and heterocyclic systems; signs are given wherever they have been determined. His article is critical and authoritative and should be very useful. Finally, BOWERS has tabulated (80 pages) the hyperfine splittings in the E.S.R. spectra of radical ions in solution.

This is a useful book and one that libraries should possess, but the price is rather high for individual ownership. There will soon be competition, for another publisher has announced that Vol. 1 of *Progress in Nuclear Magnetic Resonance Spectroscopy* is expected soon. What fertility!

A. D. BUCKINGHAM, University of Bristol

Chemical Physics of Ionic Solutions, edited by B. E. CONWAY AND R. G. BARRADAS, Wiley, New York, London and Sydney, 1966, xvii + 622 pages, £9.8s.0d.

The symposium held by the Electrochemical Society in Toronto in May 1964 may be considered as the successor to the earlier symposium of the same society held in Washington in May 1957 as well as to the Faraday Society's General Discussion on *Interaction in Ionic Solutions* in September 1957 in Oxford, and the International Symposium on Electrolytes in Trieste in 1959. In some senses the field of the present symposium is narrower than those of the earlier ones but it gains by being better focussed on the subject accurately described by the title. Many of the papers are of such difficulty that it is of great value to have them printed for close study. The editors discuss in their preface the justification for publishing the proceedings of a symposium. The excellent choice of papers together with the publication of sufficient discussion material, completely vindicates their argument. The resulting volume is outstanding among recent publications of this type and like the Faraday Society Discussions should serve as a model for those contemplating a similar enterprise. It is appropriately dedicated to the memory of F. E. W. WETMORE, who carried out so much of his well-known electrochemical research in Toronto; no better memorial could be desired.

ROGER PARSONS, University of Bristol

J. Electroanal. Chem., 14 (1967) 243

An Introduction to Fuel Cells, edited by K. R. WILLIAMS, Elsevier, Amsterdam, London and New York, 1966, xiv + 329 pages, £4.10s.0d.

Mr. WILLIAMS begins his preface by indicating the lack of a co-ordinated account of the scientific basis of fuel cells and their current status. In this excellent book he and his colleagues have filled this gap with a well-balanced text. Unlike many books with more than one author, this is written by a team which has been in existence over a period of nearly ten years. Hence it reads consistently with none of the abrupt changes of level or viewpoint usually associated with such works. It is also very clearly written. The kinetics of electrode reactions are inadequately treated in all but the most recent electrochemical textbooks, but the introductory treatment here might be read with profit by any student beginning this branch of electrochemistry. The fact that the treatment of fundamentals occupies only 85 pages could mean that it was superficial, but on the contrary the essential points are clearly brought out, not smothered in a mass of detail.

The rest of the book deals with proposed types of fuel cells, their problems and advantages. The authors have their feet planted firmly on the ground and emphasize the practical difficulties confronting the commercial exploitation of fuel cells of any type. Nevertheless in a succinct final chapter summarizing the present position, they remind us that progress in this field is greater than in those of other *new* energy converters.

The book is well produced and has useful indices. Only one serious misprint was noted: on page 81 in equation 17, the last term has a θ omitted. The reference to this equation on the following page is incorrect.

ROGER PARSONS, University of Bristol

J. Electroanal. Chem., 14 (1967) 243

Polarographic Techniques, by L. MEITES, 2nd ed., Interscience Publishers Inc., New York, London and Syndey, 1966, xvii+752 pages, 147s.

The increase in knowledge of electoanalytical techniques over the past ten years has led Professor MEITES to expand his well-known book by a factor of three. Nevertheless, it remains the same, firmly practical, laboratory book which analysts can rely on with certainty. It is full of useful practical tips, exemplified best perhaps in the first appendix on *Trouble Shooting in Polarographic Circuits* but by no means confined to one section of the book. It is also firmly centred on classical polarography although electrodes other than mercury are carefully described in chapter 8. However the chapter on *Related Techniques* gives short shrift to the modern sophisticated techniques; only 15 of the 82 pages being devoted to *Cyclic and Pulse Techniques* and this section ends with a dire warning about the unreliability of elaborate electronic apparatus which seems unreasonably gloomy. The best of this section is a diagrammatic summary of the various techniques. More than half of the chapter is concerned with various types of coulometry.

This, then is a book for the practising polarographer who would prefer not to waste time with electronics and who requires to understand the results of theoretical investigations without more than an outline of their basis. Professor MEITES is successful in supplying the latter need in most of the book but the accounts of the correlation between half-wave potentials and structure (pp. 284–8) and of the theory of the polarographic maximum (pp. 312–9) leave something to be desired. It is also surprising to read about the diffuse double-layer effect on electrode reactions (pp. 254–264) and the formation of oxide films on platinum (p. 432) without any mention of FRUMKIN; this is an indication of the unfortunate division between electrochemists and electroanalytical chemists which this Journal hopes to bridge.

This well-produced book is concluded with three useful appendices, one mentioned above and two on polarographic characteristics of inorganic and organic substances, and two excellent indices.

ROGER PARSONS, University of Bristol

ANNOUNCEMENT

THE SECOND AUSTRALIAN CONFERENCE ON ELECTROCHEMISTRY

This conference which is being organized by the Electrochemistry Division of the Royal Australian Chemical Institute will be held in Melbourne on February 19–23, 1968.

The main topics to be discussed are: aqueous electrolyte solutions, molten salts, electrode kinetics, double layer structure, non-aqueous electrochemistry, electrochemistry at high pressures and temperature, electrokinetic phenomena, electrochemical engineering, electroanalytical chemistry, electrochemical processes in solids and corrosion and tarnishing reactions.

An international representation by leading authorities in many of these topics is expected.

Papers are invited in these or related fields. It is proposed to publish a book of abstracts and contributors are requested to send a title and abstract (300 words) by August 1st 1967. Please submit abstracts and inquiries to the Secretary: Dr. D. F. A. KOCH, Division of Mineral Chemistry, C.S.I.R.O., P.O. Box 124, Port Melbourne, Vic., Australia.

VOL. 14 NO. 2 JOURNAL OF ELECTROANALYTICAL CHEMISTRY AND INTERFACIAL ELECTROCHEMISTRY JUNE 1967

CONTENTS

INTRODUCTION TO NUCLEAR CHEMISTRY

by D. J. CARSWELL

ix + 279 pages, 23 tables, 69 illus., 1967, Dfl. 32.50, 65s., $11.00

Contents: 1. The development of nuclear chemistry. 2. Fundamental particles and nuclear structure. 3. Nuclear reactions and radioactivity. 4. Properties of nuclear radiations. 5. The detection and measurement of nuclear radiation. 6. Nuclear instrumentation. 7. Radiation chemistry. 8. Isotope measurement and separation methods. 9. Charged particle accelerators, neutron sources, production and properties of the actinide elements. 10. Uses of isotopes. 11. Experimental nuclear chemistry (including 16 selected experiments). Index.

STATISTICAL THERMODYNAMICS

An Introduction to its Foundations

H. J. G. HAYMAN

ix + 256 pages, 14 illus., 1967, Dfl. 47.50, 95s., $17.00

Contents: Preface. Nomenclature. 1. An introductory survey. 2. Some simple partition functions. 3. The microcanonical assembly. 4. The second law of thermodynamics. 5. The canonical assembly. 6. The third law of thermodynamics. 7. Dilute gases. 8. The grand canonical assembly. 9. Fermi-Dirac, Bose-Einstein and imperfect gases. 10. The partition function method applied to Fermi-Dirac, Bose-Einstein and photon gases. 11. Classical statistical thermodynamics. 12. The relationship between classical and quantum statistics.
Appendices: 1. The probability integral. 2. Stirling's formula for ln $n!$. 3. The method of variation of constants. 4. The dynamic equilibrium of a microcanonical assembly. 5. The adiabatic principle. 6. Liouville's theorem. Index.

THE STRUCTURE OF INORGANIC RADICALS

An Application of Electron Spin Resonance to the Study of Molecular Structure

by P. W. ATKINS and M. C. R. SYMONS

x + 280 pages, 57 tables, 74 illus., 357 lit. refs., 1967, Dfl. 60.00, £6.0.0, $21.75

Contents: 1. Introduction. 2. An introduction to electron spin resonance. 3. Formation and trapping of radicals. 4. Trapped and solvated electrons. 5. Atoms and monatomic ions. 6. Diatomic radicals. 7. Triatomic radicals. 8. Tetra-atomic radicals. 9. Penta-atomic radicals. 10. Summary and conclusions.
Appendices: 1. The language of group theory. 2. The spin Hamiltonian. 3. Calculation of g-values. 4. Determination of spin-density distribution and bond angles. 5. Analysis of electron spin resonance spectra. Index of data. Subject index.

FUNDAMENTALS OF METAL DEPOSITION

by E. RAUB and K. MÜLLER

viii + 265 pages, 10 tables, 138 illus., 245 lit. refs., 1967, Dfl. 60.00, £6.5.0, $21.50

Contents: 1. Chemical and electrochemical principles. 2. Electrode processes. 3. The cathodic discharge of ions. 4. The structure of electrolytic metal deposits. 5. Physical and chemical properties of electrolytic metal deposits. 6. Distribution of electrolytic metal deposits on the cathode. Index.

ELSEVIER PUBLISHING COMPANY
AMSTERDAM LONDON NEW YORK